PORES, SIGNALS AND PROGRAMMED CELL DEATH IN

MYXOCOCCUS XANTHUS

by

SWAPNA BHAT

(Under the Direction of Lawrence J. Shimkets)

ABSTRACT

Fruiting body development in the δ-Proteobacterium *Myxococcus xanthus* is governed by cell-cell signaling. The identities of many signals and their pores remain unknown. The first study focuses on identification of outer membrane (OM) β-barrel and lipoproteins by bioinformatic and proteomic analyses. A bioinformatic strategy was developed that involved step-wise elimination of cytoplasmic, lipoproteins and inner membrane (IM) protein sequences using Signal P, Lipo P and TMHMM programs, respectively. β-barrel proteins were identified from the remaining sequences using the most accurate β-barrel protein were identified in the proteome of which 54 were found by LC-MS/MS analysis of vegetative OM vesicles. One β-barrel protein, Oar, was found to be essential for intercellular C-signaling, which directs aggregation and sporulation. An *oar* mutant produces CsgA, yet fails to stimulate Δ*csgA* development when mixed together. *oar* cells form unusual shapes, alleviated in a *csgA oar* double mutant, suggesting that C-signal accumulation is detrimental. To identify OM lipoproteins, N-terminal sorting signals that direct lipoproteins to various subcellular locations were identified. Protein sequence analysis of lipoproteins followed by site directed mutagenesis

and immuno transmission electron microscopy of the ECM lipoprotein FibA revealed that +7 alanine is the extracellular matrix sorting signal.

The second study focuses on lipid bodies and their role in E-signaling during development. Lipid bodies are triacylglycerol storage organelles. This work shows that lipid bodies are synthesiszed early in development, possibly from membrane phospholipids. Lipid bodies are synthesized prior to Programmed Cell Death (PCD), which lyses most of the population. As the cells undergo PCD, the number of lipid body containing cells also declines. Extracellular lipid bodies released by lysed cells are observed when fruiting bodies are opened, and coalesce to form a cap at the top of growing fruiting bodies. Lipid bodies contain a developmental morphogen, E-signal, which was purified 300-fold. The active fraction rescued sporulation of the E-signal deficient mutant at 100 ng and was found to contain the development-specific ether lipid TG-1.

INDEX WORDS: *Myxococcus xanthus*, β-barrel, lipoproteins, lipid bodies, Programmed Cell Death, E-signal.

PORES, SIGNALS AND PROGRAMMED CELL DEATH IN *MYXOCOCCUS XANTHUS*

by

SWAPNA BHAT

BS, Sardar Patel University, India, 2002

MS, Maharaja Sayaji Rao University, India, 2004

A Dissertation Submitted to the Graduate Faculty of The University of Georgia in Partial Fulfillment of the Requirements for the Degree

DOCTOR OF PHILOSOPHY

ATHENS, GEORGIA

2011

PORS, SIGNALS AND PROGRAMMED CELL DEATH IN

MYXOCOCCUS XANTHUS

by

SWAPNA BHAT

Major Professor:	Lawrence J. Shimkets
Committee:	Timothy R. Hoover
	Anna C. Karls
	Eric V. Stabb

Electronic Version Approved:

Maureen Grasso
Dean of the Graduate School
The University of Georgia
August 2011

DEDICATION

I dedicate this work to my father, who is my idol, philosopher and a mentor. This is for you Appa.

ACKNOWLEDGEMENTS

I owe a profound sense of gratitude to my adviser, Larry Shimkets, whose constant guidance and support helped me to grow as a better researcher. He gave me ample advice when needed while encouraging me to carve my own creative path in science. I know that his patience was often stretched, especially, when it came to writing all those research papers but, I am glad he never gave up on me. I am also grateful to my committee members Eric Stabb, Tim Hoover and Anna Karls, whose timely suggestions during my graduate research proved to be extremely valuable. Surely, I could not have asked for a better committee. At this juncture in my career, I wish to thank all my teachers. Their hard work and dedication have shaped me into a better person and I firmly believe "Guru devo bhava" (meaning-Teacher is God-in Sanskrit).

I thank my past and present colleagues in Shimkets- Lab for their help and support, especially, during my early days in the lab. I also extend my gratitude to all the people on the 8th floor who made my days in the lab a little less lonely. I also thank the many friends that I have made in last six year in the graduate school. Their love and friendship made Athens a home away from home for me. I cherish each one of you.

Most importantly, I would like to thank my family. To my parents: I know how hard it was for you to let me go so far away, so that I could fulfill my dream. I shall always be grateful for all your love and sacrifices. To my sister: you will always be my best friend no matter how far you are. And finally I would like to thank Shailesh, who has been a constant companion through all my trying times. With you, I have always

been myself. Thank you for your love and kindness. I don't know what I would have done without you.

TABLE OF CONTENTS

Page

ACKNOWLEDGEMENTS v

LIST OF TABLES ix

LIST OF FIGURES x

CHAPTER

1 INTRODUCTION AND LITERATURE REVIEW 1

Identification of outer membrane proteins in *M. xanthus* 1

Role of lipid bodies in intercellular E-signaling in *M. xanthus* 3

2 PROKARYOTIC DEVELOPMENT: VARIETY AND VERSATILITY 7

Introduction 8

Differentiation leading to dormancy 10

Differentiation leading to nutrient acquisition 30

Differentiation leading to cell dispersal 38

Conclusion 51

3 BIOINFORMATIC AND PROTEOMIC ANALYSIS OF OUTER MEMBRANE B-BARREL AND LIPOPROTEINS 55

Abstract 56

Introduction 58

Results 60

Discussion 85

Experimental procedures 89

4 A ROLE FOR PROGRAMMED CELL DEATH AND LIPID BODIES IN THE *MYXOCOCCUS XANTHUS* FRUITING BODY DEVELOPMENT ...108

Abstract 109

Introduction 111

Results 114

Discussion 129

Methods and Materials 130

5 DISSERTATION SUMMARY AND CONCLUSION 149

M. xanthus β-barrel proteins 149

Oar is required for C-signaling 150

Lipoprotein sorting in *M. xanthus* 152

Lipid body synthesis during fruiting body development 154

Lipid body synthesis precedes PCD 158

The E-signal 160

Relevance of lipid body study 162

APPENDIX

A CHAPTER 3 SUPPLEMENTARY TABLES 168

LIST OF TABLES

Page

Table 2-1: Types of Prokaryotic Developmental Cycles and Differentiated Cells.....9

Table 3-1: *M. xanthus* β-barrel domain proteins obtained from Pfam database.....63

Table 3-2: *M. xanthus* IM, periplasmic and ECM proteins 68

Table 3-3: OM β-barrel proteins identified by LC-MS/MS.....70

Table 3-4: OM lipoproteins identified by LC-MS/MS.....73

Table 3-5: Putative lipoproteins identified by LC-MS/MS from IM fraction 83

Table 3-6: Bacterial strains, plasmids and primers used in this study.....91

Table 4-1: Bacterial strains in this study.....131

Table 5-1: Lipoproteins with +7 alanine.....155

LIST OF FIGURES

Page

Figure 2-1: Structure of a *B. subtilis* endospore 13

Figure 2-2: *Bacillus* endospore formation.....14

Figure 2-3: Scanning electron micrographs showing four stages in development of *S. lividans* …….....19

Figure 2-4: Fruiting bodies formed by different species of myxobacteria 23

Figure 2-5: Life cycle of *Myxococccus xanthus*.....25

Figure 2-6: Schematic representation of the *Chlamydia* developmental cycle.....28

Figure 2-7: Glutamine synthase (GS)-glutamate synthase (GOGAT) pathway of ammonia assimilation 32

Figure 2-8: Heterocyst development in *Anabaena* PCC 7120.....34

Figure 2-9: Molecular interaction between a legume root and *Rhizobium*.....37

Figure 2-10: Structure of a bacterial flagellum 40

Figure 2-11: Life cycle of *Caulobacter crescentus* 42

Figure 2-12: Cyclic accumulation of the global regulators CtrA, DnaA and GcrA 44

Figure 2-13: Life cycle of *B. bacteriovorus*.....47

Figure 2-14: Swarming in *Vibrio parahaemolyticus*.....50

Figure 3-1: Scheme to identify OM proteins utilizing bioinformatic programs.....62

Figure 3-2: Role of *oar* in cell signaling.....77

Figure 3-3: Identification of *M. xanthus* lipoprotein sorting signals.....81

Figure 3-4: Pie chart classifying 228 OM β-barrel proteins according to function 87

Figure 4-1: Lipid body production in WT cells during development 115

Figure 4-2: Lipid body production in Δ*difA* and WT + Δ*difA* cells during development ..117

Figure 4-3: Lipid body synthesis in submerged culture fruiting bodies 119

Figure 4-4: Bioassay of extracted lipid 123

Figure 4-5: Regulation of lipid body production during *M. xanthus* fruiting body development 125

CHAPTER 1

INTRODUCTION AND LITERATURE REVIEW

Some bacteria undergo cellular differentiation in response to environmental changes. Bacillus species differentiate into metabolically dormant, heat and desiccation resistant endospores when faced with nutritional deprivation. Other examples of cellular differentiation in bacteria include the generation of motile cells for dispersal in Caulobacter, and the production of nitrogen-fixing heterocysts in cyanobacteria. Chapter 2 provides an overview of developmental cycles observed in a wide variety of bacterial species to produce cell types dedicated to nutrient acquisition, dispersal, or dormancy.

This dissertation focuses on the developmental cycle of *Myxococcus xanthus*, a soil dwelling, δ-Proteobacterium. *M. xanthus* feeds on organic matter and other bacteria during its vegetative cycle. When nutrients deplete, these bacteria undergo a complex developmental cycle that involves assembling multicellular fruiting bodies inside which cells undergo sporulation. Movement and differentiation of cells inside a fruiting body are regulated by intercellular signaling. The objective of this work was to 1) identify outer membrane proteins by using bioinformatic and proteomic approaches 2) identify the role of lipid bodies during development.

Identification of outer membrane proteins in *M. xanthus*

M. xanthus, a Gram-negative bacterium, possesses an outer membrane (OM) and an inner membrane (IM) separated by a peptidoglycan layer. The OM proteins play a crucial role in the transport of nutrients, enzymes, toxins, and extracellular signals. The

OM, which forms an interface between the cell and the environment, contains integral β-barrel proteins that are formed by antiparallel β-strands (Wimley, 2003). β-barrel proteins form water-filled channels to facilitate transport of molecules across the OM. β-barrel proteins are unique to the OM and hence several bioinformatic programs have been developed to identify such proteins in a genome (Punta et al., 2007). However, the accuracy of these programs varies. I determined that the program used previously to identify *M. xanthus* proteins following LC-MS/MS generates many false positives (Kahnt et al., 2010). Chapter 3 describes the identification of OM proteins using bioinformatic and proteomic techniques. In this study several β-barrel programs were examined for their ability to discriminate β-barrel proteins using known OM, IM and periplasmic proteins. Two programs, TMBETA-SVM and TMBETADISC-RBF identified β-barrel proteins most accurately, and predicted 228 β-barrel proteins from among 7331 protein coding regions (Gromiha et al., 2005, Ou et al., 2008). Proteomic analysis was carried out by isolating OM vesicles by sucrose gradient centrifugation from vegetative cells, and identification of proteins by LC-MS/MS. 54 β-barrel proteins were identified, which represents 0.7 % of the genome.

Development in *M. xanthus* requires intercellular signaling by at least six extracellular signals (Shimkets, 1999). It is not known how these signals are transmitted across the cell. Previously, an OM β-barrel protein, Oar, was found to be essential for fruiting body aggregation and sporulation (Martinez-Canamero et al., 1993). However its function is not known. In chapter 3 oar mutants were analyzed for their role in intercellular signaling, and the results suggest that Oar is required for the export of C-signal, which is essential for fruiting body development.

Lipoproteins are the second type of protein present in the OM. They are also present in IM and ECM of *M. xanthus* (Curtis et al., 2007). Sorting signals that localize lipoproteins to various compartments are not conserved in bacteria (Tokuda &Matsuyama, 2004, Bos et al., 2007). Identification of lipoprotein sorting signals can help in recognizing their subcellular localization or in targeting proteins to specific compartments. Chapter 3 describes the identification of sorting signals for ECM and IM localization of lipoproteins. Sequence analysis of ECM, IM and OM lipoproteins revealed that lysine at the +2 position of mature lipoproteins leads to IM localization while alanine at the +7 position directs them to the ECM. Site directed mutagenesis of the major ECM protein, FibA, followed by immuno electron microscopy suggests that alanine at the +7 position is essential for ECM localization.

Role of lipid bodies in intercellular E-signaling in *M. xanthus*

One of the earliest developmental markers is the production of lipid bodies, which are reserves of carbon and energy in the form of triacylglycerols (TAGs) and other glycerol-lipids surrounded by a phospholipid monolayer (Hoiczyk et al., 2009). Lipid bodies are common in eukaryotes and have evolved into performing diverse functions such as cell-signaling. For example, mammalian adipocytes are specialized for long term energy storage of triacylglycerols and rapid mobilization of this resource to generate energy or heat. Macrophage lipid bodies store arachidonic acid, which is a precursor of signaling molecule eicosanoid, required for cell proliferation, apoptosis and other cellular processes, while those in steriodogenic cells store cholesterol required for synthesis of steroids (Murphy, 2001). The lipid body biogenesis and utilization are tightly regulated by associated proteins (Farese & Walther, 2009).

During fruiting body development, *M. xanthus* cells differentiate into three main cell types, peripheral rods, cells that undergo Programmed Cell Death (PCD) and sporulating cells. Only 15% of cells produce spores while approximately 5% of cells form peripheral rods, which do not enter fruiting bodies or undergo development (O'Connor & Zusman, 1991). The majority of the cells undergo PCD, which is regulated, at least in part, by the MazF toxin and MrpC antitoxin (Shimkets, 1986, Nariya & Inouye, 2008). The role of PCD during development is not well understood. It is possible that cell lysis releases nutrients and developmental signals required for fruiting body formation. The work presented in Chapter 4 suggests that lipid bodies are produced prior to PCD. Lipid bodies from lysed cells become extracellular and deposit on the top of fruiting body forming a cap-like structure. The E-signal was purified from the lipid bodies.

References

Bos, M. P., V. Robert & J. Tommassen, (2007) Biogenesis of the Gram-negative bacteria outer membrane. Annu Rev Microbiol 61: 191-214.

Curtis, P. D., J. Atwood, 3rd, R. Orlando & L. J. Shimkets, (2007) Proteins associated with the *Myxococcus xanthus* extracellular matrix. J Bacteriol 189: 7634-7642.

Farese, R. V. & T. C. Walther, (2009) Lipid Droplets Finally Get a Little R-E-S-P-E-C-T. Cell 139: 855-860.

Gromiha, M. M., S. Ahmad & M. Suwa, (2005) TMBETA-NET: discrimination and prediction of membrane spanning beta-strands in outer membrane proteins. Nucleic Acids Res 33: W164-167.

Hoiczyk, E., M. W. Ring, C. A. McHugh, G. Schwär, E. Bode, D. Krug, M. O. Altmeyer,

J. Z. Lu & H. B. Bode, (2009) Lipid body formation plays a central role in cell fate determination during developmental differentiation of *Myxococcus xanthus*. Molecular Microbiology 74: 497-517.

Kahnt, J., K. Aguiluz, J. Koch, A. Treuner-Lange, A. Konovalova, S. Huntley, M. Hoppert, L. Sogaard-Andersen & R. Hedderich, (2010) Profiling the outer membrane proteome during growth and development of the social bacterium *Myxococcus xanthus* by selective biotinylation and analyses of outer membrane vesicles. J Proteome Res.

Martinez-Canamero, M., J. Munoz-Dorado, E. Farez-Vidal, M. Inouye & S. Inouye, (1993) Oar, a 115-kilodalton membrane protein required for development of *Myxococcus xanthus*. J Bacteriol 175: 4756-4763.

Murphy, D. J., (2001) The biogenesis and functions of lipid bodies in animals, plants and microorganisms. Prog Lipid Res 40: 325-438.

Nariya, H. & M. Inouye, (2008) MazF, an mRNA interferase, mediates programmed cell death during multicellular *Myxococcus* development. Cell 132: 55-66.

O'Connor, K. A. & D. R. Zusman, (1991) Development in *Myxococcus xanthus* involves differentiation into two cell types, peripheral rods and spores. J. Bacteriol. 173: 3318-3333.

Ou, Y. Y., M. M. Gromiha, S. A. Chen & M. Suwa, (2008) TMBETADISC-RBF: Discrimination of beta-barrel membrane proteins using RBF networks and PSSM profiles. Comput Biol Chem 32: 227-231.

Punta, M., L. R. Forrest, H. Bigelow, A. Kernytsky, J. Liu & B. Rost, (2007) Membrane protein prediction methods. Methods 41: 460-474.

Shimkets, L. J., (1986) Role of cell cohesion in *Myxococcus xanthus* fruiting body formation. J. Bacteriol. 166: 842-848.

Shimkets, L. J., (1999) Intercellular signaling during fruiting body development of *Myxococcus xanthus*. Annu Rev Microbiol 53: 525-549.

Tokuda, H. & S. Matsuyama, (2004) Sorting of lipoproteins to the outer membrane in *E.coli*. Biochim Biophys Acta 1693: 5-13.

Wimley, W. C., (2003) The versatile beta-barrel membrane protein. Curr Opin Struct Biol 13: 404-411.

CHAPTER 2

PROKARYOTIC DEVELOPMENT: VARIETY AND VERSATLITY

S. Bhat, and L. J. Shimkets. (2009). The Encyclopedia of Microbiology, 3rd Edition, edited by Moselio Schaechter, Elsevier.375-392. Reprinted here with permission of publisher.

I. Introduction

Prokaryotic life cycles differ from their eukaryotic counterparts in several fundamental ways. Prokaryotic development is strictly asexual unlike eukaryotic development where sexual reproduction generates progeny with different genotypes from the parents. Prokaryotic development is often a direct or indirect response to nutrient limitation. Often carbon, nitrogen and/or phosphorus starvation directly induce development. In *Caulobacter crescentus*, growth in oligotrophic (nutrient-limited) environments led to a life cycle whereby a sessile parent produces motile progeny that disperse to reduce competition with the parent. Here the life cycle is not directly controlled by nutritional cues, but long term selection for oligotrophic growth likely shaped the developmental cycle.

The major advantage of prokaryotic development is the division of labor facilitated by the use of multiple cell types. Cellular differentiation results in structural and functional changes that generate a cell with a different purpose than its parent. This chapter will provide an overview of several different types of prokaryotic life cycles, which can be divided into three types based on the functions of the specialized cells (1) dormancy (2) nutrient acquisition, and (3) dispersal (table 2-1).

Resting cells are generated in response to nutrient limitation and provide a metabolically quiescent or **dormant** state that permits survival during periods of famine or drought. Endospore formation by *Bacillus* spp is the most carefully studied example but spores are formed by many mechanisms as illustrated by several examples.

Specialized cells for **nutrient acquisition** are generated in some organisms, most notably nitrogen fixation by cyanobacterial heterocysts.

Table 2-1: Types of Prokaryotic Developmental Cycles and Differentiated Cells.

Function	Cell	Representative genus	Phylum
Dormancy	Endospore	*Bacillus*	Firmicutes
		Metabacterium	Firmicutes
		Epulopiscium	Firmicutes
	Aerial spore	*Streptomyces*	Actinobacteria
	Cyst	*Azotobacter*	γ Proteobacteria
		Rhodospirillum	α Proteobacteria
	Myxospore	*Myxococcus*	δ Proteobacteria
		Stigmatella	δ Proteobacteria
	Exospore	*Methylosinus*	α Proteobacteria
	Small dense cell	*Coxiella*	γ Proteobacteria
	Elementary body	*Chlamydia*	Chlamydia
	Akinete	*Anabaena*	Cyanobacteria
Nutrient Acquisition	Heterocyst	*Anabaena*	Cyanobacteria
	Bacteroid	*Rhizobium-legume*	α Proteobacteria
		Frankia-alder	α Proteobacteria
Dispersal	Baeocyte	*Pleurocapsa*	Cyanobacteria
	Hormogonium	*Nostoc*	Cyanobacteria
	Swarmer cell	*Vibrio*	γ Proteobacteria
	Swarmer cell	*Caulobacter*	α Proteobacteia
	Zoospore	*Kineococcus*	Actinobacteria
	Attack phase cells	*Bdellovibrio*	δ Proteobacteria

Motile cells generated for **dispersal** are illustrated by the swarmer cells of *Caulobacter crescentus,* but dispersal is mediated by many mechanisms as illustrated by several examples.

II. Differentiation leading to dormancy

A strategy used by some bacteria to survive nutritional stress involves forming a metabolically quiescent resting cell. Resting cells can survive long periods of dormancy and germinate when conditions favor growth. Various types of resting cells include endospores, exospores, cysts, and akinetes, which have some similarities. Dormancy is achieved by dehydrating the cytoplasm. Resistance to environmental stresses is increased by forming additional layers around the cell. Finally, storage molecules are produced to aid in germination.

Endospores:

Endospores are formed by *Bacillus* and *Clostridium* species and are extremely resistant to heat, desiccation and ultra violet (UV) radiation. Starvation induces asymmetric cell division and engulfment producing a spore within a mother cell. Then, the mother cell lyses releasing the endospore. Endospores are the most resistant and durable cells known. They can germinate and resume growth after long periods of time. Endospores have been reported to have germinated from the tombs of Egyptian pharaohs, from bees trapped in 25 to 40 million year old amber and from 250 million year old salt crystals. Endospores are easily dispersed, which makes them excellent weapons of mass-destruction as seen with anthrax disease.

Exospores:

Exospores are formed by *Methylosinus trichosporium*, which utilizes methane or methanol as the sole source of carbon. *M. trichosporium* cells form a bud in stationery phase by asymmetric cell division, which develops into an exospore.

Cysts:

Cysts are produced from a single vegetative cell by accumulation of a thick coat. Cyst formation has been observed in many bacterial genera, including *Azospirillum, Azotobacter, Methylobacter*, and the purple photosynthetic bacterium *Rhodospirillum*. In *Rhodospirillum*, development of a cyst begins with the accumulation of poly-hydroxybutyrate (PHB) storage granules followed by change in cell shape and acquisition of an outer coat.

Akinetes:

Akinetes are resting cells produced by some heterocyst-forming cyanobacteria. They are formed from a vegetative cell by enlargement and cell wall thickening. Akinetes sometimes possess storage materials such as glycogen and cyanophycin, a polymer of arginine and aspartate. Unlike other types of resting cells they maintain significant metabolic activity.

The following section provides an overview of the life cycles of some bacteria that generate resting cells.

A. Endospore formation

One of the well-studied examples of prokaryotic spore development is endospore formation in *Bacillus subtilis*. The hardiness of an endospore is attributed to its layered structure (figure 2-1). Two types of peptidoglycan layers are present between the outer

and inner membranes of the endospore, the cortex and the germ cell wall. The germ cell wall is a thin layer of peptidoglycan that forms the vegetative cell wall after germination. The spore cortex is essential for maintaining a quiescent state. The proteinaceous spore coat consists of a lamellar inner layer and a striated outer layer. Between the cortex and the inner coat layer exists an undercoat region composed of an unknown material. The spore coat is encased by a loosely bound exosporium, which consists of carbohydrates and proteins. The various layers of the spore provide protection against environmental stress. Spores have little water leading to enzyme dormancy and resistance to wet heat. Spores also contain dipicolinic acid (DPA) bound to divalent cations, mostly Ca^{+2}, which provides resistance to ultraviolet radiation. Small acid-soluble spore proteins (SASPs) bind to the DNA and protect it from heat and chemicals. SASPs also provide nutrients during germination.

Spore formation requires approximately seven hours at 37°C and can be divided into seven morphological stages (0 - VI) (figure 2-2).

Stage 0 is the commitment to sporulation and does not involve any morphological changes. Endospore formation is initiated by several environmental cues, including nutrient depletion and high cell density. Starvation leads to a stringent response, the accumulation of pppGpp (guanosine 3′-diphosphate, 5′-triphosphate) and ppGpp (guanosine 3′,5′-bispyrophosphate) synthesized by RelA, which is activated when protein synthesis stalls due to the absence of amino acids. Synthesis of (p)ppGpp leads to a reduction in GTP and GDP nucleotides, which is sensed by transcription factor CodY. Adequate cell density is signaled by extracellular oligopeptides synthesized by the *phrA* and *phrE* genes. These oligopeptides are imported by the cell and inhibit repressors of

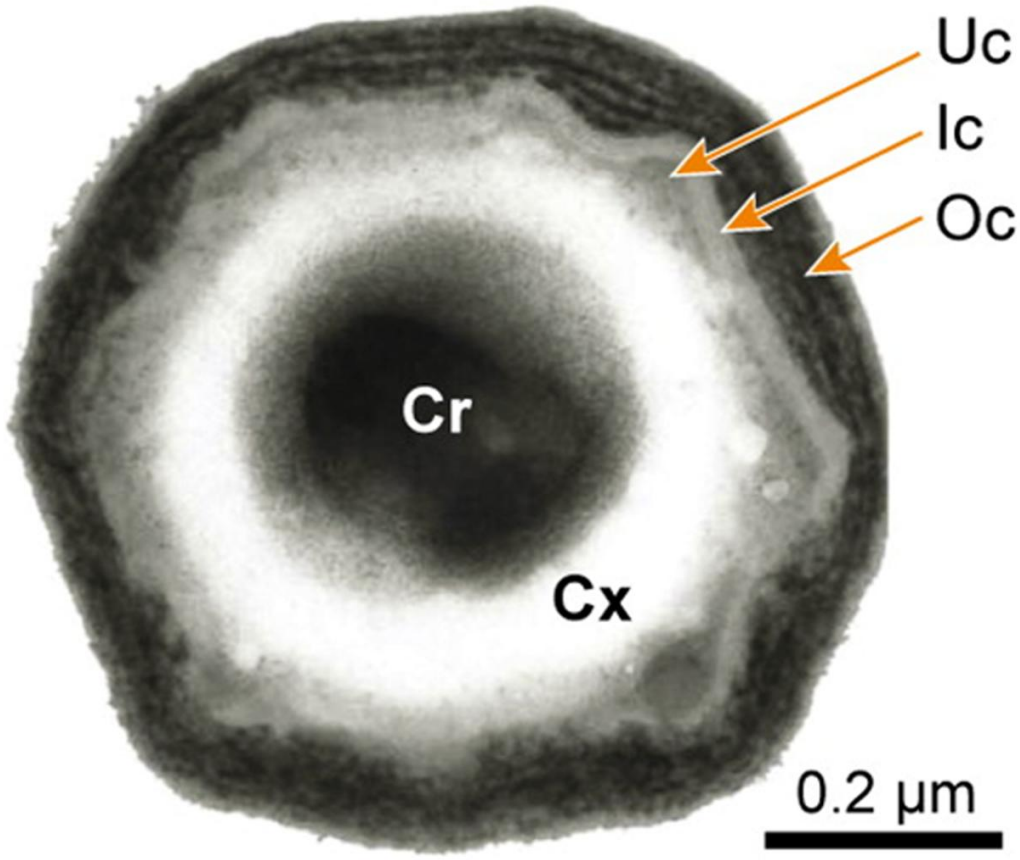

Figure 2-1: Structure of a *B. subtilis* endospore. The endospore consists of a spore core (Cr) that contains the genetic material. The spore core is surrounded by several protective layers, which include the germ cell wall (not shown) and the cortex (Cx) both composed of peptidoglycan, the proteinaceous coat layers consisting of the inner (Ic) and outer (Oc) coats, the under coat (Uc) layer of unknown composition, and the outer most layer is the loosely bound exosporium. From Henriques et al, 2007**.**

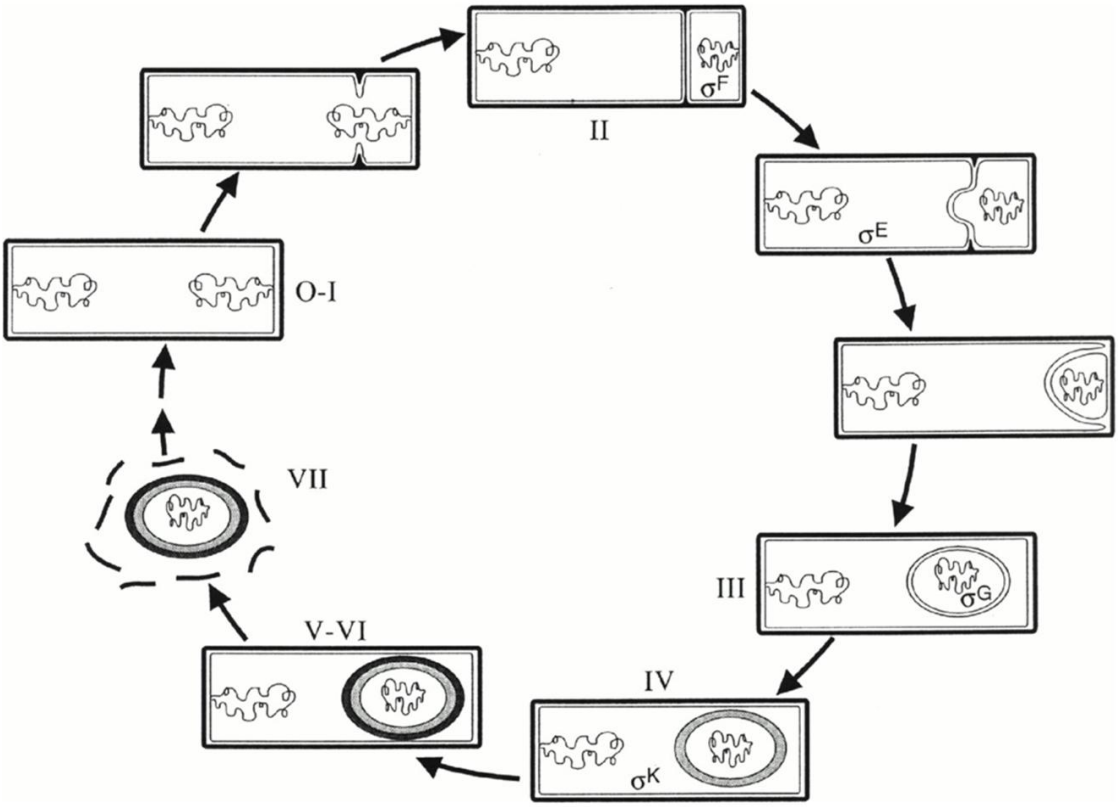

Figure 2-2: *Bacillus* endospore formation. A vegetative cell (stage 0-I) is shown as having two complete chromosomes. Stage I is the formation of an axial filament of chromatin, which stretches across the long axis of the cell (not shown). Asymmetric cell division marks stage II, dividing the cell into the larger mother cell compartment and smaller forespore compartment. At this point 30% of a chromosome is in the forespore, but the DNA translocase SpoIIIE pushes the remaining DNA into the forespore. In stage III the mother cell engulfs the forespore, which is now surrounded by two membranes of opposite orientation. Synthesis of the germ cell wall and cortex by the forespore occurs in stage IV and is represented as thickening and graying of the ellipse. Deposition of the spore coat around the forespore occurs in stage V. Stage VI is maturation, when the spore acquires its resistance properties. No morphological changes are observed at this stage.

Stage VII represents lysis of the mother cell, which releases the mature spore into the environment. From Straiger and Losick, 1996.

sporulation. The initiation of sporulation is regulated by a phosphorelay involving kinases KinA and KinB, which phosphorylate the response regulator Spo0F. Spo0B transfers the phosphate from phosphorylated Spo0F to Spo0A, the master initiator of spore formation. Spo0A~P activates genes required for several subsequent stages of spore formation including chromosome remodeling, asymmetric cell division and induction of mother cell and spore cell specific sigma factors. Sigma factors (σ) are subunits of RNA polymerase that determine promoter specificity and hence activate gene expression.

Stage I is marked by the formation of an axial filament of chromatin that stretches across the long axis of the cell. Remodeling of the chromosomes is carried out by DivIVA, a polar division protein, and RacA, which forms a bridge between DNA and DivIVA.

In **stage II** an asymmetric septum is formed, which generates small forespore and larger mother cell compartments. Asymmetric cell division is brought about by FtsZ and response regulator SpoIIE. FtsZ is a tubulin-like GTPase that polymerizes into a ring structure at the site of cell division. A DNA translocase, Spo0IIIE transports the chromosome into the forespore. Asymmetric cell division leads to compartmentalization of gene expression, established by the compartment specific sigma factors. σ^F, encoded by *spoIIA*, and σ^E, encoded by *spoIIG*, are activated in the forespore and mother cell, respectively. The sigma factors are initially synthesized in an inactive form and are activated after asymmetric cell division.

Stage III is highlighted by the mother cell engulfing the forespore. The mother cell synthesizes proteins that degrade the peptidoglycan septum. Then, the mother cell

deposits a cell membrane around the forespore releasing the forespore into the mother cell. At this point the forespore possess two membranes of opposite orientation.

In **stage IV**, the germ cell wall is deposited on the surface of the inner membrane and the cortex made of a thicker layer of peptidoglycan, is assembled on the outer membrane by forespore specific proteins. The genes for these proteins are activated by sigma factor σ^G, synthesized by *spoIIIG*, and activated soon after engulfment.

Stage V is highlighted by the formation of the spore coat around the forespore by proteins synthesized by the mother cell. The genes involved in spore coat formation include 14 *cot* genes. These *cot* genes are under the control of mother cell specific σ^K, which is activated after engulfment and after σ^G is activated in the forespore.

During **stage VI**, the spore acquires resistance to UV radiation and high temperatures. SASPs are synthesized by forespore specific genes under the control of σ^G. Dipicolinic acid synthesized by the mother cell is taken up by the forespore.

In **stage VII**, the mother cell lyses and the endospore is released.

Germination of the endospore occurs in response to nutrients that interact with receptor proteins present in the inner membrane of the spore. This leads to a cascade of events, which includes export of monovalent cations like H^+, K^+ and Na^+ from the spore core followed by the release of Ca^{+2} and dipicolinic acid. The spores swell due to uptake of water and initiate DNA replication and protein synthesis. Finally, the spores shed the spore coat and resume vegetative growth.

Some bacteria produce multiple endospores as a primary mode of reproduction instead of the traditional binary fission. *Metabacterium polyspora,* a gastrointestinal symbiont of the guinea pig, undergoes sporulation to produce several endospores from a

single mother cell. The formation of multiple endospores is achieved by producing forespores at each pole. Both forespores are engulfed by the mother cell then undergo multiple binary fissions generating additional progeny that form endospores.

Some bacteria related to *Bacillus* bypass endospore formation and produce daughter cells internally as seen in *Epulopiscium*, a gut symbiont of the surgeon fish. The mother cell possesses multiple spherical nucleoids that migrate to the cell poles during the day. These nucleoids elongate as the day progresses and eventually produce daughter cells that are released when the mother cell lyses.

B. *Streptomyces*

Streptomyces spp are soil dwelling organisms belonging to the Actinobacteria phylum. *Streptomyces* colonies contain hyphae and resemble fungi except for their distinctive prokaryotic nature. Three cell types are observed; basal hyphae, aerial hyphae and spores.

The *Streptomyces* life cycle begins with the germination of a spore under nutrient-rich conditions (figure 2-3). The spore germinates and forms multinucleate hyphae that grow into a substrate mycelium with a hydrophilic surface. Once growth of the primary mycelium has been achieved, aerial hyphae are extended vertical to the mycelial mass. Growth of the aerial hyphae uses nutrients provided by the substrate mycelia. The aerial hyphae are covered with a fibrous layer made of hydrophobin, a family of secreted proteins that form a hydrophobic layer on hyphae and spore surfaces. The aerial hyphae coil and then septate to produce chains of spores that are dispersed by wind and rain. Bald (*bld*) genes control the development of aerial hyphae and white (*whi*) genes control

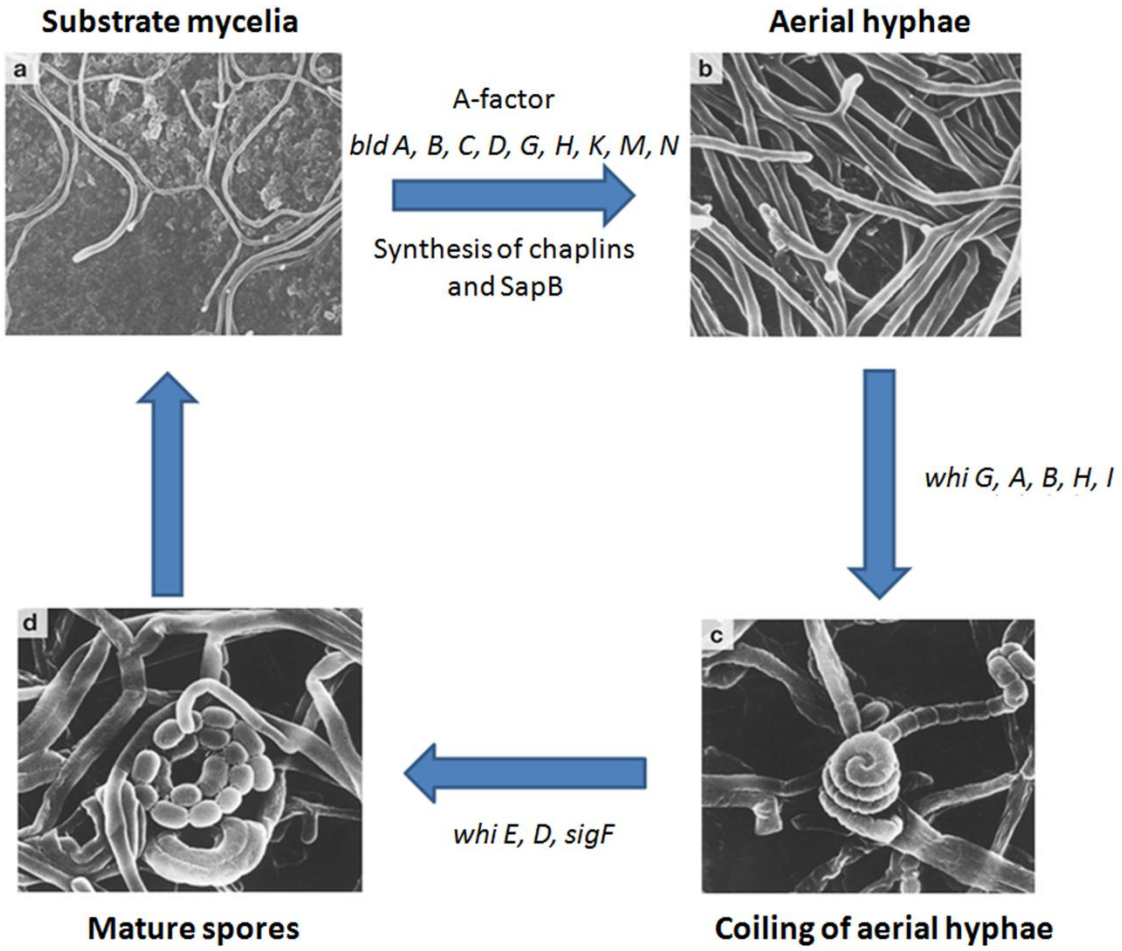

Figure 2-3: Scanning electron micrographs showing four stages in development of *S. lividans*. (a) A spore germinates and then grows into the filaments that form the substrate mycelium. The *bld* cascade is activated at this stage by several extracellular factors, one of which includes A-factor, a γ-butyrolactone. (b) The *bld* cascade culminates with the formation of hydrophobins such as SapB and chaplins that help in the escape of aerial hyphae from the substrate. (c) Once aerial hyphae are formed, the *whi* cascade is activated leading to formation of the aerial hyphae spirals. (d) The polynucleated aerial filaments are partitioned, eventually becoming spores. Figure modified from Hopwood, 2006.

the formation of aerial hyphae and spores. The *bld* mutants are unable to form aerial hyphae and hence are called 'bald' mutants while *whi* mutants are unable to sporulate and hence appear white. During mycelial growth BldD represses *bldN* and *whiG*, which encode transcriptional factors required for initiation of aerial hyphae formation. The mechanism of release of repression by BldD is not known.

The signals for aerial hyphae development include five extracellular oligopeptides and 'A'-factor, a γ-butyrolactone. The *bld* cascade involves synthesis and perception of these signals. Although the identities of the oligopeptide signals are not clear, the signal cascade ultimately leads to the synthesis of a morphogen that allows the escape of the aerial hyphae from the basal mycelia. The *bld* cascade culminates by activating the *ram* (rapid aerial mycelium) operon, which consists of four genes, *ramCSAB* that synthesize and transport the diffusible, surface-active peptide SapB. SapB, the product of *ramS*, is initially synthesized as a 42 kD protein and then processed and modified to form double cyclic structures similar to lantibiotics, a class of cyclic peptide antibiotics. Application of SapB to *bld* mutants leads to formation of aerial hyphae. The *bld* genes also induce production of other surface active proteins called chaplins. Eight types of chaplins are synthesized by genes *chpA-H*. The chaplins bind to the cell walls of the aerial hyphae while SapB is found in the culture medium and spore coat. The chaplins and SapB initiate escape of aerial hyphae from the colony surface by reducing the surface tension at the air-water interface.

The white (*whi*) genes regulate the final phase of the life cycle, the differentiation of spores along the aerial hyphae. In the growing aerial hyphae the *whi* gene cluster is activated by σ^G encoded by *whiG*. σ^G regulates the synthesis of the early

whi genes, *whiI, whiA, whiB and whiH.* WhiH and WhiI are transcriptional regulators of sporulation and septation. WhiA and WhiB prevent further growth of the aerial hyphae. WhiH activates expression of the cell division protein FtsZ, which initiates spore septation. Late sporulation regulators such as WhiD and SigF activate spore maturation and pigmentation.

The *bld* cascade acts as a checkpoint between substrate mycelia and development of aerial hyphae. The sole role of the *bld* cascade is activation of the *ram* operon to synthesize SapB. Sporulation is not well understood in *Streptomyces*. The missing pieces of the puzzle are the molecular signals that activate the *whi* cascade. Recently, another pathway, *sky,* has been proposed to act as an intermediate between *bld* and *whi*. However, the constituents of the *sky* pathway are still unclear.

C. Myxobacteria

Myxobacteria are δ Proteobacteria that move by gliding on surfaces and undergo motility-dependent multicellular morphogenesis. Myxobacteria swarm together while feeding. Multicellularity maximizes the ability of a bacterial community to feed on macromolecular substrates. Upon starvation myxobacteria aggregate to form spore-filled fruiting bodies. Formation of spores in a fruiting body allows efficient feeding of daughter cells.

Myxobacteria are predators of other micro-organisms. They also feed on insoluble macromolecules such as cell walls, proteins, lipids, polysaccharides, and nucleic acids. Myxobacteria secrete enzymes that lyse prey cells and grow on their hydrolytic products. The multicellular swarms are more efficient at digesting prey colonies than individual cells ensuring rapid degradation of prey cells or macromolecules.

The sensing of the prey cells by *M. xanthus* may be mediated by lipid chemotaxis. Prey cell membranes contain a derivative of phosphatidylethanolamine (PE) with an 18:1ω9c fatty acid (fatty acid of 18 carbons with one point of unsaturation at position 9 from the carboxyl group), which is released into the environment when cells are lysed. This fatty acid is a chemoattractant and is not made by *M. xanthus*.

Chemotaxis towards the prey cells requires motility. Myxobacteria move on a solid surface by two methods that do not depend on flagella. Social or S-motility is required for group translocation while adventurous or A-motility allows the movement of single cells or groups of cells. S-motility requires type IV pili, which are retractile appendages found on the leading cell pole and an extracellular matrix (ECM) composed of exopolysaccharides and proteins. When in close proximity, a type IV pilus extends and attaches to the ECM of a neighboring cell. Then, the pilus retracts causing the piliated cell to move forward. The mechanism of A-motility is the subject of debate. Surface motility is slow compared to swimming. Cells move approximately 3 μm/min and reverse direction every seven minutes.

Fruiting bodies are 10-1000 μm in size, and are often raised from the surface by the presence of a stalk (figure 2-4). The fruiting bodies generated by *Myxococcus* species are spherical-shaped. The *Chondromyces* and *Stigmatella* species form numerous sporangia containing spores. The sporangia are held by stalks that are branched in *Chondromyces* or consist of tubules in *Stigmatella*. The fruiting bodies contain numerous myxospores that are metabolically quiescent and resistant to heat and UV radiation. *M. xanthus* myxospores are protected by a thick electron-dense coat composed of carbohydrates and proteins.

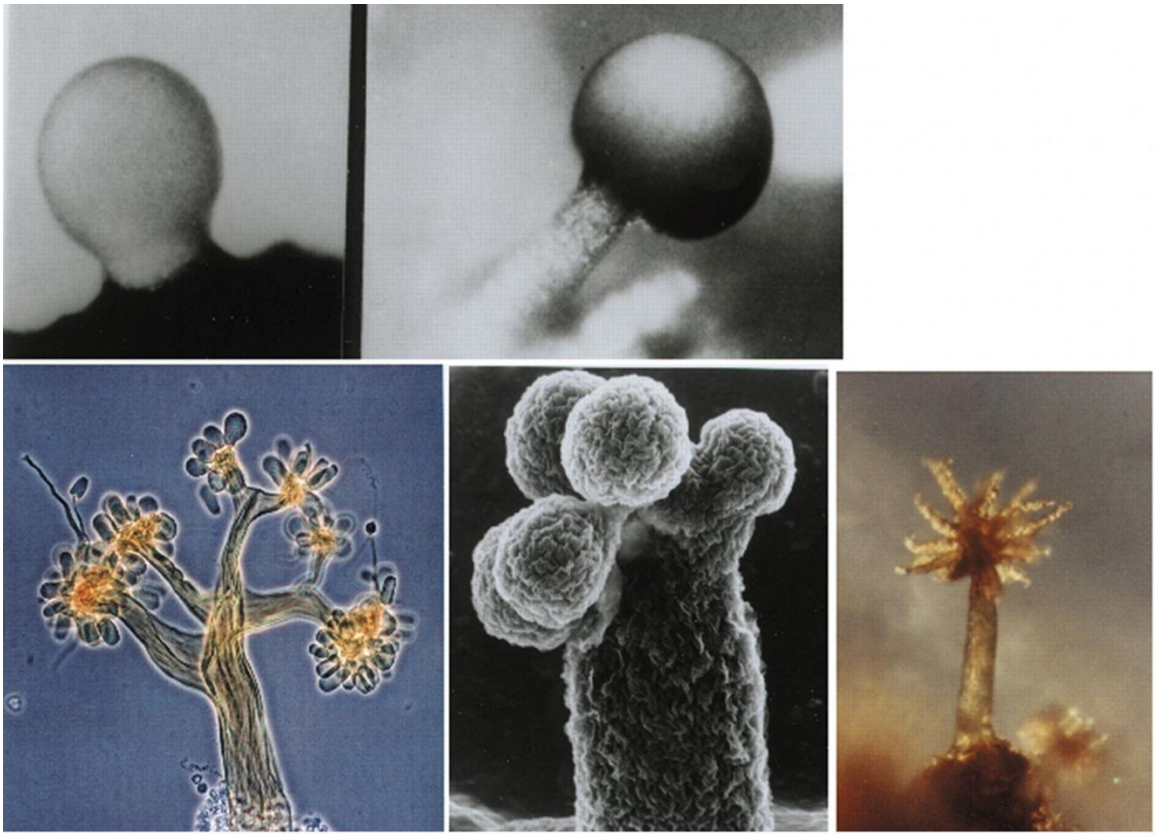

Figure 2-4: Fruiting bodies formed by different species of myxobacteria. (Top row left to right) *Myxococcus fulvus*, *Myxococcus stipitatus*; (Bottom row left to right), *Chondromyces crocatus*, *Stigmatella aurantiaca*, and *Chondromyces apiculatus.* From Kaiser, 2001.

Fruiting body development of *M. xanthus* is induced by amino acid starvation through the stringent response. Inhibition of protein synthesis stimulates pppGpp and ppGpp synthesis by RelA. ppGpp activates synthesis of an extracellular chemical signal consisting of a mixture of amino acids (Trp, Pro, Phe, Tyr, Leu, and Ile) called A-signal. A-signal is sensed by histidine protein kinase SasS, which activates the response regulator SasR. SasR along with σ^{54} activates a set of developmental genes. The B-signal, synthesized by LonD, is also required early in development though little is known about it.

During the period of A and B signaling between 0 to 8 h, no specific changes in cell arrangement can be discerned (figure 2-5). In the second phase, a sudden burst of motility is observed during which swarms of cells come together and form numerous small aggregates three or four layers thick. With time most of the small aggregates disintegrate and the cells are attracted toward larger aggregates. The formation and stability of the large aggregates require the C-, D- and E- extracellular signals and the Dif chemosensory system.

The large aggregates are lengthened vertically by adding a succession of tiers. Each tier consists of a single-layer of cells that is added over the uppermost layer. Tiers may be formed by the collision of two swarms of cells moving in opposite direction leading to a vertical pitch that allows one swarm to cross over the other swarm. The cells on the top tier expand horizontally. As more cells are recruited, multiple tiered aggregates are formed. This structure eventually becomes encapsulated in slime. Within the aggregates vegetative cells differentiate into myxospores that involve conversion of

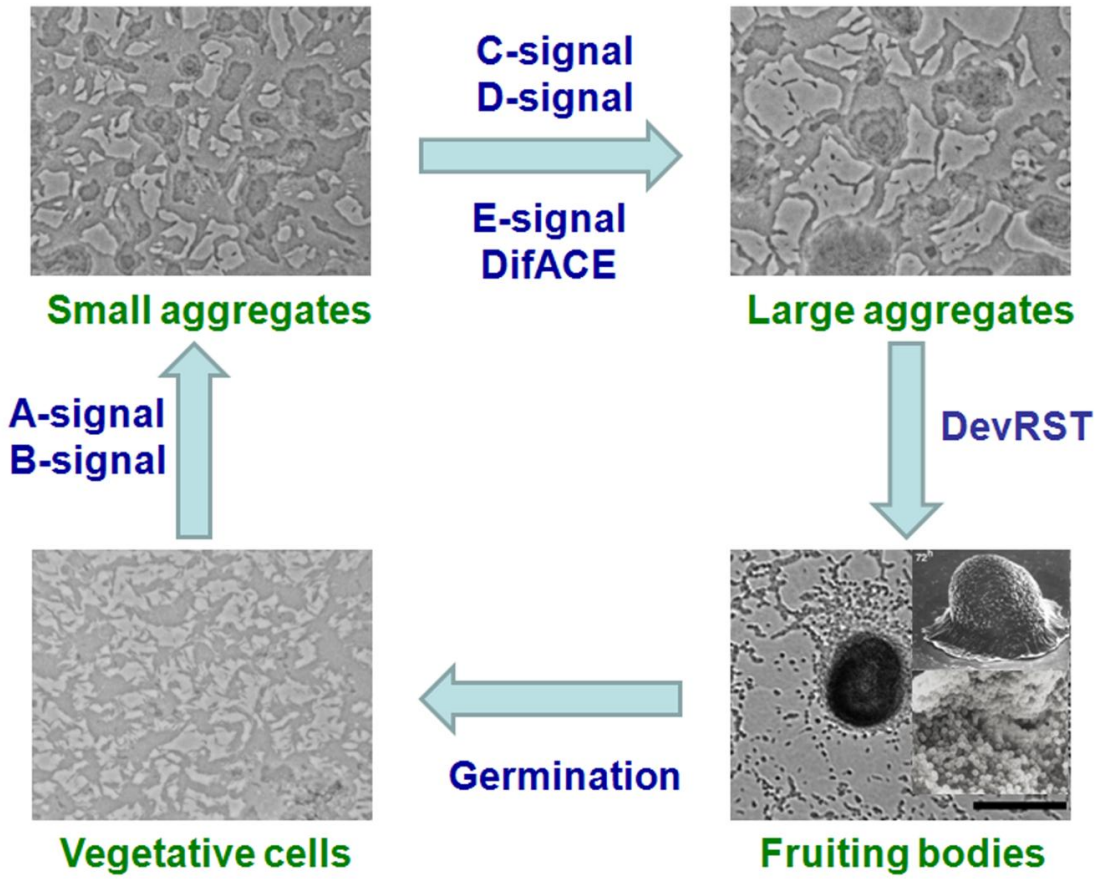

Figure 2-5: Life cycle of *Myxococccus xanthus*. Fruiting body development of *Myxococcus xanthus* can be divided into three stages. Vegetative cells are arranged in layers and sense starvation through the stringent response and cell density with the extracellular A-signal. After about 8 h, the cells show vigorous movement and form numerous small aggregates. Only few of the small aggregates form larger aggregates, which are composed of many layers of cells (the insets show electron micrographs of a fruiting body and at higher magnification spores, inside the fruiting body by scanning electron microscopy). The fruiting bodies darken due to sporulation. Germination occurs in the presence of nutrients leading to a swarm of vegetative cells. Bar is 0.1 mm. From Curtis et al, 2007 and Kuner and Kaiser, 1982.

rod shaped cells to spherical cysts. The myxospores appear to retain vegetative cell membranes and possess a capsule layer composed of slime.

The C-signal and Dif chemosensory system govern several stages of myxobacterial development. The C-signal produced by *csgA* is required for the formation of fruiting bodies as well as spores. C-signal transmission requires that cells are aligned end-to-end and leads to transcription of several developmental genes. Although FruA is synthesized in response to the A-signal and E-signal soon after starvation is sensed, FruA is phosphorylated in response to the C-signal to FruA~P, which in turn activates FrzCD a methyl-accepting chemotaxis protein (MCP). FrzCD relays the signal to FrzE, a response regulator, which controls cell reversals. FrzE~P also inhibits FrzCD methylation by a negative feedback loop. The Frz phosphorylated intermediates oscillate and is termed the 'frizillator'. The FruA~P levels are low initially because C-signals are low leading to reversal of gliding direction every eight minutes. When cells collide, the frizillator becomes synchronized due to increased C-signaling. As more C-signal is produced, cell reversal is reduced making streams of cells that move toward aggregation foci. Within the aggregation centers C-signaling is maximum leading to activation of *dev* operon by FruA~P. *devRST* expression is regulated spatially ensuring sporulation only within fruiting bodies.

The Dif chemosensory system also controls fruiting body morphogenesis and sporulation. Dif proteins DifA, a methyl-accepting chemotaxis protein (MCP), DifC, a CheW-like coupler and DifE, a CheA-like histidine kinase form a ternary signaling complex. DifACE mutants form small aggregates that are several layers thick but fail to mature beyond that stage. These results suggest that the DifACE mutants fail to

synthesize or respond to extracellular factors that are required for stable and growing aggregation centers. DifACE are essential for ECM production, S-motility and chemotaxis to lipids containing a rare fatty acid 16:1ω5c (a fatty acid of 16 carbons with one point of unsaturation at position 11 from the carboxyl group) in nature. S-motility is not the critical output because cells can make fruiting bodies using A-motility. The DifACE pathway has two sensory inputs leading to different outputs for ECM production and lipid chemotaxis. Either input mediates development but loss of both inputs eliminates fruiting body morphogenesis like *difACE* mutations. The precise signals that facilitate fruiting body development remain unknown.

D. *Chlamydia*

Chlamydia spp are obligate intracellular bacteria that cause several prevalent human diseases, including trachoma, the leading cause of human blindness and a sexually transmitted disease. Although growing cells are fragile and rapidly die outside the host, the organism produces resistant infectious cells. *Chlamydia* spp. undergo a biphasic life cycle that alternates between two morphologically distinct forms, an infectious elementary body (EB), and a noninfectious, replicating reticulate body (RB) (figure 2-6).

EBs are metabolically inactive cells ~300 nm in diameter. The DNA inside EBs is compacted by bacterial histone-like proteins HctA and HctB. Although EBs lack a peptidoglycan cell wall, proteins in the outer membrane are extensively cross-linked with disulphide bonds providing structural rigidity and osmotic stability adapted for extracellular survival. EBs also contain a type III secretion system (TTSS) that injects toxins into host cells.

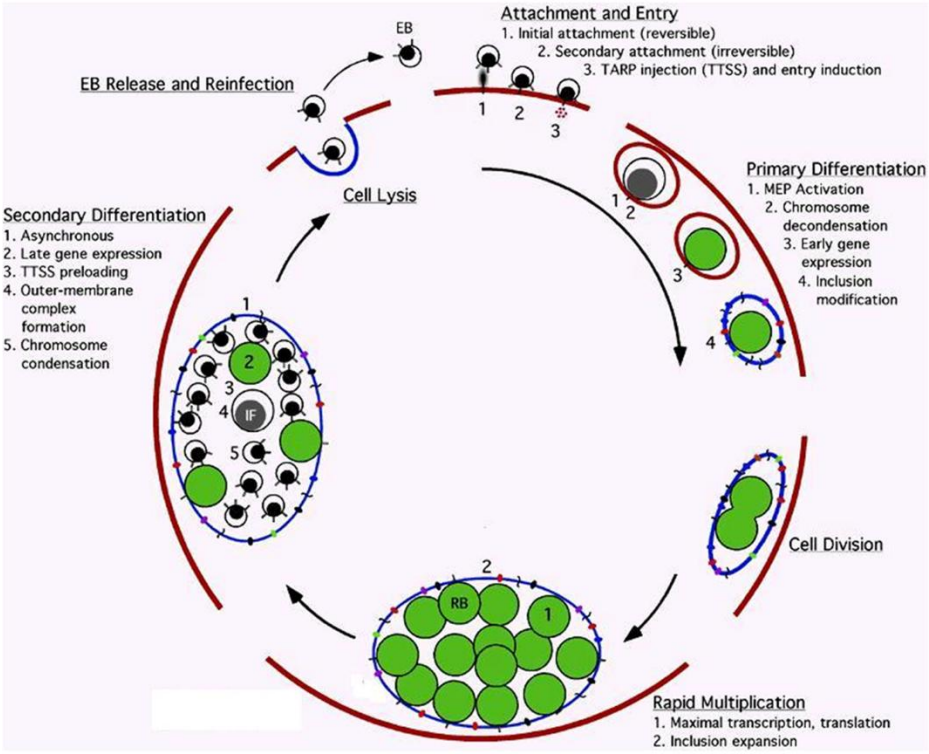

Figure 2-6: Schematic representation of the *Chlamydia* developmental cycle. The life cycle of *Chlamydia* begins with the attachment of an infectious elementary body (EB) to a host cell membrane (red line) followed by its entry into the cell by endocytosis. The uptake of an EB is achieved when it injects an actin polymerizing protein, TARP that induces phagocytosis. The EB enclosed in membrane vesicle that is soon modified to protect from the host cell. Several genes are transcribed that are required for nutrient acquisition and ATP scavenging from the host cell. Soon after endocytosis, EBs differentiate into RBs that divide rapidly by binary fission. After several cell divisions, RBs differentiate into EBs that are released by lysing the host cell or by extrusion. From Abdelrahman and Belland, 2005.

EBs bind to epithelial cells by an initial reversible attachment through electrostatic interactions and later through an irreversible attachment to an unidentified receptor on the host cell. Following irreversible binding, actin recruiting protein TARP (Translocated Actin-Recruiting Phosphoprotein) is delivered into the host cell by the TTSS. Actin undergoes polymerization to form filaments that facilitate many cellular activities, including phagocytosis, the process of ingesting large foreign particles. The actin filaments push the plasma membrane around the EB leading to internalization. An EB is internalized in a membrane vesicle, which is an extension of the plasma membrane, and called an inclusion body.

Post infection, EBs begin primary differentiation into metabolically active RBs. The RBs are larger and possess a granular cytoplasm containing fibrillar nucleic acids. The RBs divide rapidly by binary fission. Primary differentiation requires disruption of DNA-histone interactions, which is achieved by the small metabolite 2-C-methylerythritol 2, 4-cyclodiphosphate and the *euo* gene product, which is probably a histone specific protease. Although EBs are metabolically inactive, they are endowed with transcription and translation machinery, which are utilized soon after internalization to synthesize new macromolecules. Chromosome unpacking leads to active transcription of genes involved in nutrient acquisition and modification of the inclusion bodies. The genes expressed during primary differentiation encode membrane proteins to facilitate interaction with the host cell and provide protection against the host defenses. Proteins required for nutrient acquisition such as ABC transporters and oligopeptide permeases are synthesized early along with genes encoding ATP transporters suggesting that *Chlamydia* spp scavenges host ATP.

After the rapid cell division stage, RBs begin to differentiate into EBs by secondary differentiation. The genes expressed during this stage include those encoding components of the EB outer membrane complex and proteins involved in the condensation of the chromosome. During the final stages of development, the EBs occupy the entire cytoplasm of the host cell. The release of newly formed EBs can occur by either lysis of the host by degradation of the cell membrane, or extrusion, release of a fraction of the inclusion bodies leaving the host cell intact. Both release pathways occur at equal frequency. The ability of the intracellular pathogen to escape the host cell without damaging it ensures survival of the bacteria within the organism and may lead to chronic *Chlamydia* infections.

III. Differentiation leading to nutrient acquisition

Nitrogen, an essential constituent of most biomolecules, comprises 14% of the cell dry weight. Although, the major component of the Earth's atmosphere is nitrogen, N_2 is unusable by most living organisms. Only fixed (reduced) forms of nitrogen like ammonia (NH_3) or nitrate (NO_3^-) can be assimilated into biomolecules. The reduction of the extremely stable N_2 triple bond is an energy intensive process. Reduction of N_2 is carried out exclusively in a select group of microbes known as diazotrophs, which supply reduced forms of nitrogen to all living organisms. Most organisms acquire nitrogen heterotrophically from other biomolecules. Several types of differentiated cells reduce N_2. Examples include cyanobacteria heterocysts and *Rhizobium* bacteroids.

Diazotrophs use an enzyme called nitrogenase to catalyze the expensive reduction of N_2. The chemical reaction for nitrogen fixation is:

$$N_2 + 8\,H^+ + 8\,e^- + 16\,ATP \longrightarrow 2\,NH_3 + H_2 + 16\,ADP + 16\,PO_4^{-2}$$

The nitrogenase complex found in cyanobacteria and *Rhizobium* is composed of two proteins, dinitrogen reductase and dinitrogenase. The reductase binds and hydrolyzes ATP using energy to transmit electrons from a low potential reductant such as ferredoxin or flavodoxin to the dinitrogenase. Dinitrogenase binds N_2 and reduces it to ammonia. The fixation of each molecule of N_2 requires at least 16 ATP.

NH_3 is assimilated into glutamate by the glutamine synthetase (GS)-glutamate synthase (GOGAT) pathway (figure 2-7). Glutamine synthetase assimilates ammonia by converting glutamate (Glu) to glutamine (Gln). GOGAT then transfers the amido group of Gln to 2-oxoglutarate (2OG), generating two Glu. Glu and Gln transfer nitrogen to other compounds.

The nitrogenase enzyme complex is extremely sensitive to oxygen with a half-life of about 45 s in air. Hence, strict anaerobic conditions are required for activity. Aerobic bacteria and bacteria with oxygenic photosynthesis use different mechanisms to protect nitrogenase from oxygen. U*nicellular cyanobacteria show temporal separation of nitrogen fixation and photosynthesis, with nitrogen fixation occurring only in the dark and oxygenic photosynthesis occurring only in light. Filamentous cyanobacteria fix nitrogen in specialized cells known as heterocysts, which do not contain a photosynthetic apparatus and hence, do not generate* O_2. Symbiotic organisms like *Rhizobium* produce nodule structures on the surface of legume roots to generate microaerophilic (oxygen-limiting) conditions. These nodules are filled with leghaemoglobin, a red plant protein homologous to haemoglobin, which sequesters oxygen to generate the anoxic environment required for nitrogenase activity.

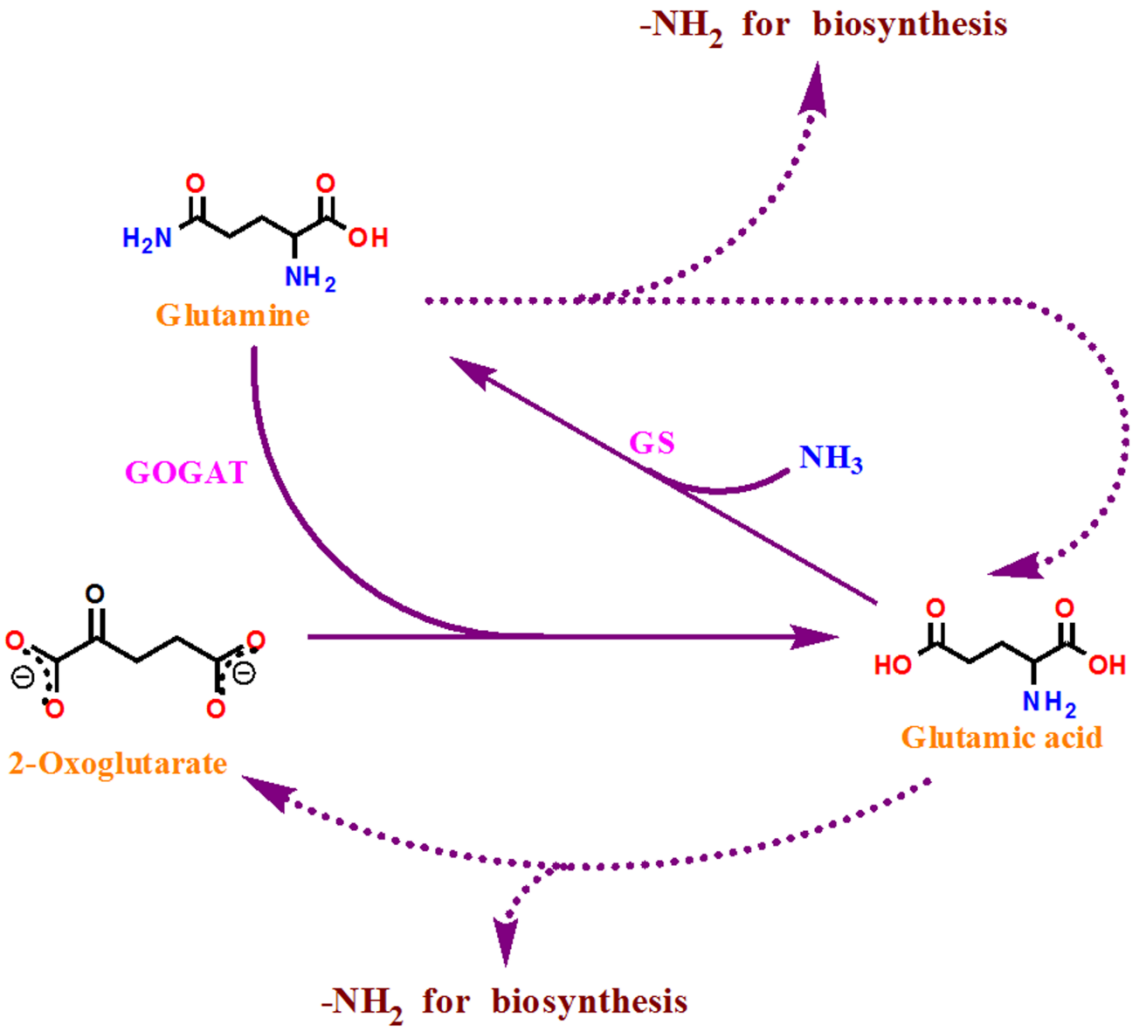

Figure 2-7: Glutamine synthase (GS)-glutamate synthase (GOGAT) pathway of ammonia assimilation. Solid lines represent reactions leading to the formation of glutamate and glutamine from 2-oxoglutarate and ammonia. Dashed lines represent the transfer of amino groups to other biosynthetic pathways. Glutamine synthetase assimilates ammonia by converting glutamate (Glu) to glutamine (Gln). GOGAT then transfers the amido group of Gln to 2-oxoglutarate (2OG), generating two Glu. Glu and Gln transfer nitrogen to other compounds. Modified from Leigh and Dodsworth, 2007.

A. Heterocyst differentiation in cyanobacteria

Cyanobacteria are the only bacteria that generate O_2 during photosynthesis and gave rise to the plant chloroplast by endosymbiosis, which performs the same process. Many multicellular cyanobacteria such as *Anabaena*, *Lyngbya*, *Scytonema*, *Stigonema*, *Tolypothrix*, and *Trichodesmium*, form filaments surrounded by a mucilaginous sheath. Filamentous species produce specialized cells like hormogonia (motile filaments for dispersal), akinetes (resting cells), and heterocysts (nitrogen fixing cells) (table 2-1).

Heterocysts are only produced when reduced nitrogen is limiting. *Anabaena* heterocysts occur along the filament at a regular interval of 10-20 vegetative cells and provide an anaerobic environment for the oxygen sensitive nitrogenase (figure 2-8). Heterocysts differentiate from vegetative cells by activating genes for nitrogen fixation and repressing genes for photosystem II. Hence, heterocysts are dependent on vegetative cells for reduced carbon. Heterocysts are larger than vegetative cells, with a thickened cell wall and less granular cytoplasm.

Heterocysts differentiate one or two generations after nitrogen depletion. α-keto glutarate (2OG) accumulates when cells have an excess of carbon but limiting reduced nitrogen, and may signal nitrogen limitation. 2OG is required for ammonium assimilation via the glutamine synthetase-glutamate synthase (GS-GOGAT) cycle. Another factor regulating heterocyst development is free calcium levels. An increase in Ca^{+2} triggers heterocyst differentiation. CcbP, a Ca^{+2} chelator, sequesters Ca^{+2} during nitrogen sufficiency and under nitrogen limitation releases Ca^{+2} to initiate heterocyst differentiation.

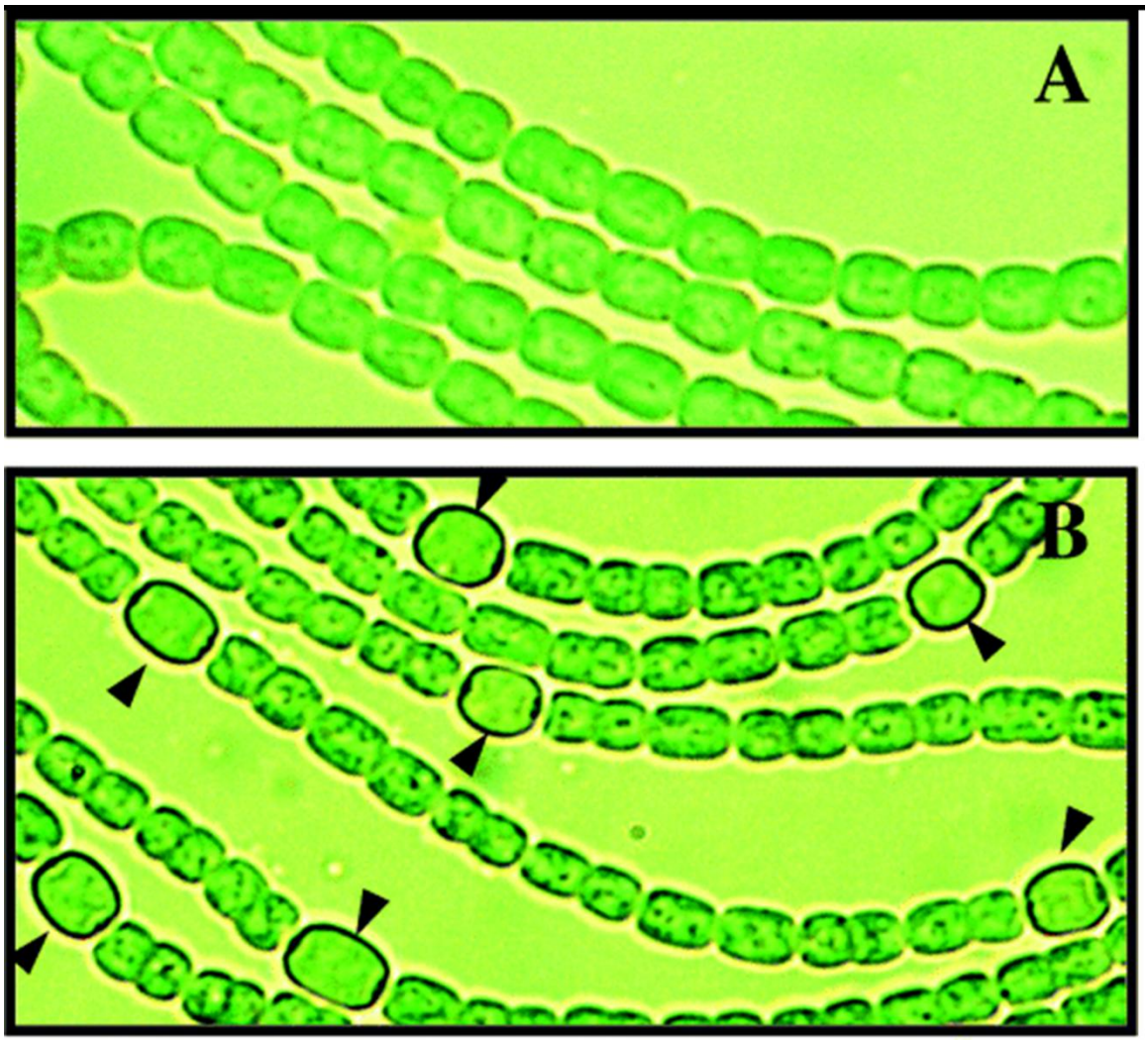

Figure 2-8: Heterocyst development in *Anabaena* PCC 7120. A. *Anabaena* cells grow as filaments of photosynthetic vegetative cells in the presence a reduced nitrogen source. B. When filaments are transferred to a nitrogen-free medium, heterocysts form within 24 h (arrows). From Zhang et al 2006.

The 2OG level is sensed by a global (nitrogen control) transcription factor, NtcA, a member of the cyclic AMP receptor protein family. The expression of the *ntcA* gene is auto-activated. 2OG increases binding of NtcA to the *ntcA* promoter thereby increasing *ntcA* transcription. NtcA is maintained at low levels in the presence of ammonium.

NtcA activates *hetR* whose protein product is necessary for heterocyst development. HetR is a self-degrading protease and a transcription factor. Although a group of cells along the filament begin to differentiate into proheterocysts (a reversible stage in heterocyst differentiation), an inhibitory signal represses heterocyst formation in all cells except one. The inhibitory signal is a small, extracellular polypeptide encoded by *patS*. HetR activates *patS* expression. Cells export an immature, full-length PatS that is hydrolyzed to the mature form during or after export, and the neighboring cells import the mature form. It is thought that the PatS to HetR ratio determines the fate of the proheterocyst.

The proheterocyst is transformed into a mature heterocyst by forming a thick cell wall, which consists of glycolipids and polysaccharides making the cell impermeable to O_2. Heterocyst maturation also involves three genomic rearrangements by site-specific recombinations that remove intervening DNA from (1) the alpha subunit of the dinitrogenase gene *nifD*, (2) a ferredoxin gene, *fdxN* (3) and a hydrogenase subunit gene, *hupL*. This ensures activation of nitrogen fixation machinery only in heterocysts. The mature heterocysts are terminally differentiated and neither grow nor revert back to vegetative cells.

B. Bacteroid Differentiation

Rhizobium spp are soil dwelling α Proteobacteria that can fix nitrogen in a symbiotic relationship with leguminous plants. Nodules develop on the roots of nitrogen-starved legumes such as peas, beans, clover and soy. Within these nodules, rhizobia differentiate into bacteroids that fix atmospheric nitrogen using nitrogenase. The rhizobia-legume symbiosis is a widely studied example of mutualism because legumes are important food crops. In return for reduced nitrogen, plants provide carbon and energy in the form of organic acids to the bacteroids.

Nodulation begins with the exchange of chemical signals (figure 2-9). Plants secrete flavonoids into the rhizosphere that activate rhizobial *nod* genes (essential for nodule formation) via the transcriptional activator NodD. *nod* gene expression leads to the synthesis of the bacterial chemical signal, Nod factor, a lipochitin oligosaccharide. The Nod factor binds to specific plant kinases initiating a signaling pathway leading to root hair curling and trapping of rhizobia.

Rhizobium cells attach to the root surface and enter the root hair through infection threads formed by the plants. The bacteria divide within the infection threads, which slowly invaginate into the root cortex. The bacteria are released into the plant cells via an infection droplet, which is formed at positions in the infection threads where the cell wall is disrupted and rhizobia come into direct contact with the plant cell plasma membrane. Exopolysaccharide (EPS) and lipopolysaccharide (LPS) on the outer surface of the bacteria are involved in suppressing the plant immune response.

Bacteria enter the plant cell lumen by endocytosis forming a symbiosome, which consists of bacteria differentiating into bacteroids enclosed in a plant cell membrane

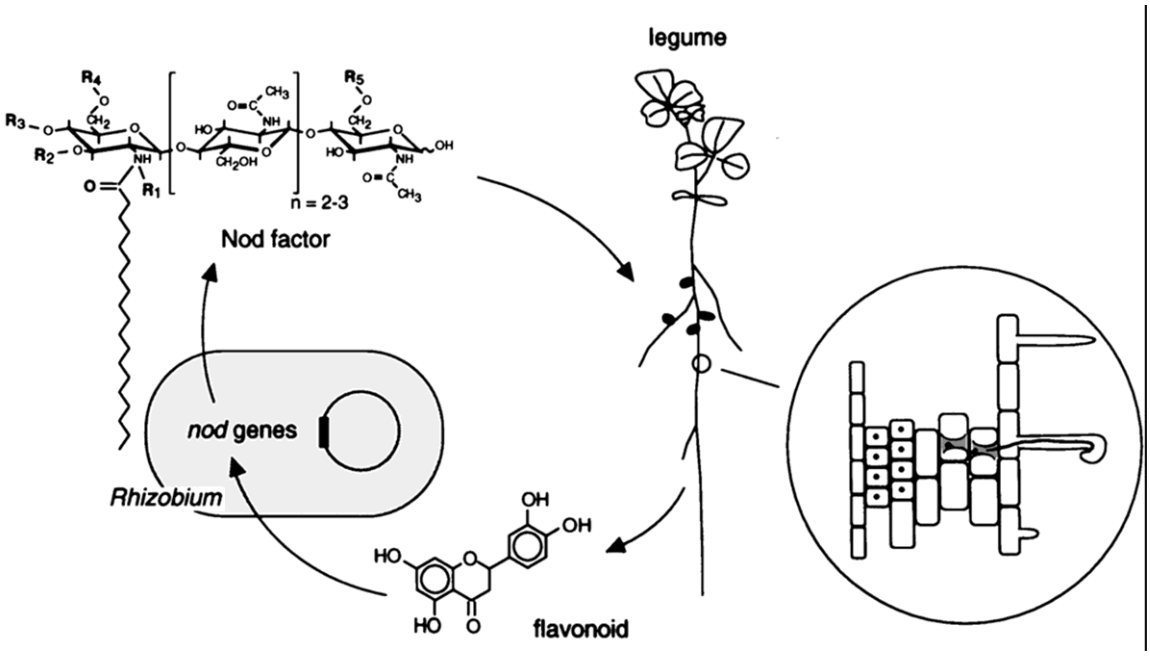

Figure 2-9: Molecular interaction between a legume root and *Rhizobium*. Legume roots secrete flavonoid that induces expression of rhizobial *nod* genes via the transcriptional activator NodD. The *nod* genes encode enzymes that synthesize a lipochitin oligosaccharide known as the Nod factor that is exported and causes several plant growth changes such as root hair deformation, and the formation of nodule primordium. Rhizobia invade the host via the infection thread, which delivers the bacteria within the nodule primordium. The bacteria differentiate into bacteroids, which can reduce atmospheric nitrogen into ammonia. The plant provides carbon in the form of organic acids to support bacteroid metabolism.

known as the peribacteroid membrane of the primordium nodule. The differentiation of the bacteroid leads to production of nitrogenase and cessation of growth. Ammonium generated through nitrogen fixation is transported to the plant cells and incorporated into glutamine by the GS-GOGAT pathway, which is inhibited in bacteroids to prevent the use of the fixed nitrogen by the bacteroid. The *Rhizobium* bacteroids seem to be unable to divide and may be terminally differentiated cells. Bacteroids function for several weeks before disintegrating.

Rhizobium infections are species-specific. Successful infections require compatible partners, which are determined by 1) the species-specific Nod factors and 2) the flavonoid-NodD interaction. The cross-talk between plants and bacteria does not stop at recognition but continues throughout nodule formation and bacteroid differentiation. Addressing questions of cell-to-cell communication during legume-*Rhizobium* interactions will improve our understanding of prokaryotic-eukaryotic relationships and increase the yields of important food crops.

IV. Differentiation leading to cell dispersal

While non-motile spores can be passively dispersed by wind and rain, this section addresses cell types that use active dispersal via motility. Dispersal of a cell is achieved by upregulating genes encoding a motility motor. As observed in *Caulobacter crescentus, Vibrio parahaemolyticus* and *Bdellovibrio bacteriovorus*, this involves generation of flagella. Motility is also observed in some dispersal cells that lack flagella. Baeocytes produced in *Pleurocapsa* cyanobacteria and hormogonia, short motile filaments that are released from filamentous cyanobacteria, move by gliding along solid surfaces without flagella (table 2-1). Although, the mechanism of gliding in hormogonia

is unknown, a protein called oscillin that forms extracellular fibrils may be essential for the process.

Motile cells of *C. crescentus* and *B. bacteriovorus* contain a single polar flagellum while *V. parahaemolyticus* swarm cells produce many lateral flagella. The bacterial flagellum rotates to enable swimming in liquid and swarming on semi-solid surfaces.

A flagellum is divided into three parts: the basal body, the hook and the filament (figure 2-10). The **basal body** is embedded within the inner cell membrane and serves as an anchor. It is composed of a rotating rod that traverses the periplasm, the area between the inner and outer membrane, and three rings. The cytoplasmic membrane supramembrane (MS) ring forms the motor apparatus that rotates the filament to propel the bacterium. The peptidoglycan (P) ring and the outer membrane lipopolysaccharide (L) ring stabilize the structure. The cytosolic C-ring is an extension of the basal body involved in switching the motor between counter-clockwise and clockwise rotation. The **filament** is a rigid helical structure composed of the protein flagellin that lies outside the cell. The **hook** is a flexible curved link between the basal body and the filament.

Flagella can rotate either counter clockwise or clockwise causing smooth swimming or tumbling of the cell. The rotational direction is often influenced by the presence of chemicals. Attractants include glucose and aspartate while repellents include alcohols or heavy metals. This process, known as chemotaxis, helps cells find food or escape from toxins. Chemical gradients are sensed by chemotaxis protein receptors present on the membrane. Information regarding the binding of a chemical to the receptor is relayed by these receptors to other proteins. The chemoattractant itself is not directly relayed but influences the phosphorylation of histidine kinase (CheA) and

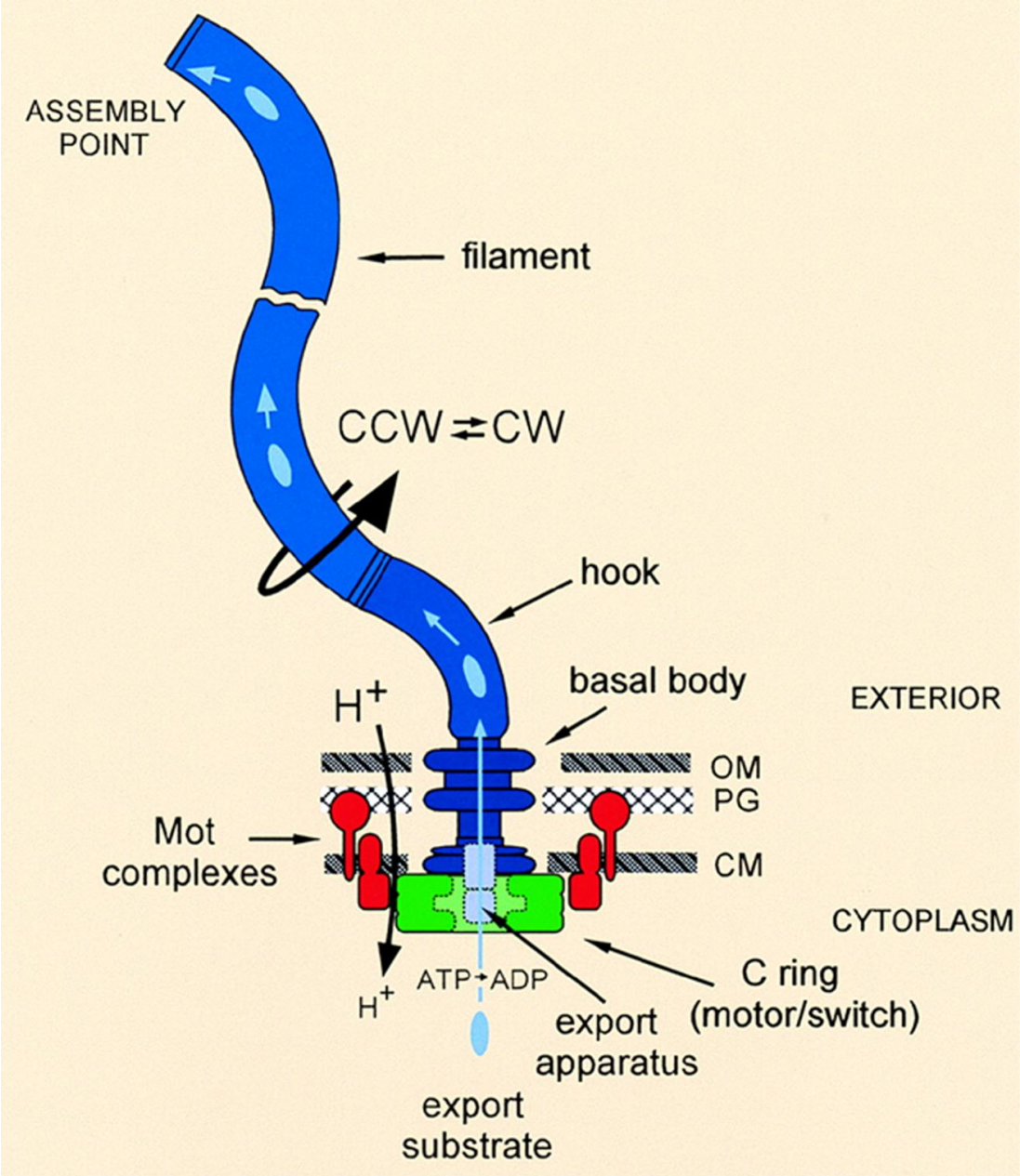

Figure 2-10: Structure of a bacterial flagellum. A flagellum has three basic parts, a rigid helical filament, a flexible hook, and a basal body composed of a rod and several rings. The flagellum is connected to a motor composed of Mot complexes and the C-ring that energizes it to rotate clockwise (CW) or counter-clockwise (CCW). A flagellum is also a type III secretion system that can export its subunits across the cytoplasmic membrane. From Macnab, 1998.

response regulator (CheY) proteins by signal transduction. CheY interacts with the flagellar motor and directs its rotation.

A. Development in *Caulobacter crescentus*

Caulobacter crescentus is common in fresh water bodies. *C. crescentus* exhibits dimorphism as an obligate component of its cell cycle. The life cycle is controlled by three master regulators that are produced in cyclic fashion and regulate the temporal and spatial formation of two cell types. The complete regulatory circuit involves approximately 550 cell-cycle dependent genes.

Two morphologically distinct cell types are involved, a stalked mother cell and a short lived, motile swarmer cell. The life cycle of *C. crescentus* begins with the production of a new **swarmer cell** by a mother cell (figure 2-11). The swarmer cell is equipped with a single polar flagellum, and a chemotaxis system. Chromosome replication is inhibited in the swarmer cells and hence these cells are unable to divide. Swarmer cells swim for a period ensuring dispersal and colonization of new niches. Because *C. crescentus* is found in oligotrophic (low nutrient) environments, this reduces the possibility that the progeny compete with the mother cell for nutrients. Then, the swarmer cell sheds its flagellum and differentiates into a **stalked mother cell** by producing a polar stalk. The stalk is a cylindrical extension of the cell envelope and anchors the cell to the substrate. The stalked cell attaches to a solid surface using a holdfast containing the strongest biological adhesive known. The stalked mother cell never swims again and engages in the reproductive phase of the *Caulobacter* life cycle. Chromosomes are replicated and partitioned into opposite poles of the cell. Before cell division (predivisional cell stage) the stalked cell elongates and a flagellum is formed at

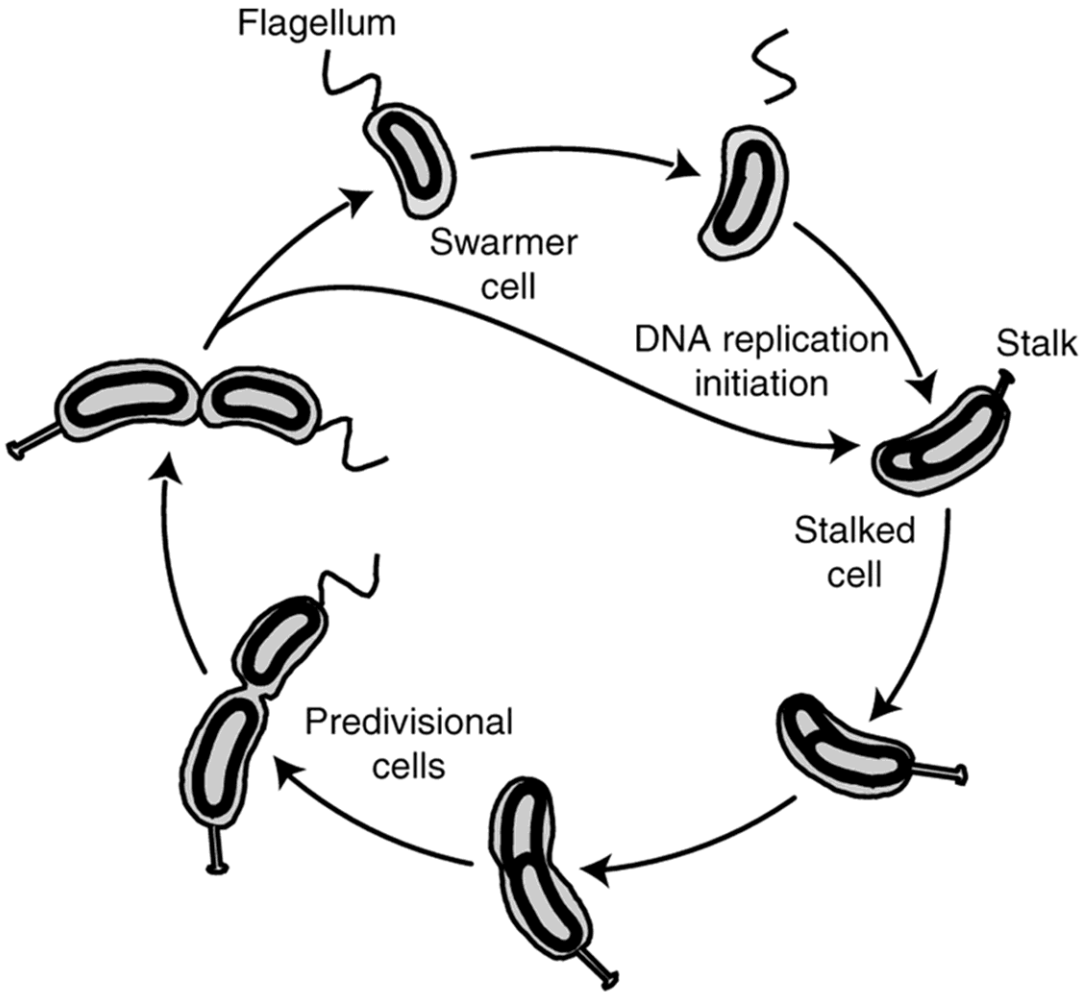

Figure 2-11: Life cycle of *Caulobacter crescentus*. The life cycle begins when a flagellated swarmer cell is produced from a stalked mother cell. Swarmer cells are unable to replicate. They swim for some time and then differentiate into stalked cells by losing their flagellum and growing a stalk. The stalked cells initiate growth and begin to elongate. A flagellum is produced at the opposite cell pole in the predivisional cell. Cell division gives rise to a swarmer cell and a stalked cell. The stalked mother cell continues to produce swarmer cells. From Goley et al, 2007.

the pole opposite the stalk. A diffusion barrier is formed to divide the predivisional cell into separate swarmer and stalked cell compartments. Subsequent cell division leads to stalked and swarmer cell progeny. The mother cell continues to produce a swarmer cell with every cell division.

The *C. crescentus* life cycle can be divided into three phases based on the DNA replication status of the cell: a pre-initiation gap phase (G1), a DNA synthesis phase (S) and a post-synthesis (division) phase (figure 2-12). The G1 phase encompasses the life of the swarmer cell. The stalked cell initiates the S phase. Three master regulator proteins CtrA, GcrA, and DnaA function at different times during the cell cycle. CtrA is a response regulator that regulates chromosome replication, synthesis of the flagellum, and chemotaxis. Phosphorylated CtrA (CtrA~P) interacts with DNA in a region called the CtrA box embedded in the origin of replication (*oriC*). In swarmer cells, CtrA binding to the CtrA boxes inhibits initiation of chromosome replication. CtrA is degraded during the swarmer-to-stalked cell transition by ClpXP, an ATP-dependent protease, releasing the major block to chromosome replication. Localization factor RcdA in complex with CtrA interacts with ClpXP at the stalked cell pole, providing a cell localization mechanism to control the degradation of CtrA.

During swarmer-to-stalked cell differentiation, degradation of CtrA is accompanied by DnaA synthesis. DnaA is the DNA replication initiator protein and binds to the DnaA boxes in *oriC*. Free DnaA is present only during the start of each cell cycle. DnaA also activates GcrA expression in the stalked cell to activate genes required for DNA replication. GcrA is not present during cell division and is repressed by CtrA in

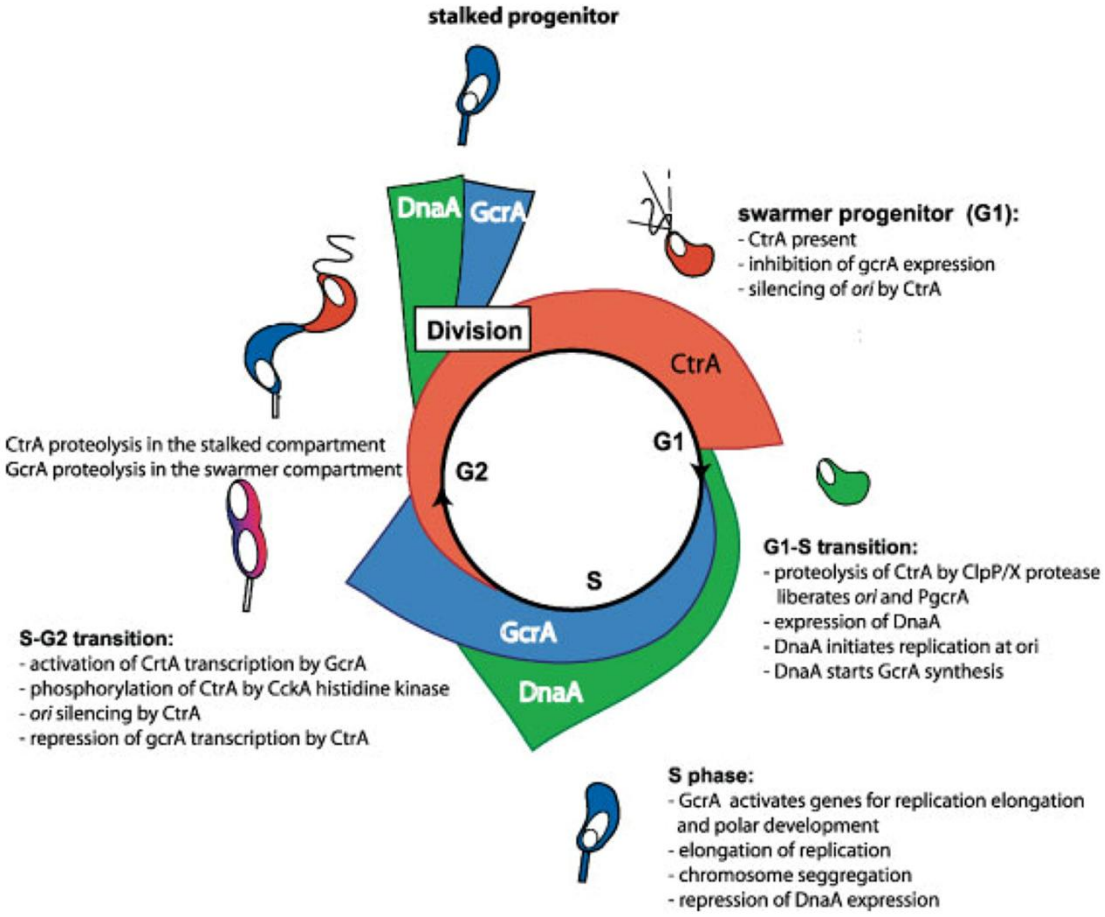

Figure 2-12: Cyclic accumulation of the global regulators CtrA, DnaA and GcrA. In swarmer cells, CtrA inhibits DNA replication and *gcrA* expression. During swarmer-to-stalked cell transition, CtrA is degraded activating DnaA, DNA replication and GcrA expression. GcrA accumulates in the stalked cell leading to DNA segregation and cell division. GcrA also activates CtrA expression, which represses GcrA expression in the late stalked cell (S–G2 transition). In the predivisional cells, DnaA is degraded while GcrA is inactivated in the swarmer compartment and CtrA is degraded in the stalked compartment. After cell division, DnaA and GcrA are synthesized in the stalked mother cell but are repressed in the swarmer cell. From Holtzendroff et al, 2006.

swarmer cells. DnaA also acts as a transcriptional regulator and brings about expression of cell division initiator FtsZ, which localizes at the site of cell division.

An essential feature of the *Caulobacter* life cycle is cell polarity, which governs correct localization of the flagellum and stalk. Cell polarity is achieved by the spatial localization of regulators of polarity, the DivJ and PleC histidine kinases and the DivK response regulator. In predivisional cells DivK oscillates between the two cell poles. DivJ controls stalk formation and cell division, and localizes to the stalked pole where it phosphorylates DivK. DivK~P indirectly inactivates CtrA. PleC regulates flagellum assembly and cell motility by localizing to the swarmer cell pole. PleC brings about dephosphorylation of DivK~P maintaining the active state of CtrA. The new pole of the cell is marked at each cell division with TipN, which is essential for the biogenesis of cell organelles. TipN is located at the division plane in the late predivisional cells and is inherited at the new pole by both progeny. TipN relocates to the new division site later in the cell cycle marking the new pole at the next division.

The various stages of *Caulobacter* development are controlled by the temporal production and spatial localization of cell cycle regulators. These regulators in turn control the critical elements of the cell cycle, replication initiation, cell division and synthesis of cell type specific organelles. Spatial and temporal regulation ensures the occurrence of such processes once per cell cycle and also conserves energy, which is essential for survival in oligotrophic environments.

B. *Bdellovibrio*

Bdellovibrio bacteriovorus is a δ Proteobacteria that preys on other bacteria. *B. bacteriovorus* cells alternate between a motile infectious attack phase and a nonmotile reproductive phase. These bacteria are tiny intracellular parasites of Proteobacteria and invade the host cell through a hole in the outer membrane. They reside in the periplasm (the region between the inner and outer membrane) of the host cell and feed on biopolymers by utilizing a large repertoire of hydrolytic enzymes. Greater than 200 genes coding for lytic enzymes have been found in the genome. Within three hours of invasion the host cell is full of progeny *Bdellovibrio*, which are released by lysing the host cell.

The life cycle of *B. bacteriovorus* can be divided into eight morphological stages (I to VIII) (figure 2-13).

Stage I is the attack phase. *B. bacteriovorus* cells are motile using a single polar flagellum. Whether they actually seek prey cells or stumble upon them by chance remains unknown. Chemotaxis toward oxygen and compounds like amino acids have been suggested as mechanisms to hunt for prey.

In **stage II,** attachment to a prey cell is reversible for a short time but becomes irreversible after the initial recognition period when *B. bacteriovorus* becomes committed to invasion and anchors tightly to the host cell.

During **stage III,** *B. bacteriovorus* generates a small opening in the prey cell outer membrane and peptidoglycan layer. This opening is resealed once *Bdellovibrio* is inside the host cell. Invasion is achieved by a mixture of hydrolytic enzymes that is applied in a locally targeted manner preventing excessive damage to the prey cell. The *Bdellovibrio*

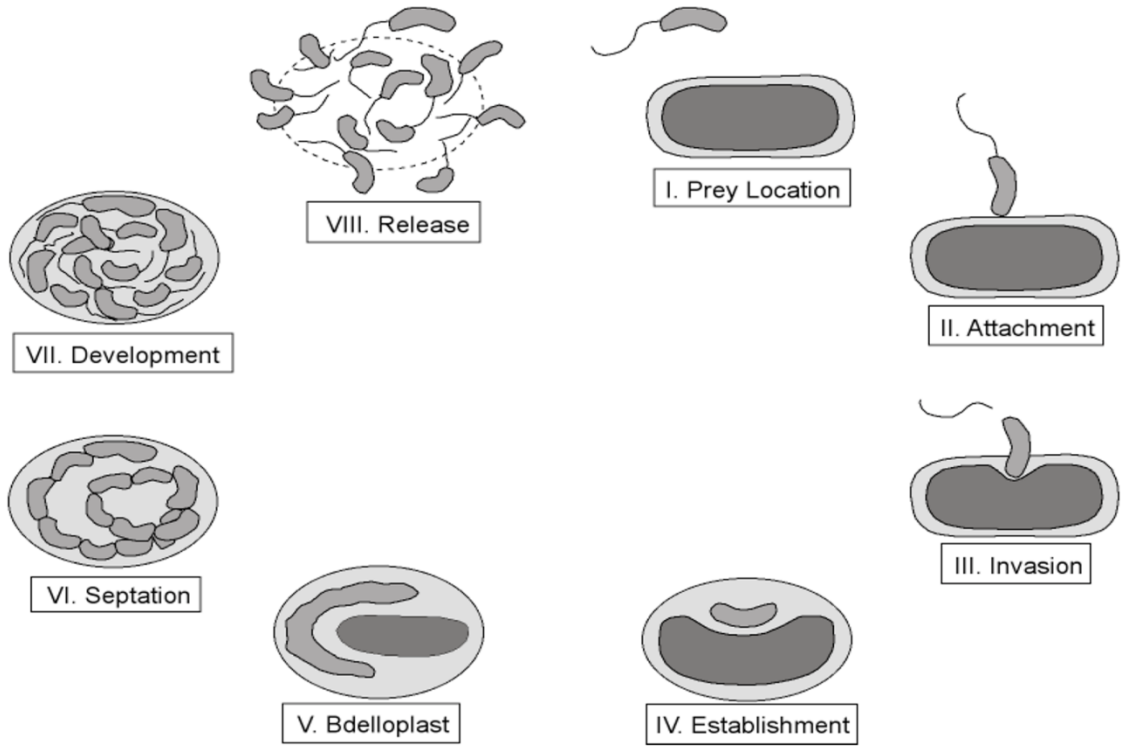

Figure 2-13: Life cycle of *B. bacteriovorus*. An attack phase cell is a motile, flagellated cell that moves toward the prey possibly by chemotaxis. *Bdellovibrio* attaches to a prey cell and enters the host periplasm by hydrolyzing the cell wall. Several host modifications occur post infection and the bdelloplast is formed. The *Bdellovibrio* feeds on degradation products of the host cell and undergoes chromosome duplication without cell division. Cell division follows when the maximum number of chromosomes is achieved. The attack phase cells mature by developing flagella. The host cell bursts to release mature attack phase cells. From Rendulic et al, 2004.

genome contains four clusters of type IV pilus genes. It has been proposed that *B. bacteriovorus* uses type IV pili to pull itself through a penetration pore formed in the outer membrane and crawl to the inner side of the prey peptidoglycan. Once inside the prey periplasm, *B. bacteriovorus* ejects its flagellum.

Stage IV is highlighted by cell growth and DNA replication without cell division to form a multinucleate filament.

In **stage V**, *B. bacteriovorus* transforms the shape of the prey cell to a spherical, osmotically stable bdelloplast where the *B. bacteriovorus* transports nutrients from the host cytosol. *B. bacteriovorus* can synthesize only 11 amino acids and is dependent on host cell amino acids for protein synthesis.

Stage VI is characterized by the septation of the filamentous *B. bacteriovorus* cell to generate several progeny cells of uniform size.

Stage VII is the maturation phase where the progeny cells develop flagella.

Stage VIII is marked by the disintegration of the outer membrane and peptidoglycan layer of the bdelloplast to release the attack phase progeny.

Regulation of the transition from one cell type to another has not been extensively investigated. *Bdellovibrio* are predators of several plant and human pathogenic bacteria but are not pathogenic to humans. Type III secretion systems, which are virulence factors found in many pathogenic bacteria, have not been found in the *Bdellovibrio* genome suggesting that *Bdellovibrio* may be developed as novel antibacterial agents without fear of causing disease.

C. Swarming in *Vibrio parahaemolyticus*

Swarming is a multicellular behavior of many Proteobacteria that occurs on solid surfaces. The differentiation from swimming cells to swarming cells involves sensing extracellular signals, differential flagellar gene expression, and regulation of cell division. Swarming aides invasion and expression of virulence genes in the host. Swarming has been studied extensively in *Vibrio parahaemolyticus*, a marine γ Proteobacteria and a causative agent of gastroenteritis. *V. parahaemolyticus* exists as a swimmer (vegetative) cell in liquid environments or as a swarmer cell on solid surfaces, allowing it to colonize a variety of niches (figure 2-14). The two cell types are significantly different from one another.

Swimmer cells have a single polar flagellum adapted for swimming in a liquid medium. Contact with a solid surface leads to differentiation into swarmer cells, which are 20 to 30 times larger than swimmer cells and possess a large number of lateral flagella. Cell division in swarmer cells is inhibited leading to polynucleated, elongated cells. Swarming occurs for several hours and then ceases leading to rapid division of multinucleate swarmer cells to swimmer cells, a process known as consolidation. Concentric rings or terraces are formed on agar plates due to repeated cycles of active swarming and consolidation.

Swarmer cell differentiation is induced by growth on solid surfaces or viscous environments, which is sensed by the polar flagellum of swimmer cells. Resistance to polar flagellum rotation signals differentiation into swarm cells. Thus, the polar flagellum acts as a mechanosensor by measuring the viscosity of the medium. A second trigger that controls swarmer cell differentiation is iron limitation. The transition from

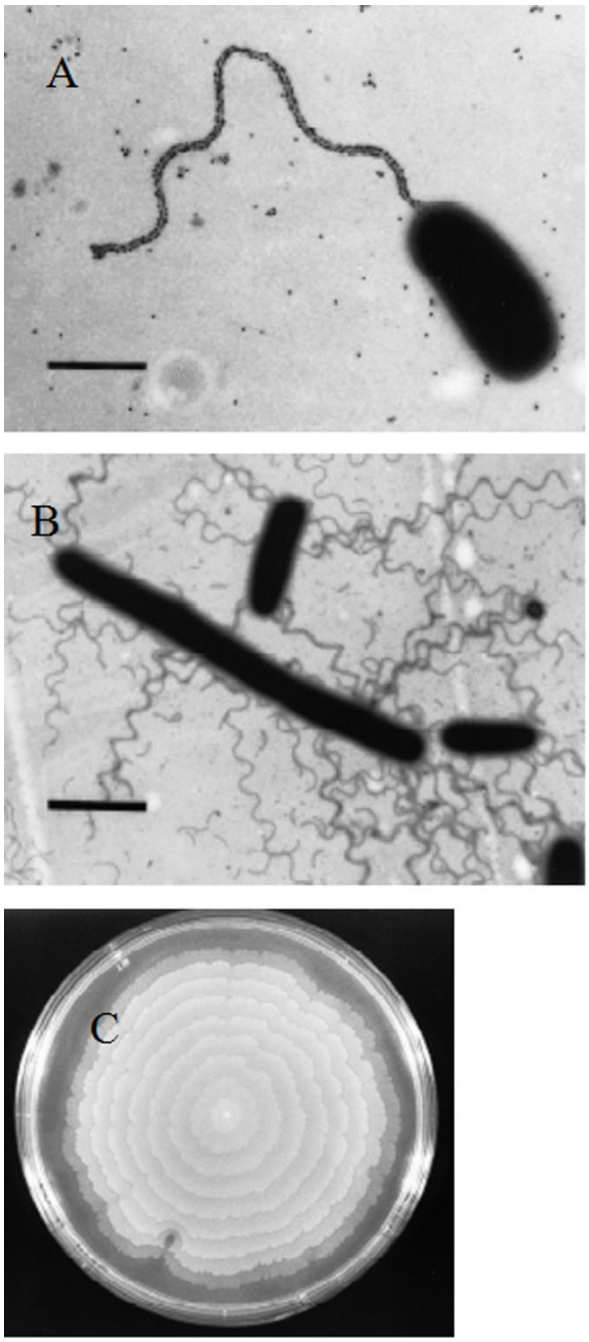

Figure 2-14: Swarming in *Vibrio parahaemolyticus*: (A) Electron micrograph of a swimmer cell with a single polar flagellum. Bar is 1 µm (B) Swarmer cells with numerous lateral flagella. Bar is 3 µm. (C) Concentric growth patterns often seen due to periodic swarmer cell differentiation and consolidation on a solid medium. From McCarter, 1999.

swimmer cell to swarmer cell blocks cell division but not cell growth generating elongated cells. An ATP dependent protease, LonS is essential for swarmer cell differentiation. It is predicted that LonS activates the transcriptional activator of the lateral flagellar gene system and also serves as an inhibitor of cell division.

Swarmer cells are characterized by the presence of numerous lateral flagella. The lateral flagella are different from the polar flagellum. The polar flagellum contains four flagellin subunits, FlaA, B, C and D while the lateral flagella contain a single flagellin protein LafA. The polar flagellum is protected by a membranous sheath, which is absent in the lateral flagella. Although the energy used for both types of motility is the electrochemical gradient, the coupling ions are different. The polar flagellum utilizes Na^+ ions while the lateral flagella use H^+. Both flagellar systems are thought to share a common chemotaxis system.

V. Conclusion

Development of multiple cell types is beneficial to prokaryotic cells because it enables them to occupy different niches and helps sustain them in unfavorable environmental conditions. Differentiation and multicellularity help achieve a division of labor. The advantage of maximizing resources is probably the driving force that led to evolution of different types of developmental programs. Although bacterial differentiation is controlled by spatial and temporal regulation of sensory pathways, an important question that has eluded developmental biologists is how bacteria sense and integrate environmental cues into their developmental program.

Bibliography

Abdelrahman Y. M. and Belland R. J. (2005) The chlamydial developmental cycle. *FEMS Microbiol Rev* **29**(5), 949-59.

Claessen D., DE Jong W., Dijkhuizen L. and Wosten H. A. (2006) Regulation of *Streptomyces* development: reach for the sky! *Trends Microbiol* **14**(7), 313-9.

Collier J. and Shapiro L. (2007) Spatial complexity and control of a bacterial cell cycle. *Curr Opin Biotechnol* **18**(4), 333-40.

Curtis P. D., Taylor R. G., Welch R. D. and Shimkets L. J. (2007) Spatial organization of *Myxococcus xanthus* during fruiting body formation. *J Bacteriol* **189**(24), 9126-30.

Goley E. D., Iniesta A. A. and Shapiro L. (2007) Cell cycle regulation in *Caulobacter*: location, location, location. *J Cell Sci* **120**(Pt 20), 3501-7.

Henriques A. O. and Moran C. P., JR. (2007) Structure, assembly, and function of the spore surface layers. *Annu Rev Microbiol* **61**, 555-88.

Hilbert D. W. and Piggot P. J. (2004) Compartmentalization of gene expression during *Bacillus subtilis* spore formation. *Microbiol Mol Biol Rev* **68**(2), 234-62.

Holtzendorff J., Reinhardt J. and Viollier P. H. (2006) Cell cycle control by oscillating regulatory proteins in *Caulobacter crescentus*. *Bioessays* **28**(4), 355-61.

Hopwood D. A. (2006) Soil to genomics: the *Streptomyces* chromosome. *Annu Rev Genet* **40**, 1-23.

Kaiser D. (2001) Building a multicellular organism. *Annu Rev Genet* **35**, 103-23.

Kim J. and Rees D. C. (1994) Nitrogenase and biological nitrogen fixation. *Biochemistry* **33**(2), 389-97.

Kneip C., Lockhart P., Voss C. and Maier U. G. (2007) Nitrogen fixation in eukaryotes--new models for symbiosis. *BMC Evol Biol* **7**, 55.

Kuner J. M. and Kaiser D. (1982) Fruiting body morphogenesis in submerged cultures of *Myxococcus xanthus*. *J Bacteriol* **151**(1), 458-61.

Lambert C., Morehouse K. A., Chang C. Y. and Sockett R. E. (2006) *Bdellovibrio*: growth and development during the predatory cycle. *Curr Opin Microbiol* **9**(6), 639-44.

Leigh J. A. and Dodsworth J. A. (2007) Nitrogen regulation in bacteria and archaea. *Annu Rev Microbiol* **61**, 349-77.

Macnab R. M. (1999) The bacterial flagellum: reversible rotary propellor and type III export apparatus. *J Bacteriol* **181**(23), 7149-53.

McCarter L. (1999) The multiple identities of *Vibrio parahaemolyticus*. *J Mol Microbiol Biotechnol* **1**(1), 51-7.

McCarter L. and Silverman M. (1990) Surface-induced swarmer cell differentiation of *Vibrio parahaemolyticus*. *Mol Microbiol* **4**(7), 1057-62.

Meeks J. C., Campbell E. L., Summers M. L. and Wong F. C. (2002) Cellular differentiation in the cyanobacterium *Nostoc punctiforme*. *Arch Microbiol* **178**(6), 395-403.

Peters J. W. and Szilagyi R. K. (2006) Exploring new frontiers of nitrogenase structure and mechanism. *Curr Opin Chem Biol* **10**(2), 101-8.

Prell J. and Poole P. (2006) Metabolic changes of rhizobia in legume nodules. *Trends Microbiol* **14**(4), 161-8.

Rendulic S., Jagtap P., Rosinus A., Eppinger M., Baar C., Lanz C., Keller H., Lambert C., Evans K. J., Goesmann A., Meyer F., Sockett R. E. and Schuster S. C. (2004) A

predator unmasked: life cycle of *Bdellovibrio bacteriovorus* from a genomic perspective. *Science* **303**(5658), 689-92.

Schultze M. and Kondorosi A. (1998) Regulation of symbiotic root nodule development. *Annu Rev Genet* **32**, 33-57.

Setlow P. (2006) Spores of *Bacillus subtilis*: their resistance to and killing by radiation, heat and chemicals. *J Appl Microbiol* **101**(3), 514-25.

Stragier P. and Losick R. (1996) Molecular genetics of sporulation in *Bacillus subtilis*. *Annu Rev Genet* **30**, 297-41.

Titus J. A., Reed W. M., Pfister R. M. and Dugan P. R. (1982) Exospore formation in *Methylosinus trichosporium*. *J Bacteriol* **149**(1), 354-60.

Vandahl B. B., Birkelund S. and Christiansen G. (2004) Genome and proteome analysis of *Chlamydia*. *Proteomics* **4**(10), 2831-42.

Zhang C. C., Laurent S., Sakr S., Peng L. and Bedu S. (2006) Heterocyst differentiation and pattern formation in cyanobacteria: a chorus of signals. *Mol Microbiol* **59**(2), 367-75.

CHAPTER 3

BIOINFORMATIC AND PROTEOMIC ANALYSIS OF *MYXOCOCCUS XANTHUS* OUTER MEMBRANE β-BARREL AND LIPOPROTEINS

Bhat, S., Zhu, X., Patel, R., Orlando, R., and Shimkets, LJ. To be submitted to Mol Microbiol.

Abstract

Typical of δ-Proteobacteria, *Myxococcus xanthus* DK1622 contains an outer membrane (OM) and an inner membrane (IM) separated by a periplasm containing a peptidoglycan layer. Integral membrane β-barrel proteins are found exclusively in the OM where they form pores allowing the passage of nutrients, waste products and signals. Several prediction programs were evaluated for their ability to discriminate β-barrel proteins using known *M. xanthus* OM, IM and periplasmic proteins. TMBETA-SVM and TMBETADISC-RBF identified β-barrel proteins most accurately. These programs predicted 228 β-barrel proteins from among 7331 protein coding regions, representing 3.1% of total genes. Sucrose density gradients were used to separate IM and OM vesicles using vegetative cells, and LC-MS/MS of OM proteins identified 54 β-barrel proteins. One OM β-barrel protein, Oar, is required for intercellular communication of the C-signal. An *oar* mutant produces the C-signaling protein CsgA but is unable to stimulate *csgA* mutants to develop or to be stimulated for development by WT cells. Another class of membrane proteins are lipoproteins, which are anchored in the membrane via a lipid moiety at the N-terminus. Lipoproteins are distributed between the IM, OM and ECM according to an N-terminal sorting sequence that varies among species. 44 OM proteins identified by LC-MS/MS were predicted lipoproteins. Lipoprotein sorting was studied to identify sorting signals that direct lipoproteins to the correct subcellular location. Sequence analysis of predicted extracellular matrix (ECM) and IM lipoproteins revealed conservation of alanine at the +7 position of mature ECM lipoproteins, and lysine at the +2 position of IM lipoproteins. Site directed mutagenesis and immuno transmission electron microscopy showed that alanine at the +7 position is essential for sorting of the

lipoprotein FibA into the ECM. FibA appears at normal levels in the ECM even when a +2 lysine is added to the signal sequence. These results suggest that ECM proteins are not subject to the Lol system IM retention rule. This approach provides a way to target lipoproteins to specific IM, OM and ECM locations.

Introduction

The life cycle of the δ-proteobacterium, *Myxococcus xanthus* involves a vegetative stage, in which cells feed on bacteria and organic detritus, and a developmental stage in which thousands of cells aggregate to form a multicellular fruiting body containing spores. Fruiting body development involves intercellular communication with at least six extracellular signals (Shimkets, 1999). However, the receptors and sensory pathways of these signaling pathways are largely unknown. Identification of outer membrane (OM) proteins in *M. xanthus* may reveal components of these signaling pathways that are used to export or import signals.

The OM acts as a selective barrier that allows the passage of nutrients, water and chemical signals through pores formed by porin proteins. In porins, antiparallel β-strands are arranged to form a cylindrical β-barrel structure lined with hydrophilic residues that create a water-filled channel (Wimley, 2003). Some porins allow passive diffusion of small solutes with molecular weights up to 600 Da (Nikaido, 2003). Active diffusion of specific nutrients through porins is carried out by TonB systems, which utilize energy provided by the inner membrane (IM) to mediate solute passage through the OM (Postle, 2007). Some porins allow passage of specific substrates, such as fatty acids in the case of FadL (van den Berg, 2005). Porins are synthesized as precursors with an N-terminal signal sequence that aids transport across the IM via the general secretory (Sec) pathway (Bos *et al.*, 2007a). The signal sequences are hydrolyzed by signal peptidases present in the IM. Chaperones in the periplasm facilitate protein folding and insertion into the OM using the Omp85 machinery (Voulhoux *et al.*, 2003).

Databases such as Pfam can help identify OM proteins, but only if the protein contains a domain with appreciable identity to a domain of known function (Finn *et al.*, 2006). Unfortunately, most bacterial genomes contain hypothetical proteins that are not represented in the Pfam database, for example, the *M. xanthus* genome encodes 40% hypothetical proteins (Kahnt *et al.*, 2010). Thus, bioinformatic programs that can predict the OM protein β-barrel structure would be useful since this structure is unique to OM proteins (Punta *et al.*, 2007).

The IM and OM contain lipoproteins that are anchored by a lipid-modified N-terminal cysteine residue. Lipoproteins are transported as precursors via the Sec pathway to the IM where they are processed at the conserved N-terminal lipobox of the prolipoprotein. The lipobox consists of four amino acids (L_{-3}-[A/S/T]$_{-2}$-[G/A]$_{-1}$-C_{+1}) around the signal peptide cleavage site with the +1 cysteine serving as the site of covalent modification (Hutchings *et al.*, 2009). Lipoprotein maturation involves attachment of a diacylglycerol group to the +1 cysteine sulfhydryl group to form a thioester linkage, cleavage of the signal peptide, and acylation of the +1 α-amino group. The lipid moieties anchor the N-terminus of the proteins in lipid bilayers.

In *Escherichia coli*, localization of lipoproteins to the IM requires aspartate at the +2 position of the mature lipoprotein (Seydel *et al.*, 1999). Lipoproteins lacking this sorting signal are transported to the OM via the Lol pathway, which is an ABC transport system located in the IM (Masuda *et al.*, 2002). The signal sequences directing Lol avoidance differ among bacteria. In *Pseudomonas aeruginosa*, lysine and serine at positions +3 and +4 lead to IM retention of lipoproteins (Tanaka *et al.*, 2007). Some bacteria secrete lipoproteins outside the cells, and may possess novel mechanisms to sort

lipoproteins to the external environment (Tokuda & Matsuyama, 2004). *M. xanthus* secretes at least 11 lipoproteins that are associated with the extracellular matrix (ECM) whose mechanism of targeting is unknown (Curtis *et al.*, 2007).

In this paper we identified OM proteins using bioinformatic and proteomic tools. Two prediction programs TMBETA-SVM and TMBETADISC-RBF identified 228 β-barrel OM proteins in the genome, of which 54 were detected in DK1622 vegetative cells by LC-MS/MS. We show that one of these proteins, Oar, is essential for C-signal transmission during fruiting body development. Lipoprotein sorting into IM, OM, and extracellular compartments was also examined. Alanine at the +7 position mediates ECM localization even when a signal for IM localization is also present suggesting that there are at least two lipoprotein secretion pathways.

Results

The first goal of this study was to identify *M. xanthus* OM β-barrel proteins and lipoproteins using bioinformatic and proteomic approaches. We generated a database of putative OM proteins using bioinformatic programs against which proteomic results were compared. The second goal of this study was to identify the trafficking signals for IM, OM and ECM lipoproteins. Site directed mutagenesis was then used to identify the ECM trafficking signal for the major ECM lipoprotein FibA.

β-barrel prediction in *M. xanthus* proteome. Integral OM proteins are synthesized with an N-terminal signal sequence. The signal sequence enables transport of proteins across the IM by the Sec system, and can be predicted using the program Signal P. The *M. xanthus* proteome was examined for candidates with a signal peptide score (S prob) of >0.1, which generated 2493/7331 candidates (Figure 3-1). In the next step, all predicted

signal peptide containing proteins were classified as lipoproteins or non-lipoproteins using the Lipo P program. 425 out of the potential 2493 signal peptide containing proteins were predicted to be lipoproteins (Figure 3-1). The non-lipoproteins were further segregated into IM and non-IM proteins. Integral IM proteins have alpha helices that are rich in hydrophobic amino acids. Proteins with at least two putative transmembrane helices using the TMHMM program were classified as IM proteins (Krogh et al., 2001). 560/2068 proteins with putative signal peptides in *M. xanthus* were identified as IM proteins.

The remaining 1508 signal peptide containing proteins, comprising periplasmic, secreted, and OM proteins, were subjected to β-barrel prediction programs to identify integral OM proteins. Six prediction programs were evaluated, TMBETA-NET, PRED-TMββ, TMBETA-SVM, TMBETADISC-RBF, BOMP, and TMB-HUNT using 40 *M. xanthus* protein sequences with predicted β-barrel domains obtained from the Pfam database (Table 3-1). These proteins are homologous to well-studied OM proteins from other organisms as demonstrated by BLASTP. The 40 proteins span 10 protein families including TonB dependent receptors, Omp85 and OmpH, secretins, efflux proteins, and organic solvent tolerance proteins (Koski *et al.*, 1990, Reizer *et al.*, 1993, Johnson & Church, 1999, Bos *et al.*, 2007b). Except for BOMP **(**10%**)** and TMB-HUNT (63%) all prediction programs identified >77% of the 40 OM proteins (Table 3-1). PRED-TMββ identified the most β-barrel proteins (38/40) (95%). TMBETADISC-RBF, TMBETA-SVM and TMBETA-NET identified 34/40 (85%), 33/40 (83%) and 31/40 (78%) β-barrel proteins respectively.

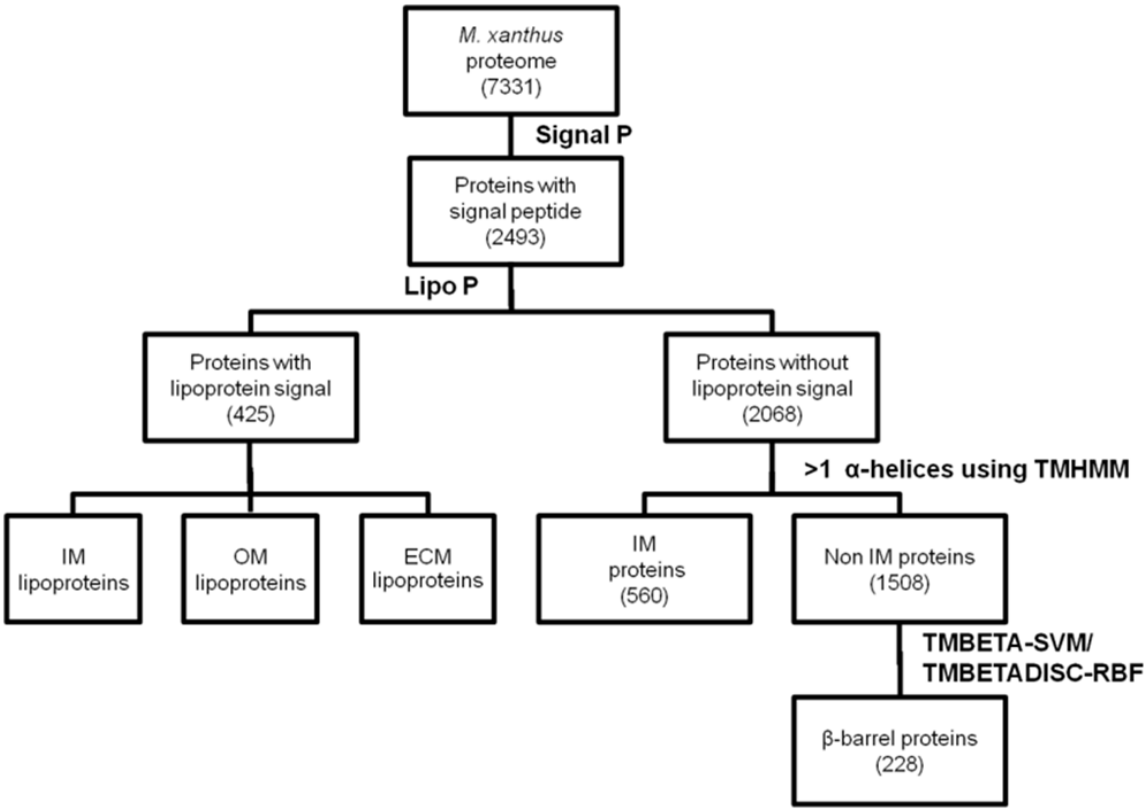

Figure 3-1. Scheme to identify OM proteins utilizing bioinformatic programs. The Signal P program identified 2493 signal peptide containing proteins among the putative 7331 member *M. xanthus* proteome. Of these 425 lipoproteins were identified using Lipo P. Of the 2068 proteins without a lipoprotein signal 560 were integral IM proteins identified using TMHMM. The non-IM proteins include periplasmic proteins, secreted proteins and OM proteins. Finally, integral OM proteins containing a β-barrel domain were identified using TMBETA-SVM plus TMBETADISC-RBF.

Table 3-1. *M. xanthus* β-barrel domain proteins obtained from the Pfam database.

MXAN	Function	1[a]	2[b]	3[c]	4[d]	5[e]	6[f]
MXAN0272	TonB dependent receptor	+	+	+	+	+	+
MXAN0518	TonB dependent receptor	+	+	+	-	-	-
MXAN0562	Phosphate selective porin (PhoE)	+	+	+	+	-	+
MXAN0990	Outer membrane efflux protein	+	-	+	-	-	-
MXAN1316	TonB dependent receptor	+	+	+	+	+	-
MXAN1450	TonB dependent receptor (Oar)	+	+	+	+	+	-
MXAN2514	Secretin (GspD)	+	+	+	+	-	-
MXAN2708	Organic solvent tolerance protein (OstA)	+	+	+	+	+	-
MXAN3106	Secretin (GspE)	+	+	+	+	+	-
MXAN3431	Outer membrane efflux protein	+	+	+	-	-	-
MXAN3883	Fimbrial usher protein (FUP)	+	+	+	+	+	-

MXAN3905	Outer membrane efflux protein	+	+	+	+	+	-
MXAN4176	Outer membrane efflux protein	+	+	+	+	+	-
MXAN4198	Outer membrane efflux protein	+	+	+	+	+	-
MXAN4559	TonB dependent receptor	+	+	+	+	+	-
MXAN4727	Structural protein (OmpH)	+	+	-	-	+	-
MXAN4728	Omp85 protein	+	+	+	-	-	-
MXAN4746	TonB dependent receptor	+	+	+	+	+	-
MXAN4772	OmpA protein	-	+	-	-	+	-
MXAN5023	TonB dependent receptor	+	+	+	+	-	-
MXAN5030	Outer membrane efflux transporter	+	+	+	+	+	-
MXAN5042	OmpA protein	+	-	-	-	-	-
MXAN5069	Aquaporin Z (ApqZ)	+	-	-	-	+	-
MXAN5772	Secretin (PilQ)	+	+	+	+	+	-
MXAN5956	Major intrinsic protein	+	-	+	-	-	-

MXAN6044	TonB dependent receptor	+	+	+	+	+	-
MXAN6176	Outer membrane efflux protein	+	+	+	+	+	-
MXAN6246	OmpA	+	-	-	-	-	-
MXAN6487	Outer membrane efflux protein	+	+	+	+	+	-
MXAN6547	TonB dependent receptor	+	+	+	+	-	-
MXAN6579	TonB dependent receptor	+	+	+	+	+	-
MXAN6716	TonB dependent receptor	+	+	+	+	-	-
MXAN6845	TonB dependent receptor	+	+	+	+	+	-
MXAN6911	TonB dependent receptor	+	+	+	+	+	+
MXAN7037	OmpA	+	+	+	+	+	-
MXAN7040	Fatty acid transport (FadL)	+	+	+	+	+	+
MXAN7238	Outer membrane efflux protein	+	+	-	+	+	-
MXAN7331	TonB dependent receptor	+	+	+	+	-	-
MXAN7397	OmpA	-	-	-	-	+	-
MXAN7436	Outer membrane efflux protein	+	+	+	+	-	-

Programs that correctly predicted a β-barrel protein is indicated by a positive sign (+) while failing to do so is indicated by a negative sign (–).

[a] PRED-TMββ

[b] TMBETADISC-RBF

[c] TMBETA-SVM

[d] TMBETA-NET

[e] TMB-HUNT

[f] BOMP

TMBETA-NET, TMBETA-SVM, TMBETADISC-RBF and PRED-TMββ were tested on 21 known *M. xanthus* IM, periplasmic, and ECM proteins to eliminate programs that generate false positives. (Table 3-2). The IM and periplasmic proteins were obtained from the Pfam database while the ECM proteins were previously identified by Curtis et al for proteomic studies (Curtis et al., 2007). PRED-TMββ prediction showed 11/20 (55%) false positives, TMBETA-NET and TMBETADISC-RBF generated 2/20 (9.5%) false positives, and TMBETA-SVM produced no false positives. In the absence of a stand-alone program for TMBETA-NET, β-barrel proteins were identified using TMBETA-SVM and TMBETADISC-RBF.

TMBETA-SVM and TMBETADISC-RBF predicted 240/1508 and 414/1508 proteins respectively. 228 proteins were identified by both programs equivalent to ~3.1% of the genome (Supplementary table A-1). This number is consistent with analyses of several Gram-negative bacteria, where 2-3% of the genome encodes β-barrel proteins (Punta et al., 2007).

Identification of OM proteins in *M. xanthus* by LC-MS/MS. In order to identify OM proteins in *M. xanthus*, separation of IM and OM was carried out using a protocol developed by Simunovic et al (Simunovic *et al.*, 2003), then subjected to LC-MS/MS. 90 proteins were identified of which 26 were predicted β-barrel proteins. Another 28 β-barrel proteins were identified when 88% phenol was used to aid solubilization of OM proteins. In all, LC-MS/MS analysis identified 54 predicted β-barrel proteins (Table 3-3) plus 44 lipoproteins (Table 3-4). 73 proteins in the OM preparation were highly abundant cytoplasmic contaminants including ribosomal proteins, DNA polymerase

Table 3-2. *M. xanthus* IM, periplasmic and ECM proteins[1].

MXAN	Function	Predicted localization	1 [a]	2 [b]	3 [c]	4 [d]
MXAN2832	permease	Periplas	-	-	-	-
MXAN2951	ABC transporter, periplasmic substrate binding protein	Periplasm	-	-	-	-
MXAN1066	PTS system, IIA component	Periplasm	+	-	-	-
MXAN0977	di-haem cytochrome-c peroxidase	Periplasm	-	-	-	-
MXAN1389	alkaline phosphatase	Periplasm	+	-	-	-
MXAN0468	peptidylprolyl cis-trans isomerase	Periplasm	+	-	-	-
MXAN3420	multicopper oxidase (CumA)	Periplasm	-	-	-	-
MXAN0274	biopolymer transport protein, ExbD/TolR family	IM	-	-	-	-
MXAN0559	ABC transporter, ATP-binding protein (Mac1)	IM	+	-	-	-

MXAN2570	acetate--CoA ligase	IM	-	-	-	-
MXAN4829	isoquinoline 1-oxidoreductase, beta subunit (IorB)	IM	+	-	-	-
MXAN5123	sensor histidine kinase MrpA (MrpA)	IM	+	+	-	-
MXAN2505	general secretory pathway protein K (GspK)	IM	-	-	-	+
MXAN3182	Serine threonine kinase	IM	+	-	-	-
MXAN1493	unknown	ECM	+	-	-	-
MXAN3885	Spore coat U	ECM	+	-	-	+
MXAN5686	unknown	ECM	+	-	-	-
MXAN1424	unknown	ECM	+	+	-	-
MXAN2375	unknown	ECM	-	-	-	-
MXAN0075	amidohydrolase	ECM	-	-	-	-

[1] IM and periplasmic proteins were obtained from the Pfam database while ECM proteins were previously identified by Curtis et al (Curtis et al., 2007).

Table 3-3. OM β-barrel proteins identified by LC-MS/MS.

Locus id	Function	No. of peptides
MXAN0219	Hypothetical protein	1
MXAN0518	TonB-dependent receptor	1
MXAN0659	Putative lipoprotein	5
MXAN0662	Hypothetical protein	3
MXAN0751	Conserved domain protein	4
MXAN0855	Putative chemotaxis MotB protein	5
MXAN0924	Hypothetical protein	2
MXAN1426	Hypothetical protein	2
MXAN1450	TonB-dependent receptor (Oar)	40
MXAN1689	Conserved hypothetical protein	1
MXAN2417	Conserved hypothetical protein	1
MXAN2462	Hypothetical protein	1
MXAN2514	General secretion pathway protein D	4
MXAN2536	Putative long-chain-fatty-acid-CoA ligase	6
MXAN2659	Hypothetical protein	17
MXAN2906	Penicillin acylase family protein	8
MXAN3106	Bacterial membrane secretin (secretin) family	10
MXAN3160	Peptidase, M13 (neprilysin) family	22
MXAN3774	Conserved Hypothetical protein	11
MXAN3780	Patatin-like phospholipase family protein	3
MXAN3953	Hypothetical protein	2

MXAN4085	Peptidylprolyl cis-trans isomerase, FKBP-type	1
MXAN4293	Hypothetical protein	4
MXAN4295	Patatin-like phospholipase family protein	6
MXAN4365	Outer membrane receptor family	1
MXAN4652	Putative Flp pilus assembly protein CpaB	1
MXAN4728	OMP85 family protein	4
MXAN4746	TonB-dependent receptor	5
MXAN5023	TonB dependent receptor	5
MXAN5152	OmpA family protein	3
MXAN5194	OmpA domain protein	2
MXAN5453	Hypothetical protein	6
MXAN5685	Hypothetical protein	2
MXAN5743	Hypothetical protein	11
MXAN5756	TolB protein	2
MXAN5931	Hypothetical protein	7
MXAN6079	Putative molybdopterin oxidoreductase, iron-sulfur binding subunit	15
MXAN6090	Hypothetical protein	10
MXAN6196	Hypothetical protein	3
MXAN6487	Outer membrane efflux protein domain protein	11
MXAN6521	Putative lipoprotein	1
MXAN6829	Hypothetical protein	4
MXAN6891	Hypothetical protein	2

MXAN6911	TonB-dependent receptor	8
MXAN7037	Putative chemotaxis MotB protein	1
MXAN7039	Putative lipoprotein	34
MXAN7040	FadL	13
MXAN7104	M3 (thimet oligopeptidase) family peptidase	10
MXAN7112	Conserved Hypothetical protein	3
MXAN7196	Hypothetical protein	1
MXAN7203	Putative 28 kDa outer membrane protein	5
MXAN7407	Hypothetical protein	6
MXAN7436	Outer membrane efflux protein	4
MXAN7513	Hypothetical protein	1

Table 3-4. OM lipoproteins identified by LC-MS/MS

MXAN	Function	No. of peptides
MXAN0283	Putative lipoprotein	1
MXAN0522	Putative lipoprotein	2
MXAN0533	NAD dependent epimerase/dehydratase family	1
MXAN0662	Hypothetical protein	3
MXAN0751	Conserved domain protein	4
MXAN0934	Protease DO family protein	14
MXAN1063	Putative lipoprotein	1
MXAN1162	Putative lipoprotein	5
MXAN1176	Peptidylprolyl cis-trans isomerase, cyclophilin-type	1
MXAN1342	Putative lipoprotein	1
MXAN1451	Putative lipoprotein MlpA	4
MXAN1623	peptidase, M16 (pitrilysin) family	8
MXAN1689	Conserved hypothetical protein	1
MXAN2091	Peptidase, M16 (pitrilysin) family	3
MXAN2286	Peptidyl-dipeptidase Dcp	4
MXAN2417	Conserved hypothetical protein	1
MXAN2470	5'-nucleotidase family protein	1
MXAN2660	Putative lipoprotein	6
MXAN2968	Efflux transporter, RND family, MFP subunit	4
MXAN3060	Adventurous gliding motility protein CglB	4

MXAN3084	Social gliding motility protein Tgl	2
MXAN3103	Putative lipoprotein	3
MXAN3440	Peptidase, M13 (neprilysin) family	4
MXAN3581	Peptidyl-dipeptidase A	4
MXAN4641	Hypothetical protein	1
MXAN4747	Putative lipoprotein	1
MXAN4900	Putative lipoprotein	15
MXAN4966	Putative lipoprotein	10
MXAN5331	Putative lipoprotein	2
MXAN5361	Putative 5`-nucleotidase	1
MXAN5390	Putative lipoprotein	1
MXAN5684	Putative lipoprotein	5
MXAN5933	Peptidase, M48 (Ste24 endopeptidase) family	5
MXAN6381	Hypothetical protein	1
MXAN6521	Putative lipoprotein	1
MXAN6660	Hypothetical protein	3
MXAN6720	Putative lipoprotein	2
MXAN6978	Putative lipoprotein	2
MXAN6985	Hypothetical protein	1
MXAN7108	Putative lipoprotein	1
MXAN7110	Peptidyl-prolyl cis-trans isomerase, FKBP-type	8
MXAN7220	Putative lipoprotein	1

MXAN7333	Putative lipoprotein	4
MXAN7438	Putative cobalt-zinc-cadmium resistance protein	3

subunits, translational elongation factors, and polyketide synthases (Supplementary table A-2).

A total of 18 known IM and periplasmic proteins were also identified including subunits of NADH dehydrogenase, cytochromes, and membrane transporters. Periplasmic proteins included disulfide oxidoreductase DbsA proteins, alkyl peroxidase and alkaline phosphatase (Supplementary table A-2).

Oar is required for C-signaling. Porins form hydrophilic channels that may allow export or import of extracellular signals. *oar* mutants exhibit delayed aggregation and are unable to sporulate (Martinez-Canamero *et al.*, 1993). Because Oar appears to be a TonB dependent receptor, it is possible that one or more essential developmental signals pass through it. To test this hypothesis, *oar* cells were mixed pair wise with mutants unable to produce each of the essential developmental signals A, B, C, D, E and S (Shimkets, 1999). If *oar* is proficient in producing a signal, it would be expected to rescue development of a mutant unable to produce such a signal. *oar* cells were mixed in 1:1 ratio with mutants from each signal producing class and found to be specifically defective in C-signaling (Figure 3-2A).

The *esg* gene product is required for the synthesis of a branched chain fatty acid required for the production of the E-signal (Toal *et al.*, 1995). The *esg* mutants show delayed aggregation and are unable to sporulate. However, *esg* mutations do not eliminate synthesis of branched chain fatty acids because there is a second pathway that can also produce them, albeit at smaller concentrations, causing some sporulation to occur as observed in Figure 3-2A (Bode *et al.*, 2009). When *oar* cells were mixed with *esg* mutant cells, fruiting body development was restored (Figure 3-2A). The *csgA* gene

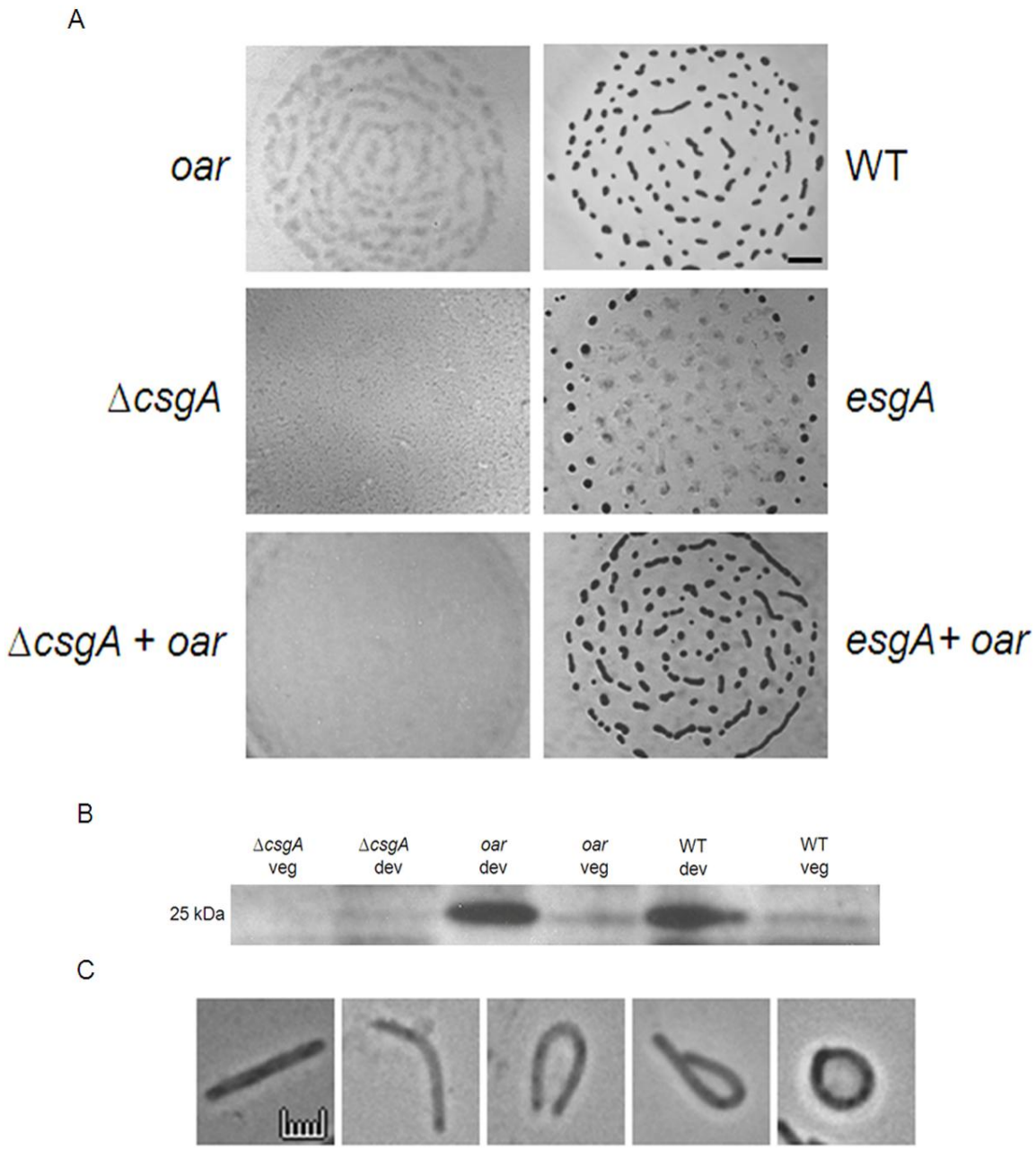

Figure 3-2. Role of *oar* in cell signaling. **(**A) Extracellular complementation of *oar* (LS2453) cells with Δ*csgA* (LS2441) and *esg* (JD300). WT (DK1622) cells were used as a control. Bar is 1 mm (B) Western blot analysis of vegetative cells and 24 h developing cells using anti-CsgA primary antibody. (C) Morphology of *oar* cells during

development. The first panel represents 24 h developing WT cells while the subsequent panels represent various oar cell shapes observed at 24 h into starvation. Bar is 1 μm.

is required for the production of the C-signal (Shimkets *et al.*, 1983). Δ*csgA* cells can be rescued for development by mixing with *csgA*$^{+}$ cells even if those cells are also developmentally defective (Hagen *et al.*, 1978). The mixtures containing *oar* and Δ*csgA* cells failed to undergo fruiting body development suggesting that *oar* cells are unable to provide C-signal to Δ*csgA* cells.

Western blot analysis of vegetative and 24 h developing cells was carried out to determine whether *oar* cells produce CsgA,. Figure 3-2B shows that *oar* cells produce CsgA during development at levels comparable to WT cells. These results suggest that *oar* has difficulty transmitting the C-signal. When the *oar* mutant was mixed with WT cells 99% of the spores that germinated were of WT origin suggesting that the oar developmental defect cannot be bypassed with an extracellular signal.

While 24 h developing WT cells show rod-shaped morphology, the *oar* cells were bent into horseshoe shaped cells that eventually form spheroplasts (Figure 3-2c). 100 cells were counted in both WT and *oar* mutant strains. In case of *oar*, 62% of cells had transformed into spheroplasts while all of the WT cells were intact. These defects were not observed in *oar* vegetative cells (data not shown). In a *csgA oar* double mutant, only 8% of cells had *oar*-like, morphology. These results suggested that CsgA accumulation is toxic.

ECM and IM lipoproteins utilize different sorting signals in *M. xanthus*. In other organisms, lipoproteins are sorted into the IM and OM using amino acid residues near the lipid modification site. ECM localization mechanisms have not been examined in detail since *E. coli* does not export proteins. Therefore the lipobox and the first eight amino acids of the mature ECM and IM lipoproteins were examined by multiple sequence

alignment using WebLogo (Crooks *et al.*, 2004). 7/10 ECM proteins, including by far the most abundant ECM protein FibA, possess alanine at the +7 position, while three known OM proteins, Tgl, CglB and MlpA have aspartate at the +7 position (Figure 3-3A). This result suggests that the +7 position may have a role in lipoprotein targeting. 12 putative IM lipoproteins were identified by LC-MS/MS from purified inner membranes (Table 3-5). 8/12 IM lipoproteins have lysine at the second position suggesting that lysine at the +2 position may be an IM retention signal (Figure 3-3B). Recently it was shown that the signal sequence of MXAN1176, a lipoprotein with lysine at the +2 position, localized in the IM (Wei *et al.*). These results suggest that lysine at the +2 position serves as an IM sorting signal while alanine at the +7 position is required for ECM localization.

Site directed mutagenesis of *fibA* was carried out to determine whether alanine at the +7 position is essential for ECM localization. Since no amino acid conservation was observed in the N-terminus of OM lipoproteins, alanine (GCC) was changed to aspartate (GAC) at the 27^{th} position (+7 in mature FibA) as this substitution involved minimal nucleotide modification. The modified *fibA* gene was expressed extrachromosomally in pZJY156 under control of the constitutive *pilA* promoter and introduced into Δ*fibA* strain LS2208. As a positive control, WT *fibA*, was introduced into LS2208 with the same vector system. Both strains produced comparable amounts of FibA as revealed by Western analysis of whole cells (Figure 3-3C). Immuno transmission electron microscopy was carried out to examine whether FibA is localized to the ECM. Cells were allowed to form biofilms on formvar coated nickel grids in a submerged culture (Kuner & Kaiser, 1982). Development was then induced by incubating the grids in cohesion buffer. The cells were probed with anti-FibA (Mab2105) followed by anti-

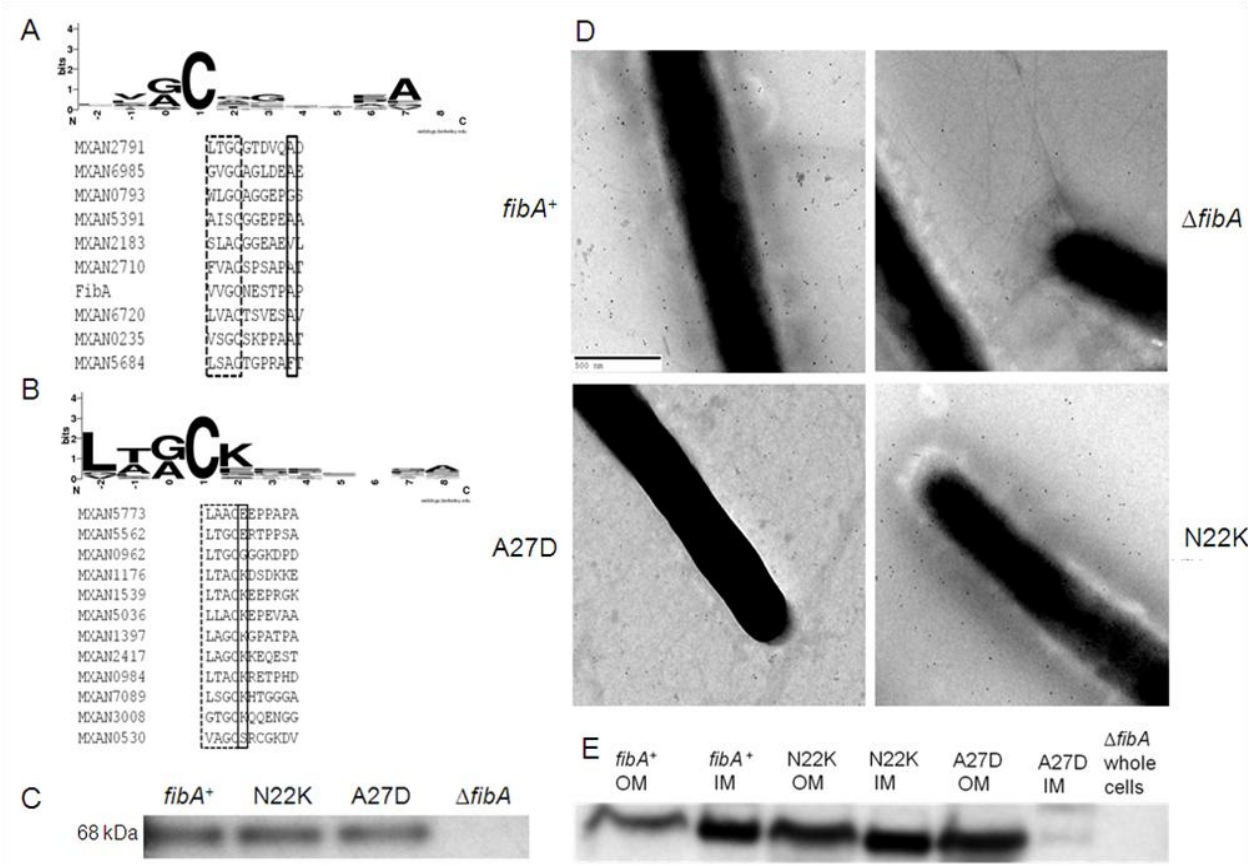

Figure 3-3. Identification of *M. xanthus* lipoprotein sorting signals. (A) Multiple sequence alignment of ECM proteins using WebLogo. The lipobox (highlighted by a box made of dashed lines) and the following seven amino acids of the N-terminal region of mature lipoproteins were aligned using WebLogo. Seven ECM lipoproteins have alanine at the 7th position (highlighted by a solid

box). (B) 8/12 predicted IM lipoproteins have lysine at the 2nd position (highlighted by a solid box). (C) Western blot analysis of 18 h developing cells using Mab2105 primary antibody. Strains used include LS2760 (WT FibA), LS2208 (Δ*fibA*), LS2761 (N22K FibA), LS2764 (A27D FibA). (D) Immuno transmission electron microscopy of developing cells using monoclonal antibody Mab2105. *M. xanthus* cells were allowed to form a biofilm on a formvar-carbon-coated nickel grid for 3 h. The cells were probed with Mab2105, which reacts primarily with FibA followed by anti-mouse antibodies conjugated with 10 nm colloidal gold particles. Bar is 500 nm. (E) Western blot analysis of membrane fractions purified from 7-8 h developing cells.

Table 3-5. Putative lipoproteins identified by LC-MS/MS from IM fraction.

MXAN	Function	No. of peptides
MXAN 0530	Putative lipoprotein	1
MXAN 0962	Putative lipoprotein	2
MXAN 0984	Heavy metal efflux transporter, RND family, MFP subunit	3
MXAN 1176	Peptidylprolyl cis-trans isomerase, cyclophilin-type	5
MXAN 1397	PBS lyase HEAT-like repeat protein	3
MXAN 1539	Putative lipoprotein	6
MXAN 2417	Conserved hypothetical protein	8
MXAN 3008	Adventurous gliding motility protein AglU	5
MXAN 5036	Conserved domain protein	4
MXAN 5562	Putative lipoprotein	3
MXAN 5773	Putative lipoprotein	3
MXAN 7089	Putative lipoprotein	1

mouse antibody conjugated to 10 nm gold particles, and then examined by transmission electron microscopy. Gold particles on or around 10-12 cells were enumerated.

Approximately 70 gold particles cell^{-1} are associated with the ECM and the cell surface of strain LS2760, which produces WT FibA (Figure 3-3D). In contrast only a few gold particles were attached to the surfaces of LS2208 (Δ*fibA)* or LS2764 (A27D) (3.1 and 6.1 particles cell^{-1}, respectively). This suggests that the +7 position is essential for localizing FibA to the ECM. Membrane separation of 7 h developing cells was performed in order to examine the localization of FibA to IM and OM locations. WT FibA is distributed almost equally in IM and OM during starvation suggesting that transport of FibA to the ECM occurs stepwise (Figure 3-3E). Conversly, the A27D change led to exclusively OM localization.

Because lysine was conserved at the +2 position of the majority of lipoproteins identified from the IM sample, we wondered whether modified FibA with +2 lysine would be retained in the IM. Site directed mutagenesis was carried out with FibA where an asparagine (AAC) codon was changed to lysine (AAG) at the 22nd position (+2 in mature FibA). The modified *fibA* gene with N22K was also expressed in pZJY156 under control of the constitutive *pilA* promoter and introduced into LS2208. The strain produced comparable amounts of FibA to the WT (Figure 3-3D). Immuno transmission electron microscopy of this strain showed large numbers of gold particles associated with the ECM (112 particles cell^{-1}) suggesting that the N22K substitution does not abort ECM localization of FibA. Membrane separation of developing cells containing the modified FibA showed similar FibA distribution to the WT further confirming that lysine at the +2 position does not exclusively target FibA to the IM. These results suggest that ECM

lipoproteins are sorted differently than those retained in the IM. An ECM lipoprotein with alanine at the +7 position is exported to the ECM even when it contains the IM retention signal, lysine at the +2 position.

Discussion

Bioinformatic analysis of the *M. xanthus* OM proteome using TMBETA-SVM and TMBETADISC-RBF identified 228 putative β-barrel proteins. To avoid false positives, these two programs were used only on those proteins that possessed signal peptide I but were devoid of transmembrane helices. This stepwise approach dramatically reduced the number of false positives. For example, when TMBETADISC-RBF was used on the whole *M. xanthus* proteome, it identified 915 β-barrel proteins (12%) of the genome, which is far greater than is typical of Gram-negative bacteria. Therefore, it is important to remove cytoplasmic, IM and lipoproteins prior to the use of β-barrel prediction programs.

Out of 228 putative β-barrel proteins, 54 were identified by LC-MS/MS of OM vesicles isolated from vegetative cells. Kahnt et al used biotinlyation of *M. xanthus* whole cells and OM vesicles to identify 63 β-barrel proteins (Kahnt et al., 2010). However, only 20 β-barrel proteins were identified by both studies. Kahnt et al used the program PRED-TMββ to identify β-barrel proteins from among the biotinylated proteins, which we found to generate over 50% false positives. When we reexamined their data using our step-wise approach, we found that 21 (33%) out of 63 β-barrel proteins identified by Kahnt et al were predicted to be false positives. Furthermore, 22 biotinylated proteins that were not predicted to be β-barrel proteins in the Kahnt et al study are predicted by our work to be β-barrel proteins. Therefore, selection of a

bioinformatic strategy requires careful examination. Because most membrane protein enrichment methods cannot avoid protein contamination from other cellular compartments use of bioinformatics can help accurately identify integral OM proteins from a pool of enriched candidates. As the bioinformatic programs improve, it may be possible to eliminate fractionation altogether.

The *M. xanthus* integral OM proteins can be classified based on function (Figure 3-4). The majority (~60%) of the predicted OM proteins have no known functions. Many putative β-barrel proteins are predicted to be involved in transport. Of these, TonB dependent receptors predominate. TonB dependent receptors are involved in energy dependent uptake of specific substrates, such as iron, which may be poorly permeable across the membrane or may be present in very low concentrations in the environment. The energy is derived from the proton motive force across the IM generated by a protein complex consisting of TonB, ExbB and ExbD. *M. xanthus* potentially encodes 17 TonB dependent receptors of which only five were detected by proteomics.

One *M. xanthus* TonB dependent receptor, Oar, is essential for C-signaling during development. *M. xanthus* produces at least six intercellular signals during development recognized by six classes of mutants that complement one another when mixed in pairs (Shimkets, 1999). The C-signal is an extracellular signal produced by the *csgA* gene. close contact between cells is essential for C-signaling. When Δ*csgA* cells are physically separated from wild-type cells by a porous membrane, C-signaling is blocked (Kim & Kaiser, 1990b). Likewise when Δ*csgA* cells are mixed with non-motile *mglAB* cells, C-signaling ceases even though *mglAB* cells can produce C-signal (Kim & Kaiser, 1990b). However, when *mglAB* cells were aligned end-to-end C-signaling was restored leading to

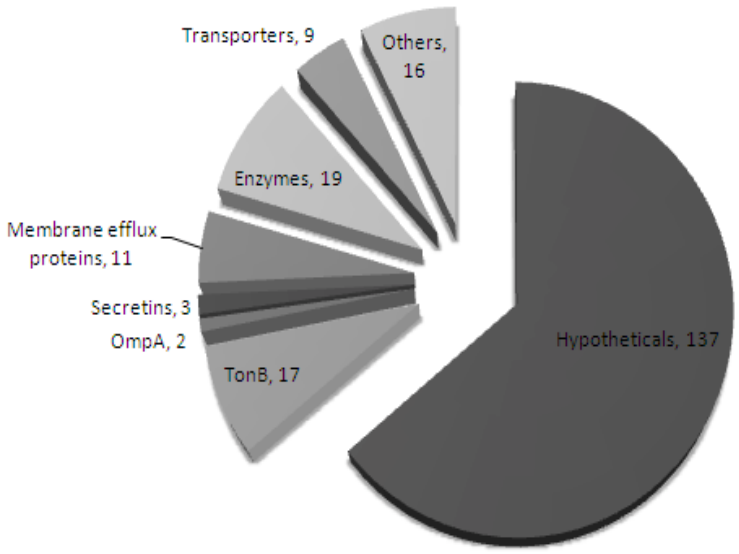

Figure 3-4. Pie chart classifying 228 OM β-barrel proteins according to function. Most *M. xanthus* OM proteins have no known function. The second major class of proteins includes TonBs, which are required for transport of a specific substrate. Transport of small molecules are carried out by transporters and OmpA, membrane efflux proteins are required for export of toxins and secretins form a large OM pore that allow export by Type II secretion system.

sporulation (Kim & Kaiser, 1990a). These results suggest that C-signaling requires proper alignment of cells. The inability of the *oar* mutant to rescue Δ*csgA* development could arise due to improper alignment of cells caused by abnormal shapes produced by the *oar* cells. These shapes include bend, hooked and rounded cells that may inhibit C-signaling between cells. Although 60% of cells undergo bending and eventual spheroplasting, 40% cells retain normal cell morphology, yet they fail to rescue Δ*csgA* aggregation and sporulation. Another possibility is that *oar* is an OM channel, involved in export of the C-signal. Either way, loss of C-signaling appears to adversely affect cell shape, which has not been observed in other C-signaling deficient mutants such as the *mglAB* mutant that can produce CsgA but fail to transmit the signal due to cell alignment problems. As normal cell morphology is restored in the *oar csgA* double mutant, it appears as if the C-signal is toxic. Indirect evidence suggests that CsgA is an enzyme that acts on lipid molecules (Avadhani *et al.*, 2006). It is possible that the product of this enzyme reaction may destabilize the cell membrane.

The most abundant ECM lipoprotein is FibA (Curtis et al., 2007, Kearns et al., 2002). Alanine at the +7 position appears to be conserved in most ECM proteins (Curtis et al., 2007). In developing WT cells FibA is found in equal amounts in IM and OM suggesting stepwise passage through the cell envelope. An amino acid change from alanine to aspartate at the +7 position (A27D) in FibA leads to exclusively OM retention, suggesting that the +7 position is crucial for export to the ECM.

Substitution of asparagine with lysine at the +2 position might be expected to cause FibA to accumulate in the IM since it seems to be the first transit point in a temporal sequence. However, this substitution did not block export to the OM and ECM.

These results suggest that *M. xanthus* utilizes two different mechanisms for lipoprotein sorting. *Klebsiella oxytoca* also possesses two mechanisms for lipoprotein transport, a Lol system for IM retention using +2 aspartate as the sorting signal, and a type II secretion system for the export of the cell surface exposed lipoprotein PulA (Pugsley, 1993, Poquet *et al.*, 1993). The *M. xanthus* genome predicts the presence of two type II secretion systems. Future studies should reveal whether these are utilized for lipoprotein export. While, the mechanism of ECM lipoprotein trafficking remains unknown, our study provides a valuable tool to identify subcellular location of various lipoproteins based on sequence information, and a method to target specific proteins to IM, OM or ECM.

Experimental procedures

Bioinformatic analysis. *M. xanthus* protein sequences were obtained from NCBI (ftp://ftp.ncbi.nih.gov/genomes/Bacteria/Myxococcus_xanthus_DK_1622/NC_008095.faa). Prediction of signal peptide, lipoprotein, and transmembrane helices in protein sequences were made using Signal P (http://www.cbs.dtu.dk/services/SignalP/), Lipo P (http://www.cbs.dtu.dk/services/LipoP/) and TMHMM (http://www.cbs.dtu.dk/services/TMHMM/) respectively (Krogh *et al.*, 2001, Juncker *et al.*, 2003, Bendtsen *et al.*, 2004). *M. xanthus* β-barrel domain proteins were obtained from the Pfam database (http://pfam.janelia.org/). The majority of the β-barrel domain proteins belong to the OM β-barrel protein (MBB) superfamily.

Six β-barrel prediction methods were evaluated for their ability to discriminate *M. xanthus* β-barrel proteins including TMB-HUNT (http://bmbpcu36.leeds.ac.uk/~andy/betaBarrel/AACompPred/aaTMB_Hunt.cgi),

TMBETA-SVM (http://tmbeta-svm.cbrc.jp/), TMBETA-NET (http://psfs.cbrc.jp/tmbeta-net/), TMBETADISC-RBF (http://rbf.bioinfo.tw/~sachen/OMPpredict/TMBETADISC-RBF.php), PRED-TMBB (http://bioinformatics.biol.uoa.gr/PRED-TMBB/input.jsp) and BOMP (http://services.cbu.uib.no/tools/bomp) (Bagos *et al.*, 2004, Berven *et al.*, 2004, Garrow *et al.*, 2005, Gromiha *et al.*, 2005, Ou *et al.*, 2008, Park *et al.*, 2005).

Bacterial strain and growth condition. Table 3-6 lists the bacterial strains, plasmids and primers used in this study. *M. xanthus* DK1622 cells were grown in CYE medium [1% Bacto casitone (Difco), 0.5% yeast extract (Difco), 10 mM 4-morpholinepropanesulfonic acid (MOPS) buffer (pH 7.6), and 0.1% $MgSO_4$)] at 32°C with vigorous shaking. To solidify the media, Bacto agar (Difco) was added at a concentration of 1.5%. *E. coli* cells were grown in Luria-Bertani (LB) medium. Kanamycin was added to CYE or LB media at a final concentration of 50 μg ml^{-1}.

Membrane separation. Membrane separation was carried out as described by Simunovic et al with a few modifications (Simunovic *et al.*, 2003). A 1 L culture of *M. xanthus* DK1622 cells was grown to a density of 2 $x10^8$ cells ml^{-1}. Cells were harvested by centrifugation, washed with chilled distilled water, and resuspended in 40 to 50 ml of 23.5% sucrose in 20 mM N-2-hydroxyethylpiperazine-N'-2-ethanesulfonic acid (HEPES), pH 7.6. Freshly prepared chicken egg white lysozyme (300 μg ml^{-1}) (Sigma Chemical Co., St. Louis, Mo.) and EDTA (pH 7.6) (1 mM) were added, and the cell suspension was incubated overnight at 4°C with gentle stirring. The cells were resuspended in 6 ml of ice-cold double-distilled water with vigorous pipetting to induce spheroplast formation, and stirred for 30 min at 4°C. Spheroplasts were collected by centrifugation at 12,000 x *g* for 10 min at 4°C. The supernatant was collected and saved,

Table 3-6. Bacterial strains, plasmids and primers used in this study.

Strains, plasmids, and primers	**Genotype**	**Reference or source**
***M. xanthus* strains**		
DK1622	Wild type	(Kaiser, 1979)
LS2208	Δ*fibA*	Lawrence Shimkets
LS2441	Δ*csgA*	Lawrence Shimkets
LS2453	*oar*, Km^r	Lawrence Shimkets
LS2760	LS2208 containing plasmid pSTB31, Km^r	This study
LS2761	LS2208 containing plasmid pSTB27, Km^r	This study
LS2764	LS2208 containing plasmid pSTB28.1, Km^r	This study
JD300	*esgA*, Km^r	(Downard *et al.*, 1993)
***E.coli* strains**		
TOP10		Invitrogen
Plasmids		
pCR2.1-TOPO	Cloning vector	Invitrogen
pZJY156	Shuttle vector	(Zhao et al., 2008)

pUC19	Cloning vector	
pSTB20	pCR2.1-TOPO carrying *pilA* promoter and *fibA* gene	This study
pSTB21	pCR2.1-TOPO carrying full length *fibA*	This study
pSTB22	pUC19 carrying 500 bp, XbaI-SalI fragment from pSTB20	This study
pSTB23	pSTB22 with N22K substitution in the FibA	This study
pSTB24.1	pSTB22 with A27D substitution in the FibA	This study
pSTB25	500 bp, XbaI-SalI from pSTB23 cloned into pSTB21	This study
pSTB26.1	500 bp, XbaI-SalI from pSTB24.1 cloned into pSTB21	This study
pSTB27	pZJY156 carrying *pilA* promoter and modified *fibA* from pSTB25	This study
pSTB28.1	pZJY156 carrying *pilA* promoter and modified *fibA* from pSTB26.1	This study
pSTB31	pZJY156 carrying *pilA* promoter and WT *fibA* from pSTB20	This study
Primers		
A	5’TCTAGAGGGAGCGCTTCGGATGCGTAGGCTGATCG 3’	
B	5’CTTCTGCACGAGCATGGGGGTCCTCAGAGAAGGTTGCAACG	
C	5’ ACCCCCATGCTCGTGCAGAAGAGAGTTCGCGGAGCG 3’	
D	5’ GGTACCCCTCGAGCCGCTGCCCAAGTAG 3’	
FibA2DF	5’ GAGTCCACCCCTGACCCCGAGGCCGAC 3’	
FibA2DR	5’ GTCGGCCTCGGGGTCAGGGGTGGACTC3’	
FibAKF	5’ GTTGTCGGTTGCAAGGAGTCCACCCCTGCC 3’	
FibAKR	5’ GGCAGGGGTGGACTCCTTGCAACCGACAAC 3’	

Underline indicates an overlap of 21 nucleotides.

and the pellet was resuspended in 3 volumes of 5 mM EDTA (pH 7.6). One tablet of complete EDTA-free protease inhibitor (Roche, Indianapolis, Ind.) was added, and the suspension stirred for 1 h. The supernatant was added back to the suspension and stirred for an additional 30 min. 1 ml of RNase A (10 mg ml^{-1}, Sigma Chemical Co.) and 1 ml of DNase type II (10 mg ml^{-1}, Sigma Chemical Co.) were added, and stirred for another 30 min. Rod-shaped cells were pelleted by centrifugation at 5000 × g. Spheroplasts were collected by ultracentrifugation at 100,000 x *g* for 3 h at 4°C in a 70.1 Ti rotor (Beckman Coulter, Fullerton, Calif.). Membrane pellets were resuspended in 23.5% sucrose in 20 mM HEPES, 5 mM EDTA, pH 7.6 using a Dual 21 tissue homogenizer (Kimble Kontes, Vineland, N.J.), and incubated overnight with gentle stirring at 4°C. The membrane suspension was loaded on top of a three-step gradient consisting of 10 ml of 60% sucrose, 10 ml of 48% sucrose, 10 ml of 35% sucrose in 20 mM HEPES, 5 mM EDTA, pH 7.6. The membrane fractions were separated by ultracentrifugation at 120,000 x *g* for 4 h at 4°C in a Beckman swinging bucket rotor (SW28). The membrane enrichment that migrated to the middle of the 35% sucrose layer consisted of OM vesicles, which was collected, diluted with HE0.1 buffer [20 mM HEPES, 0.1 mM EDTA, pH 7.6], concentrated by ultracentrifugation at 120,000 x *g* for 3 h at 4°C in a 70.1 Ti rotor, and then stored at -20°C.

The heavy density membrane enrichment that migrated at the 48/60% sucrose layer interface consisted of IM and hybrid membrane (HM) vesicles, which were collected and concentrated by ultracentrifugation using a SW28 rotor at 120,000 x *g* for 4 h at 4°C. Concentrated enrichments were layered on top of a discontinuous sucrose gradient consisting of 4 ml of a 70% sucrose, 4 ml of a 60% sucrose, 15 ml of a 55%

sucrose, 3 ml of a 40% sucrose, and 3 ml of a 30% sucrose in 20 mM HEPES, 5 mM EDTA, pH 7.6. The gradients were centrifuged using SW28 rotor at 70,000 x *g* for 20 h. The membrane enrichment that migrated between the 60 and 70% sucrose layers consisted of IM vesicles. This fraction was collected, concentrated by ultracentrifugation, then stored at -20°C,

Membrane separation of developing cells was carried out by growing a 500 ml culture to a final density of 5×10^8 cell ml^{-1}. The cells were harvested by centrifugation and resuspended in 10 ml water. The cells were spread on two 33- by 22-cm trays and incubated at 32°C for 7 h. Developing cells were harvested with a razor blade and resuspended in 40 to 50 ml of 23.5% sucrose in 20 mM HEPES, pH 7.6. The membrane separation was carried out as described above.

Phenol extraction of OM proteins. Phenol extraction of OM proteins was carried out as described in Hancock and Nikaido (Hancock & Nikaido, 1978). An equal volume of 88% phenol, pH 6.8, was added to the OM protein sample and incubated at 70°C for 10 min. The mixture was immediately cooled on ice for 10 min, and then centrifuged for 10 min at 5000 x *g*. The upper, aqueous layer was discarded. To the interface and the phenol phase an equal volume of distilled water was added, incubated at 70°C for 10 min, cooled on ice, and centrifuged at 5000 x *g* for 10 min. After the aqueous phase was discarded, protein was extracted from the phenol phase using two volumes of acetone each time. The acetone fractions were combined and the acetone was removed by air-drying. The pellet was resuspended in 100 µl of 1x PBS buffer [137 mM NaCl, 2.7 mM KCl, 4.3 mM Na_2HPO_4, 1.47 mM KH_2PO_4, pH 7.4].

In-gel trypsin digestion. 150 µg protein was boiled in loading buffer [52.5 mM Tris-HCl, pH 6.8, 2% SDS, 25% glycerol, 0.01% bromophenol blue, 100 mM dithiothreitol (DTT)] for 10 min and cooled on ice for 10 min. The sample was loaded on a 4-20% gradient polyacrylamide gel. The gel was run at 70 V until the dye entered the gel. Protein detection was performed using Bio-safe Coomassie Stain (Bio-Rad). The portion of the gel containing protein was cut into small pieces, and destained with 100 µl of water for 15 min. The gel pieces were washed sequentially for 15 minutes each with 50% acetonitrile, 100% acetonitrile, and 100 mM ammonium bicarbonate containing 50% acetonitrile (vol/vol). The gel pieces were dried under vacuum, treated with 100 µl of 10 mM DTT in 40 mM ammonium bicarbonate at 56°C for 45 min, alkylated with 100 µl of 55 mM iodoacetamide, 40 mM ammonium bicarbonate, and incubated for 30 min at room temperature in the dark. The gel pieces were washed with acetonitrile for 15 min, and then dried under vacuum. The gel pieces were rehydrated with 2 µg μl^{-1} proteomics-grade trypsin (Promega) in 40 mM ammonium bicarbonate and incubated at 37°C overnight. Solutions from multiple trypsin digestions were pooled. The gel slices were washed once with 50% acetonitrile in 25 mM ammonium bicarbonate, twice with 5% formic acid, and twice with acetonitrile for 15 min each. The washes were combined with the solutions from the previous step and dried under vacuum.

Identification of OM proteins. LC/MS-MS was carried out as described by Curtis et al (Curtis et al., 2007)**.** The peptides obtained from trypsin digestion were loaded on a PicoFrit C_{18} column (8-cm by 50-µm) (New Objective, Woburn, MA), and separated on an Agilent 1100 capillary LC (Palo Alto, CA), which interfaced directly to a LTQ linear ion trap mass spectrometer (Thermo Electron, San Jose, CA). The mobile phases

consisted of A (H_2O and 0.1% formic acid) and B (acetonitrile and 0.1% formic acid). The peptides were first desalted for 10 min with 0.1% formic acid, and then eluted into the mass spectrometer at a flow rate of 200 ηl min^{-1}. MS/MS spectra was acquired on the nine most abundant precursor ions from each MS scan with a repeat count and duration of 3 and 15 s each. The MS/MS spectra was converted into peak lists by ReAdW and mzMXL2Other software (Pedrioli *et al.*, 2004).

Database searches were performed using Mascot 1.9 software (Matrix Science, Boston, MA) against a *M. xanthus* protein database obtained from NCBI. The search parameters included full tryptic enzymatic cleavage up to three missed cleavages, peptide tolerance of 1000 ppm, fragment ion tolerance of 0.6 Da, and variable modification including methionine oxidation, deamination and carboxyamidomethylation. The proteins identified were statistically validated using PROVALT software (Graham *et al.*, 2006). Only proteins with a false-discovery rate of less than 1% were considered to be statistically significant.

Extracellular complementation. *M. xanthus* cells were grown to a cell density of 5×10^8 cells ml^{-1}, harvested and resuspended to a final concentration of 5×10^9 cells ml^{-1}. *oar* cells were mixed with various strains in 1:1 ratio and 10 µl of the cell mixture was spotted on TPM agar plates. The plates were incubated at 32°C and after five days digital images were acquired.

Microscopic analysis. 5×10^8 *M. xanthus* cells were spotted on TPM agar plates and incubated for 24 h. Cells were resuspended in a drop of TPMF buffer [TPM containing 10% ficoll], and examined with a phase contrast microscope (Leica Microsystems,

DM55008). Digital images were obtained at 1000x magnification using a QIQICAM FAST 1394 camera (Compix Inc).

Site directed mutagenesis and cloning of *fibA*. The *fibA* gene was expressed from pZJY156 (Zhao *et al.*, 2008). The *fibA* gene was fused with the *pilA* promoter using the gene splicing by overlap extension (SOEing PCR) method (Horton, 1995). The primers are listed in Table 6. Primers A and B were used for amplification of the *pilA* promoter including the ribosomal binding site and the start codon (Wu & Kaiser, 1997). Primers C and D were used for the amplification of full length *fibA*. Primers B and C were designed to have an overlap of 21 nucleotides (underlined region). *M. xanthus* DK1622 genomic DNA was used as a template. The two PCR products and primer pair A and D were then used for SOEing PCR. PCR products were separated on 0.8% agarose, excised, extracted using the Gel Extraction kit (Qiagen), and cloned into pCR2.1-TOPO (Invitrogen) to create pSTB20. Full length *fibA* was cloned into pCR2.1-TOPO to create pSTB21. A 500 bp, XbaI-SalI fragment containing the *pilA* promoter and the N-terminal region of FibA from pSTB20 was cloned into pUC19 to create pSTB22, which was used as the template for site directed mutagenesis. The primers used for the site directed mutagenesis are listed in Table 6. Primers FibA2DF and FibA2DR were used for replacing alanine with aspartate at 27th position while FibAKF and FibAKR were used for replacing asparagine with lysine at the 22nd position (Table 6). PCR was carried out using a high fidelity DNA polymerase I (Expand High Fidelity PCR system, Roche). The PCR products obtained were treated with DpnI to eliminate the methylated template, and then transformed into *E. coli* Top10 cells. Plasmids were isolated from transformants and sequenced. The plasmids encoding FibA with N22K or A27D amino acid substitutions

were called pSTB23 and pSTB24.1 respectively. The 500 bp, XbaI-SalI from pSTB23 and pSTB24.1 were cloned at the same site in pSTB21 to create pSTB25 and pSTB26.1, respectively. The new plasmids contained full length *fibA* encoding the N22K or A27D substitutions expressed from the *pilA* promoter. The plasmids, pSTB25 and pSTB26.1 were digested with XbaI and EcoRI, and the 2800 bp fragment containing the *pilA* promoter and *fibA* gene was cloned into pZJY156 to create pSTB27 and pSTB28.1 plasmids. These plasmids were then transformed into *M. xanthus* LS2208 to create LS2761 and LS2764. Full length *fibA* expressed from the *pilA* promoter was cloned into pZJY156 to create pSTB31 and also transformed into *M. xanthus* LS2208 to create LS2760. Expression of *fibA* from the *pilA* promoter was verified by western blotting using monoclonal antibody Mab2105 (Behmlander & Dworkin, 1991).

Western blot analysis. 5 µg of cell lysate or 10 µg of membrane fractions, were separated on a 4-20% SDS-PAGE gradient gel (Bio Rad). Proteins were transferred to an Immobilin-P, PVDF membrane (Milipore). The membrane was blocked with 3% bovine serum albumin (BSA) in PBST (1x PBS containing 0.1% Tween 20). The proteins were probed with the Mab2105 (1:500 dilution) or anti-CsgA (1:5000) that was prepared in PBST containing 0.1% BSA (Behmlander & Dworkin, 1991). This was followed by washing three times with PBST. The membrane blot was then probed with horseradish peroxidase-conjugated goat anti-mouse IgG or anti-rabbit IgG, which were diluted to 1:10,000 in PBST containing 0.1% BSA. The membrane was washed three times with PBST and developed with the ECL luminescence detection kit (Amersham).

Electron microscopy: *M. xanthus* cells were grown to a density of 5×10^8 cells ml^{-1} and diluted to 3.3×10^6 cells ml^{-1}in CYE or CYEK (CYE containing 50 µg ml^{-1} kanamycin)

broth. 4 ml of the cell suspension and a formvar-carbon-coated nickel grid (Electron Microscope Sciences) was transferred to a petri plate (60 × 15 mm). The plate was incubated at 32°C for 12 h. A thin biofilm on the surface of the grid was allowed to form. Starvation was induced by replacing the CYE or CYEK broth with cohesion buffer [10 mM MOPS, pH 6.8, 1 mM $MgCl_2$, 1 mM $CaCl_2$] and incubated for 3 h at 32°C. The grid was treated with 2% glutaraldehyde for 15 min at room temperature followed by washing five times with the cohesion buffer. The grid was blocked with 5% bovine serum albumin (BSA) in cohesion buffer for 45 min at room temperature. The grid was treated with Mab2105 antibody (1:20 dilution) prepared in cohesion buffer containing 5% BSA for 45 min at room temperature followed by washing three times with cohesion buffer (Behmlander & Dworkin, 1991). The grid was then treated with anti-mouse antibody (1:100 dilutions) conjugated to 10 nm colloidal gold particles (Sigma-Aldrich), and incubated for 30 min at room temperature. The grid was washed three times with the cohesion buffer. The grid was washed three times with water, allowed to air dry, and observed under a FEI Technal transmission electron microscope operated at 200 kV.

Acknowledgements

We would like to thank Jan Mrazek for helpful discussions and Krishna Bayyareddy for technical help. We would also like to thank Dr. John P. Shields and Dr. Jianguo Fan of the Center for Ultra Structural Research for their assistance with TEM. This work was supported by research grant MCB 0742976 from the National Science Foundation.

References

Avadhani, M., R. Geyer, D. C. White & L. J. Shimkets, (2006) Lysophosphatidylethanolamine is a substrate for the short-chain alcohol dehydrogenase SocA from *Myxococcus xanthus*. *J Bacteriol* **188**: 8543-8550.

Bagos, P. G., T. D. Liakopoulos, I. C. Spyropoulos & S. J. Hamodrakas, (2004) PRED-TMBB: a web server for predicting the topology of beta-barrel outer membrane proteins. *Nucleic Acids Res* **32**: W400-404.

Behmlander, R. M. & M. Dworkin, (1991) Extracellular fibrils and contact-mediated cell interactions in *Myxococcus xanthus. J Bacteriol* **173**: 7810-7820.

Bendtsen, J. D., H. Nielsen, G. von Heijne & S. Brunak, (2004) Improved prediction of signal peptides: SignalP 3.0. *J Mol Biol* **340**: 783-795.

Berven, F. S., K. Flikka, H. B. Jensen & I. Eidhammer, (2004) BOMP: a program to predict integral beta-barrel outer membrane proteins encoded within genomes of Gram-negative bacteria. *Nucleic Acids Res* **32**: W394-399.

Bode, H. B., M. W. Ring, G. Schwär, M. O. Altmeyer, C. Kegler, I. R. Jose, M. Singer & R. Müller, (2009) Identification of additional players in the alternative biosynthesis pathway to Isovaleryl-CoA in the myxobacterium *Myxococcus xanthus*. *ChemBioChem* **10**: 128-140.

Bos, M. P., V. Robert & J. Tommassen, (2007a) Biogenesis of the Gram-negative bacterial outer membrane. *Annu Rev Microbiol* **61**: 191-214.

Bos, M. P., V. Robert & J. Tommassen, (2007b) Functioning of outer membrane protein assembly factor Omp85 requires a single POTRA domain. *EMBO Rep* **8**: 1149-1154.

Crooks, G. E., G. Hon, J. M. Chandonia & S. E. Brenner, (2004) WebLogo: a sequence logo generator. *Genome Res* **14**: 1188-1190.

Curtis, P. D., J. Atwood, 3rd, R. Orlando & L. J. Shimkets, (2007) Proteins associated with the *Myxococcus xanthus* extracellular matrix. *J Bacteriol* **189**: 7634-7642.

Downard, J., S. V. Ramaswamy & K. S. Kil, (1993) Identification of *esg*, a genetic locus involved in cell-cell signaling during *Myxococcus xanthus* development. *J. Bacteriol.* **175**: 7762-7770.

Finn, R. D., J. Mistry, B. Schuster-Bockler, S. Griffiths-Jones, V. Hollich, T. Lassmann, S. Moxon, M. Marshall, A. Khanna, R. Durbin, S. R. Eddy, E. L. Sonnhammer & A. Bateman, (2006) Pfam: clans, web tools and services. *Nucleic Acids Res* **34**: D247-251.

Garrow, A. G., A. Agnew & D. R. Westhead, (2005) TMB-Hunt: a web server to screen sequence sets for transmembrane beta-barrel proteins. *Nucleic Acids Res* **33**: W188-192.

Graham, R. L., C. E. Pollock, S. N. O'Loughlin, N. G. Ternan, D. B. Weatherly, P. J. Jackson, R. L. Tarleton & G. McMullan, (2006) Multidimensional proteomic analysis of the soluble subproteome of the emerging nosocomial pathogen *Ochrobactrum anthropi*. *J Proteome Res* **5**: 3145-3153.

Gromiha, M. M., S. Ahmad & M. Suwa, (2005) TMBETA-NET: discrimination and prediction of membrane spanning beta-strands in outer membrane proteins. *Nucleic Acids Res* **33**: W164-167.

Hagen, D. C., A. P. Bretscher & D. Kaiser, (1978) Synergism between morphogenetic mutants of *Myxococcus xanthus*. *Dev Biol* **64**: 284-296.

Hancock, R. E. & H. Nikaido, (1978) Outer membranes of gram-negative bacteria. XIX. Isolation from *Pseudomonas aeruginosa* PAO1 and use in reconstitution and definition of the permeability barrier. *J Bacteriol* **136**: 381-390.

Horton, R., (1995) PCR-mediated recombination and mutagenesis. *Molecular Biotechnology* **3**: 93-99.

Hutchings, M. I., T. Palmer, D. J. Harrington & I. C. Sutcliffe, (2009) Lipoprotein biogenesis in Gram-positive bacteria: knowing when to hold 'em, knowing when to fold 'em. *Trends Microbiol* **17**: 13-21.

Johnson, J. M. & G. M. Church, (1999) Alignment and structure prediction of divergent protein families: periplasmic and outer membrane proteins of bacterial efflux pumps. *J Mol Biol* **287**: 695-715.

Juncker, A. S., H. Willenbrock, G. Von Heijne, S. Brunak, H. Nielsen & A. Krogh, (2003) Prediction of lipoprotein signal peptides in Gram-negative bacteria. *Protein Sci* **12**: 1652-1662.

Kahnt, J., K. Aguiluz, J. Koch, A. Treuner-Lange, A. Konovalova, S. Huntley, M. Hoppert, L. Sogaard-Andersen & R. Hedderich, (2010) Profiling the outer membrane proteome during growth and development of the social bacterium *Myxococcus xanthus* by selective biotinylation and analyses of outer membrane vesicles. *J Proteome Res*.

Kaiser, D., (1979) Social gliding is correlated with the presence of pili in *Myxococcus xanthus*. *Proc Natl Acad Sci U S A* **76**: 5952-5956.

Kearns, D. B., P. J. Bonner, D. R. Smith & L. J. Shimkets, (2002) An extracellular matrix-associated zinc metalloprotease is required for dilauroyl

phosphatidylethanolamine chemotactic excitation in *Myxococcus xanthus*. *J Bacteriol* **184**: 1678-1684.

Kim, S. K. & D. Kaiser, (1990a) Cell alignment required in differentiation of *Myxococcus xanthus*. *Science* **249**: 926-928.

Kim, S. K. & D. Kaiser, (1990b) Cell motility is required for the transmission of C-factor, an intercellular signal that coordinates fruiting body morphogenesis of *Myxococcus xanthus*. *Genes Dev* **4**: 896-904.

Koski, P., L. Hirvas & M. Vaara, (1990) Complete sequence of the *ompH* gene encoding the 16-kDa cationic outer membrane protein of *Salmonella typhimurium*. *Gene* **88**: 117-120.

Krogh, A., B. Larsson, G. von Heijne & E. L. Sonnhammer, (2001) Predicting transmembrane protein topology with a hidden Markov model: application to complete genomes. *J Mol Biol* **305**: 567-580.

Kuner, J. M. & D. Kaiser, (1982) Fruiting body morphogenesis in submerged cultures of *Myxococcus xanthus*. *J. Bacteriol.* **151**: 458-461.

Martinez-Canamero, M., J. Munoz-Dorado, E. Farez-Vidal, M. Inouye & S. Inouye, (1993) Oar, a 115-kilodalton membrane protein required for development of *Myxococcus xanthus*. *J Bacteriol* **175**: 4756-4763.

Masuda, K., S. Matsuyama & H. Tokuda, (2002) Elucidation of the function of lipoprotein-sorting signals that determine membrane localization. *Proc Natl Acad Sci U S A* **99**: 7390-7395.

Nikaido, H., (2003) Molecular basis of bacterial outer membrane permeability revisited. *Microbiol Mol Biol Rev* **67**: 593-656.

Ou, Y. Y., M. M. Gromiha, S. A. Chen & M. Suwa, (2008) TMBETADISC-RBF: Discrimination of beta-barrel membrane proteins using RBF networks and PSSM profiles. *Comput Biol Chem* **32**: 227-231.

Park, K. J., M. M. Gromiha, P. Horton & M. Suwa, (2005) Discrimination of outer membrane proteins using support vector machines. *Bioinformatics* **21**: 4223-4229.

Pedrioli, P. G. A., J. K. Eng, R. Hubley, M. Vogelzang, E. W. Deutsch, B. Raught, B. Pratt, E. Nilsson, R. H. Angeletti, R. Apweiler, K. Cheung, C. E. Costello, H. Hermjakob, S. Huang, R. K. Julian, E. Kapp, M. E. McComb, S. G. Oliver, G. Omenn, N. W. Paton, R. Simpson, R. Smith, C. F. Taylor, W. Zhu & R. Aebersold, (2004) A common open representation of mass spectrometry data and its application to proteomics research. *Nat Biotech* **22**: 1459-1466.

Poquet, I., M. G. Kornacker & A. P. Pugsley, (1993) The role of the lipoprotein sorting signal (aspartate +2) in pullulanase secretion. *Mol Microbiol* **9**: 1061-1069.

Postle, K., (2007) TonB system, in vivo assays and characterization. *Methods Enzymol* **422**: 245-269.

Pugsley, A. P., (1993) The complete general secretory pathway in gram-negative bacteria. *Microbiol Rev* **57**: 50-108.

Punta, M., L. R. Forrest, H. Bigelow, A. Kernytsky, J. Liu & B. Rost, (2007) Membrane protein prediction methods. *Methods* **41**: 460-474.

Reizer, J., A. Reizer & M. H. Saier, Jr., (1993) The MIP family of integral membrane channel proteins: sequence comparisons, evolutionary relationships, reconstructed pathway of evolution, and proposed functional differentiation of the two repeated halves of the proteins. *Crit Rev Biochem Mol Biol* **28**: 235-257.

Seydel, A., P. Gounon & A. P. Pugsley, (1999) Testing the '+2 rule' for lipoprotein sorting in the Escherichia coli cell envelope with a new genetic selection. *Mol Microbiol* **34**: 810-821.

Shimkets, L. J., (1999) Intercellular signaling during fruiting body development of *Myxococcus xanthus. Annu Rev Microbiol* **53**: 525-549.

Shimkets, L. J., R. E. Gill & D. Kaiser, (1983) Developmental cell interactions in *Myxococcus xanthus* and the spoC locus. *Proc Natl Acad Sci U S A* **80**: 1406-1410.

Simunovic, V., F. C. Gherardini & L. J. Shimkets, (2003) Membrane localization of motility, signaling, and polyketide synthetase proteins in *Myxococcus xanthus*. *J Bacteriol* **185**: 5066-5075.

Tanaka, S. Y., S. Narita & H. Tokuda, (2007) Characterization of the Pseudomonas aeruginosa Lol system as a lipoprotein sorting mechanism. *J Biol Chem* **282**: 13379-13384.

Toal, D. R., S. W. Clifton, B. A. Roe & J. Downard, (1995) The *esg* locus of *Myxococcus xanthus* encodes the E1 alpha and E1 beta subunits of a branched-chain keto acid dehydrogenase. *Mol Microbiol* **16**: 177-189.

Tokuda, H. & S. Matsuyama, (2004) Sorting of lipoproteins to the outer membrane in *E. coli*. *Biochim Biophys Acta* **1693**: 5-13.

van den Berg, B., (2005) The FadL family: unusual transporters for unusual substrates. *Curr Opin Struct Biol* **15**: 401-407.

Voulhoux, R., M. P. Bos, J. Geurtsen, M. Mols & J. Tommassen, (2003) Role of a highly conserved bacterial protein in outer membrane protein assembly. *Science* **299**: 262-265.

Wei, X., D. T. Pathak & D. Wall, Heterologous protein transfer within structured myxobacteria biofilms. *Mol Microbiol*.

Wimley, W. C., (2003) The versatile beta-barrel membrane protein. *Curr Opin Struct Biol* **13**: 404-411.

Wu, S. S. & D. Kaiser, (1997) Regulation of expression of the *pilA* gene in *Myxococcus xanthus*. *J Bacteriol* **179**: 7748-7758.

Zhao, J. Y., L. Zhong, M. J. Shen, Z. J. Xia, Q. X. Cheng, X. Sun, G. P. Zhao, Y. Z. Li & Z. J. Qin, (2008) Discovery of the autonomously replicating plasmid pMF1 from *Myxococcus fulvus* and development of a gene cloning system in *Myxococcus xanthus*. *Appl Environ Microbiol* **74**: 1980-1987.

CHAPTER 4

A ROLE FOR PROGRAMMED CELL DEATH AND LIPID BODIES IN *MYXOCOCCUS XANTHUS* FRUITING BODY DEVELOPMENT

Bhat, S., Pham, D., and Shimket, L.J. To be submitted.

Abstract

Lipid bodies are carbon and energy storage organelles found in most eukaryotes but few prokaryotes. *Myxococcus xanthus* lipid bodies are synthesized during fruiting body formation, a bacterial developmental cycle involving directed movement and cellular differentiation. In this work we show that lipid bodies contain a developmental morphogen, the E-signal, which is released by programmed cell death (PCD). Lipid body synthesis begins early in development as cells begin to shorten suggesting that they form from recycling of membrane phospholipids into triacylglycerides (TAG). During development, PCD lyses up to 80% of the cell population while most of the remaining cells form spores. Three lines of evidence suggest that lipid body synthesis begins prior to PCD. First, the population of lipid body containing wild type cells declines in proportion with PCD as development progresses. Second, in mixture with *difA-gfp* cells, the *difA-gfp* mutant preferentially undergoes PCD while the wild type forms spores. In this mixture lipid bodies are observed in *difA-gfp* cells prior to PCD. Finally, extracellular lipid bodies are observed in fruiting bodies, and form a large cap on top of nascent fruiting bodies. Lipid body lipids rescue sporulation of an E-signal deficient mutant. The lipids were fractionated using solid phase extraction and thin layer chromatography, which led to a 50-fold purification of the E-signal. MALDI analysis of the active fraction identified TG-1, a triacylglyceride containing one ether-linked *iso* 15:0 fatty acid and two ester-linked *iso* 15:0 fatty acids. TG-1 was previously shown to be one of the major components of lipid bodies. 33 developmental mutants were analyzed for lipid body synthesis most of which exhibited aberrant accumulation suggesting that similar to

eukaryotes, the lipid body regulon is subject to diverse levels of control involving many genes that are not specifically involved in fatty acid synthesis or degradation.

Introduction

Many organisms store carbon and energy in the form of neutral lipids such as triacylglycerides (TAGs). These energy reserves are compartmentalized into organelles by a phospholipid monolayer to form lipid bodies or lipid droplets. In mammals and insects, lipid bodies are predominantly found in specialized cells known as the adipocytes and fat cells, respectively, while in plants they are found in the seeds (Murphy, 1993, Murphy & Vance, 1999, Law & Wells, 1989). Although the use of TAGs as storage compounds is ubiquitous in eukaryotes, they are relatively rare in prokaryotes. Lipid body formation has been observed in the actinomycetes *Rhodococcus* and *Streptomyces* under conditions where there is an excess of carbon, but other nutrients, such as nitrogen, are growth limiting (Alvarez & Steinbüchel, 2002, Waltermann & Steinbuchel, 2005).

Recently, lipid bodies were observed during development in *Myxococcus xanthus*, a δ-Proteobacterium that responds to amino acid deprivation by inducing a multicellular developmental cycle that culminates in spore-filled fruiting bodies (Hoiczyk et al., 2009). These lipid bodies seem remarkably similar to eukaryotic lipid bodies in form and function as they consist of triacylglycerols (TAGs) surrounded by a phospholipid monolayer. *M. xanthus* TAGs presumably provide energy for sporulation since lipid bodies appear early in development but disappear by the time the spore matures (72 h) (Hoiczyk et al., 2009). β-oxidation of TAGs provides more energy compared with the more common bacterial storage compound poly hydroxyl butyrate (PHB) (Alvarez & Steinbüchel, 2002). *M. xanthus* TAGs contain both ether- and alkyl–linked fatty acids, depending on the molecular species (Hoiczyk et al., 2009). The phospholipid membrane consists of phosphatidylethanolamine with a vinyl-linked fatty acid, similar to eukaryotic

plasmalogens, whose deficiency has been linked to spermatogenesis defects, cataract development, and central nervous system myelination problems in mice (Hoiczyk et al., 2009, Rodemer *et al.*, 2003, Teigler *et al.*, 2009).

Besides energy storage, eukaryotic lipid bodies are also involved in many physiological functions, depending on the cell type. Lipid bodies of macrophages store arachidonic acid, which is a precursor of signaling molecule eicosanoid required for cellular processes such as apoptosis (Bozza et al., 1996). Similarly steroidogenic cells store cholesterol required for the synthesis of steroids (Almahbobi & Hall, 1990). When lipid accumulation occurs unchecked in these cells, it may lead to various disorders such as obesity, type II diabetes and atherosclerosis (Li *et al.*, 2007, Sell *et al.*, 2006, Bell *et al.*, 2008, Lang & Insull, 1970). An important step in developing treatment methods for these diseases is to understand how lipid body synthesis and utilization are regulated by cells.

M. xanthus development is regulated by intercellular communication in which lipid bodies may play a crucial role. Mutants lacking the ability to produce the major lipid body fatty acid, *iso* 15:0, exhibit delayed aggregation and produce few spores (Toal et al., 1995). *iso* 15:0 is synthesized by the *esg* gene product, which is also required for the synthesis of an extracellular signal of unknown structure called the E-signal (Downard *et al.*, 1993, Downard & Toal, 1995). The *esg* gene encodes the E1 component of branched-chain keto acid dehydrogenase (Bkd enzyme complex), which produces the short branched chain fatty acid primer isovaleric acid from leucine (Toal et al., 1995). This primer is extended by fatty acid synthase into the long chain fatty acids *iso*15:0 and *iso*17:0. A second, novel pathway involving LiuC, MvaS, MXAN4264, MXAN4265 and

MXAN4266 can also synthesize isovalerate (Bode *et al.*, 2006b, Bode *et al.*, 2009). This alternative pathway is highly induced during fruiting body formation and in *esg* mutants. Mutants blocked in both pathways are deficient in sporulation, which can be restored when the mutant is mixed with wild type cells suggesting that the mutant is defective in the synthesis of an extracellular molecule called the E-signal. Development can also be restored by addition of isovaleric acid or *iso*15:0 suggesting that *iso*15:0 or a molecule containing it may be the E-signal.

Fruiting body development leads to differentiation of three distinct cell types, peripheral rods that remain outside the fruiting body, myxospores, and cells that undergo programmed cell death (PCD) (O'Connor & Zusman, 1991, Søgaard-Andersen & Yang, 2008, Shimkets, 1999, Nariya & Inouye, 2008). PCD is activated approximately 12 h into development, and claims up to 80% of the cell population (Wireman & Dworkin, 1975, Shimkets, 1986, Nariya & Inouye, 2008). PCD is mediated by the MazF toxin, an RNA interferase, and inhibited by the antitoxin MrpC, which forms a protein-protein complex with MazF (Nariya & Inouye, 2008). MrpC is also a transcriptional activator of many developmental genes including *mazF* and *mrpC* (Sun & Shi, 2001b, Nariya & Inouye, 2008, Sun & Shi, 2001a). MrpC is phosphorylated by the Pkn14 serine/threonine kinase to inhibit transcriptional activity during growth (Nariya & Inouye, 2008). Although the role of PCD during development remains unknown, mutants that are blocked in PCD, such as *mazF*, are unable to complete development suggesting that PCD is an essential component (Nariya & Inouye, 2008).

In this paper we examine the role of lipid bodies in cell-cell signaling during development. Our data indicates that lipid bodies are synthesized before cells commit to a

developmental fate. Cells undergoing PCD release lipid body lipids into the fruiting body. Among the extracellular lipids is the E-signal, which was purified 50-fold and identified as TG-1 (1-i15:0-alkyl-2,3-di-i15:0-acyl glycerol) a development-specific TAG containing ether linked *iso* 15:0. Many developmental mutants exhibit aberrant lipid body formation indicating that lipid production and utilization are closely coupled with the developmental program.

Results

Lipid body production in developing WT cells. Lipid bodies are first observed about 6-12 h after fruiting body development is initiated by amino acid deprivation (figure 4-1A). As there are no exogenous nutrients, the carbon sources for lipid body synthesis appear to be derived from turnover of cellular material. Myxospores are formed from long, thin rod-shaped cells that shorten then develop into spherical spores, which indicate that the cells have to degrade their membranes. In fact, two-thirds of the cellular membrane is lost during spore formation (Hoiczyk et al., 2009). Lipid bodies may be synthesized from membrane phospholipids since enzymes required for their de novo synthesis are not associated with the lipid bodies (Hoiczyk et al., 2009).

Lipid body area and cell length of developing wild type (DK1622) cells were quantified by fluorescence and phase contrast microscopy using the lipophilic dye Nile red (Hoiczyk et al., 2009). Early on, several small lipid bodies appear close to the membrane (figure 4-1A). The cell length is reduced by 40% at 18 h, when lipid body production reaches its peak, while lipid body size increases approximately 8-fold compared with 6-12 h (figure 4-1B).

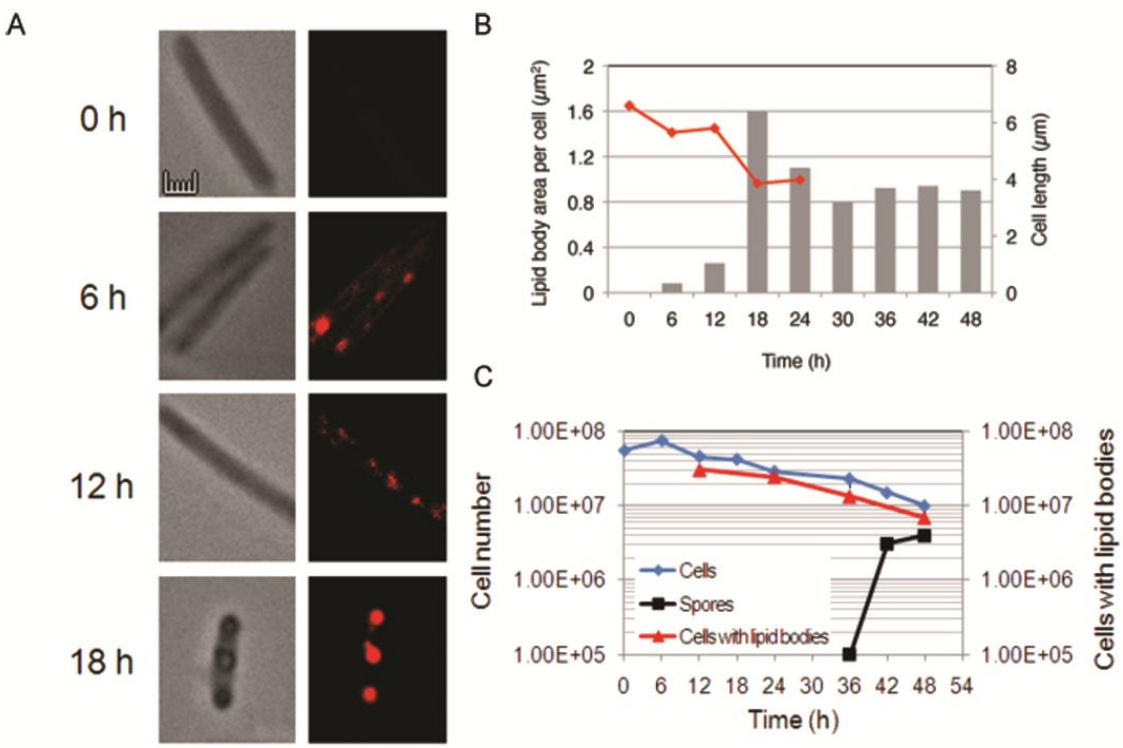

Figure 4-1: Lipid body production in WT cells during development. (A) WT cells stained with Nile red at various times during development. Phase (left panels), fluorescence (right panels). Bar is 1 μm (B) Lipid bodies were quantified by measuring the average area of lipid bodies per cell (grey bars). Cell length was measured using phase contrast images of 30 cells (red line). (C) Changes in WT cell number during development as determined by direct counts. Rod-shaped cells (blue); myxospores (black). Lipid body containing cells were enumerated by Nile red staining (red).

The area occupied by lipid bodies at the peak production is about 1.6 μm^2. There are usually two large lipid bodies located near the poles of the cell (figure 4-1A). Sometimes there is a third lipid body located in the center of the cell. The lipid bodies are so prominent they are seen as darkened areas in cells observed by phase contrast microscopy, for example the cells shown in figure 4-1A. Lipid bodies decline in area and number after 18-24 h suggesting that their contents are utilized by the cell. In the case of sporulating cells, lipids bodies are no longer visible after spore maturation though some of the lipids remain (Bode et al., 2009, Hoiczyk et al., 2009).

Cells undergoing PCD produce lipid bodies. At peak production nearly 90% of the cells contain lipid bodies (figure 4-1C). The peripheral rods, which comprise about 10% of the population, do not make lipid bodies (Hoiczyk et al., 2009). *M. xanthus* development involves population reduction by PCD (Nariya & Inouye, 2008). During wild type DK1622 development an 80% decline in cell number was accompanied by a corresponding decline in the number of cells containing lipid bodies (figure 4-1C). These results suggest that cells undergoing PCD produce lipid bodies. This phenomenon was studied in more detail by taking advantage of the fact that in certain mixtures of strains one cell type preferentially undergoes PCD while the other cell type preferentially sporulates. One such mixture is Δ*difA* mixed with DK1622 cells.

When allowed to develop alone Δ*difA* cells fail to undergo either PCD or sporulation (figure 4-2A). Lipid body synthesis is delayed relative to wild type cells but eventually the majority of the cells produce lipid bodies. The number of lipid bodies in Δ*difA* cells is far greater than in wild type cells but they are smaller and do not have the same spatial distribution (figure 4-2B).

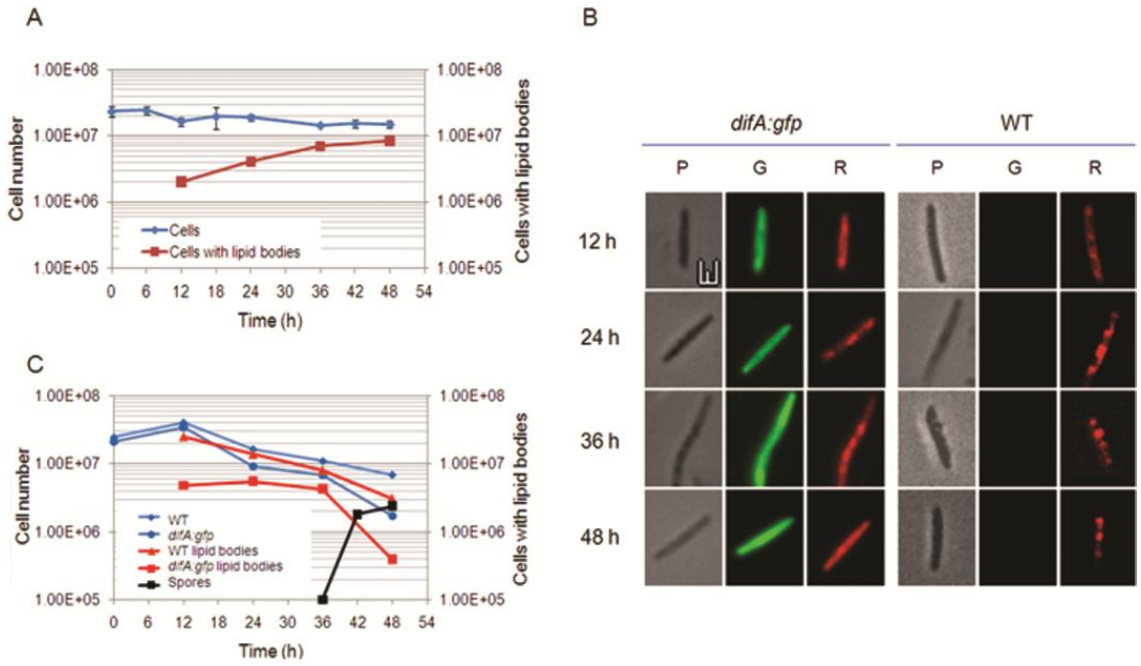

Figure 4-2: Lipid body production in Δ*difA* and WT + Δ*difA* cells during development. (A) Changes in LS2472 (Δ*difA*, P_{pilA}-*gfp*) cell number at various time during development as determined by direct counts (blue). Lipid body containing cells (red). B) WT and LS2472 were mixed 1:1 and stained with Nile red at various times. Phase (P), green fluorescence (G), and red fluorescence (R). Bar is 1 µm (C) Changes in WT and LS2472 cell number were enumerated by direct counts of rod-shaped cells (blue) and myxospores (black). LS2472 cells were identified by using the green channel. Lipid body containing cells were identified by Nile red staining.

The total area of the lipid bodies in Δ*difA* cells is about half of that found in wild type cells at 24 h due in part to delayed synthesis. In these experiments the *difA* mutant contained a constitutively expressed gene encoding the green fluorescent protein (*gfp*) to distinguish Δ*difA* cells from wild type cells. Δ*difA* and WT cells were mixed in equal ratio and allowed to develop on TPM agar. The developing cells were stained with Nile red every 6 h and examined under a fluorescence microscope (figure 4-2B). Cells were also enumerated in the green channel to examine population changes of Δ*difA* cells (figure 4-2C). Overall Δ*difA* cells decline in number by over 90% as development progresses. Δ*difA* cells form only 0.1% of the spore population (data not shown) suggesting that WT cells stimulate Δ*difA* PCD. In this mixture, production of lipid bodies by the Δ*difA* cells is still delayed relative to WT cells (Figure 4-1). Reflecting this delay the number of lipid body containing Δ*difA* cells initially increase then declines steadily after 24 h. Wild type cells also undergo some PCD, though not as extensively as Δ*difA* cells since they form 99.9% of the spores.

Lipid bodies become extracellular during development. PCD would be expected to release lipid bodies into the fruiting body. The presence of extracellular lipid bodies in wild type fruiting bodies was examined in submerged culture in order to minimize artificial cell lysis. Fruiting bodies were stained with Nile red, then opened by gently pressing the coverslip against a clean glass slide in the presence of ficoll to stabilize the cell membrane. Free lipid bodies could be observed at both 24 (figure 4-3A) and 48 h.

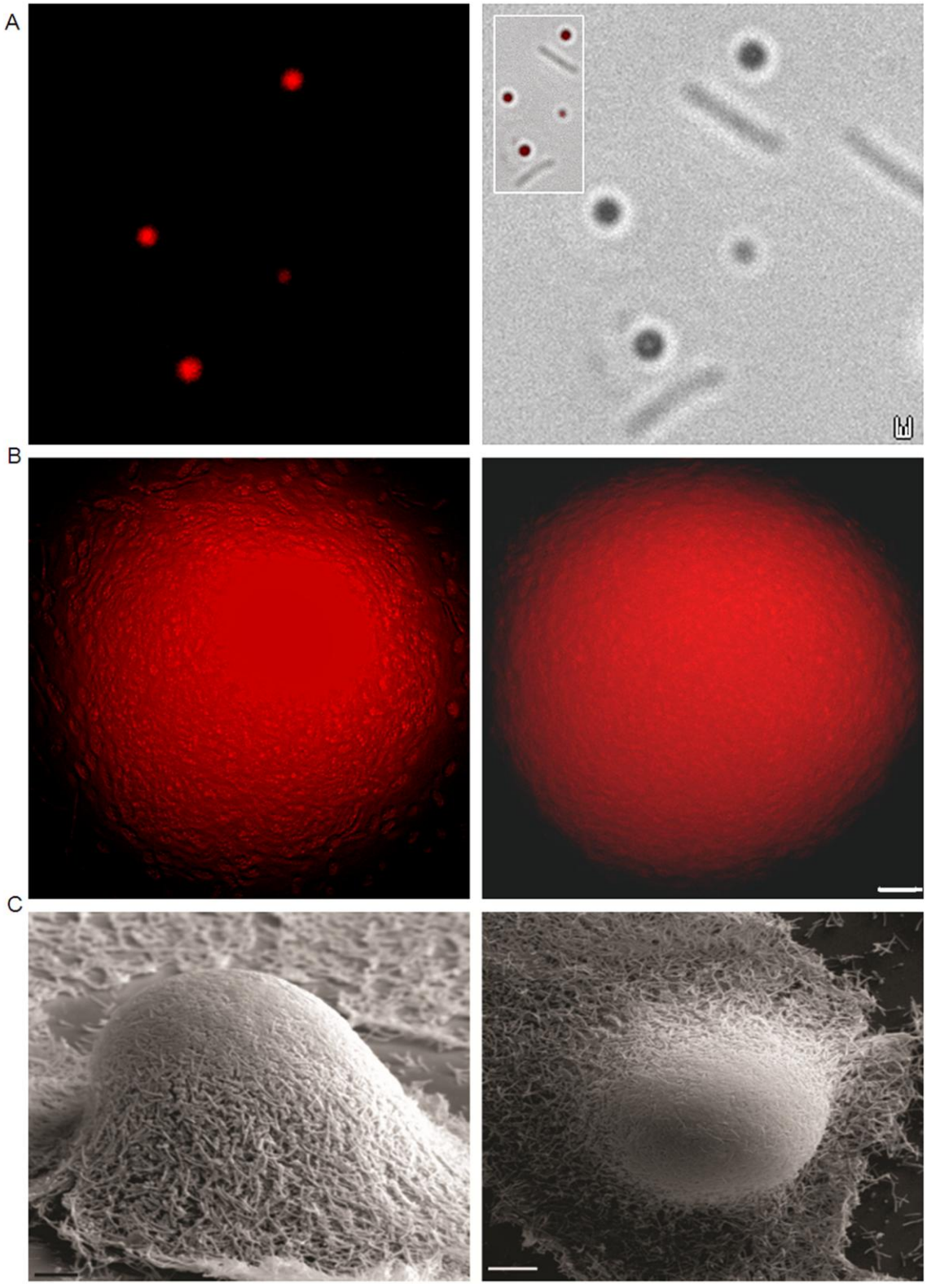
A
B
C

Figure 4-3: Lipid body synthesis in submerged culture fruiting bodies. (A) 24 h Nile red stained fruiting bodies were broken by gently putting pressure against a glass slide to release their contents. Nile red (left) and phase (right) images. Inset is merged image of phase and fluorescence images. Bar is 1 µm (B) 48 h developing fruiting bodies were stained with Nile red and optically sectioned under a fluorescence microscope. Uppermost section (left) and middle section (right) Bar is 2 µm (C) SEM of 48 h fruiting bodies. Images were taken from side (left), bar is 10 µm and top (right), bar is 20 µm.

The location of the lipid bodies within the fruiting body was determined in 48 h fruiting bodies that were imaged from the top down in a series of 0.1 μm optical sections. Figure 4-3C compares an optical section of the uppermost layer (left) with a middle section (right). Both sections reveal the presence of lipid bodies within cells. However, the uppermost section contains free lipid that appears to coat the surface of the fruiting body.

Fruiting bodies examined by scanning electron microscopy appear to have a cap-like structure at the top of the fruiting body that extends partway down the sides (Figure 4-3C). The material in the cap may also contain polysaccharide and protein (Behmlander & Dworkin, 1994). The developmental defects of *difA* and *difE* mutants can be partially corrected by addition of ECM material suggesting that it has morphogenic properties, though the morphogen has not been identified (Chang & Dworkin, 1994, Yang *et al.*, 2000).

Lipid bodies contain E-signal. Having established that cells undergoing PCD release their lipid bodies, we wanted to determine whether lipid bodies contain developmental morphogens. The E-signal is an extracellular signal required for sporulation whose chemical structure is unknown. The E-signal is thought to contain *iso* 15:0 since elimination of E-signal production requires mutation of two metabolic pathways, each of which produce the primer for the synthesis of *iso* 15:0.

We attempted to purify the E-signal by taking advantage of the capacity of lipid body lipids to restore development of an *esg MXAN4265* double mutant, which makes <10% of the WT level of *iso* 15:0 (Bode et al., 2009). *M. xanthus* DK5614, which is unable to synthesize straight chain fatty acids, was used as a source of E-signal since it is

highly enriched in branched chain fatty acids (Bode et al., 2006a). Lipids were extracted after 24 h of development and fractionated by solid phase extraction on silica gel with solvents of increasing polarity. Five lipid fractions were assayed for their ability to rescue *esg MXAN4265* sporulation. Different amounts of lipid were applied to Whatman filter paper disks then applied to mutant cells undergoing development. During the four day incubation period the cells climb on to the disks and, if a stimulatory lipid is present, form myxospores. The undifferentiated vegetative cells were killed by taking advantage of their sensitivity to heat. Spores on filter discs were germinated on nutrient rich CYEK medium. After 24-48 h of incubation, the spores germinate and swarms of cells migrate away from the filter paper disks. Swarming is a social behavior and the rate of swarm expansion is directly proportional to the original number of cells (Kaiser & Crosby, 1983). Thus, the higher the number of spores that germinate, the more rapidly the swarm expands. The bioactivity of each lipid fraction was quantified by identifying the lipid amount that caused half maximal swarm expansion from a plot of lipid amount vs. swarm expansion (figure 4-4A).

All fractions rescued *esg MXAN4265* development to some extent, though fraction 1 was by far most active at 5 µg/disk (figure 4-4B). Fraction 2, enriched in ester-linked triglycerides, fraction 4, enriched in mono- and diacylglycerides, and fraction 5, enriched in phospholipids, were active only at concentrations 20-500 fold higher than fraction 1 (data not shown). As these fractions contain lipids with *iso* 15:0, we suspect that extracellular lipases produce free *iso* 15:0 that is used to synthesize the E-signal, thereby bypassing the mutational block (Moraleda-Munoz & Shimkets, 2007). Likewise, fraction 3, enriched in free fatty acids, could provide ample *iso* 15:0 substrate for E-signal

A

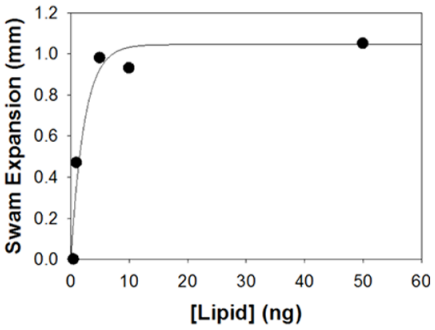

B

Purification step	Purification method	Bioactivity (µg/disk)	Fold purification
Crude lipid	Methanol/Chloroform extraction	30	
Step 2	LC-Si solid phase extraction	5	6
Step 3	TLC	0.1	300

C

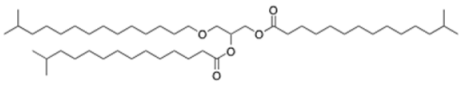

TG-1 (1-i15:0-alkyl-2,3-di-i15:0-acyl glycerol)

Figure 4-4: Bioassay of extracted lipid. (A) An example of a plot of a lipid fraction vs swarm distance. (B) Stepwise purification of E-signal. Bioactivity refers to lipid concentration for 1/2max swarm expansion. (C) Chemical structure of the principle TAG in the active fraction.

synthesis. Fraction 3 was 6-fold less active than fraction 1. Because of its impressive activity, fraction 1 is the most likely candidate fraction for the E-signal.

Lipids in fraction 1, were further separated by preparative silica gel thin layer chromatography, which produced five lipid spots, each of which was extracted, quantified and assayed. Only one fraction was able to produce spores with the *esg MXAN4265* mutant. This fraction had an R_f value of 0.4 and the ½ max concentration that rescued development was 0.1 µg representing a 50-fold purification over the previous step.

Matrix-assisted laser desorption/ionization (MALDI) was used to analyze the active fraction. MALDI uses a soft ionization technique, which creates large fragments and therefore is ideal for identifying large organic molecules. MALDI analysis revealed the ether lipid, TG-1 (figure 4-4C) as one of the components (data not shown). A second component included a closely related derivative of TG-1 containing *iso* 17:0, rather than *iso* 15:0, at the *sn*-2 position. No other lipids with branched chain fatty acids were identified. These results suggested that these ether lipids are the E-signal.

Many developmental mutants are unable to synthesize lipid bodies. 33 developmental mutants were examined for lipid body formation at 18 h, the peak of lipid body production in wild type. Cells were stained with Nile red, and the lipid body area per cell was averaged from 30 cells and given as a percent of WT cells (figure 4-5A). At least six extracellular signals are required for fruiting body development (Shimkets, 1999). We examined the relevance of each signal to lipid body production by quantifying lipid bodies in signaling deficient mutants. Figure 4-5B provides a simplistic model of the lipid body regulon in *M. xanthus* during various stages of development.

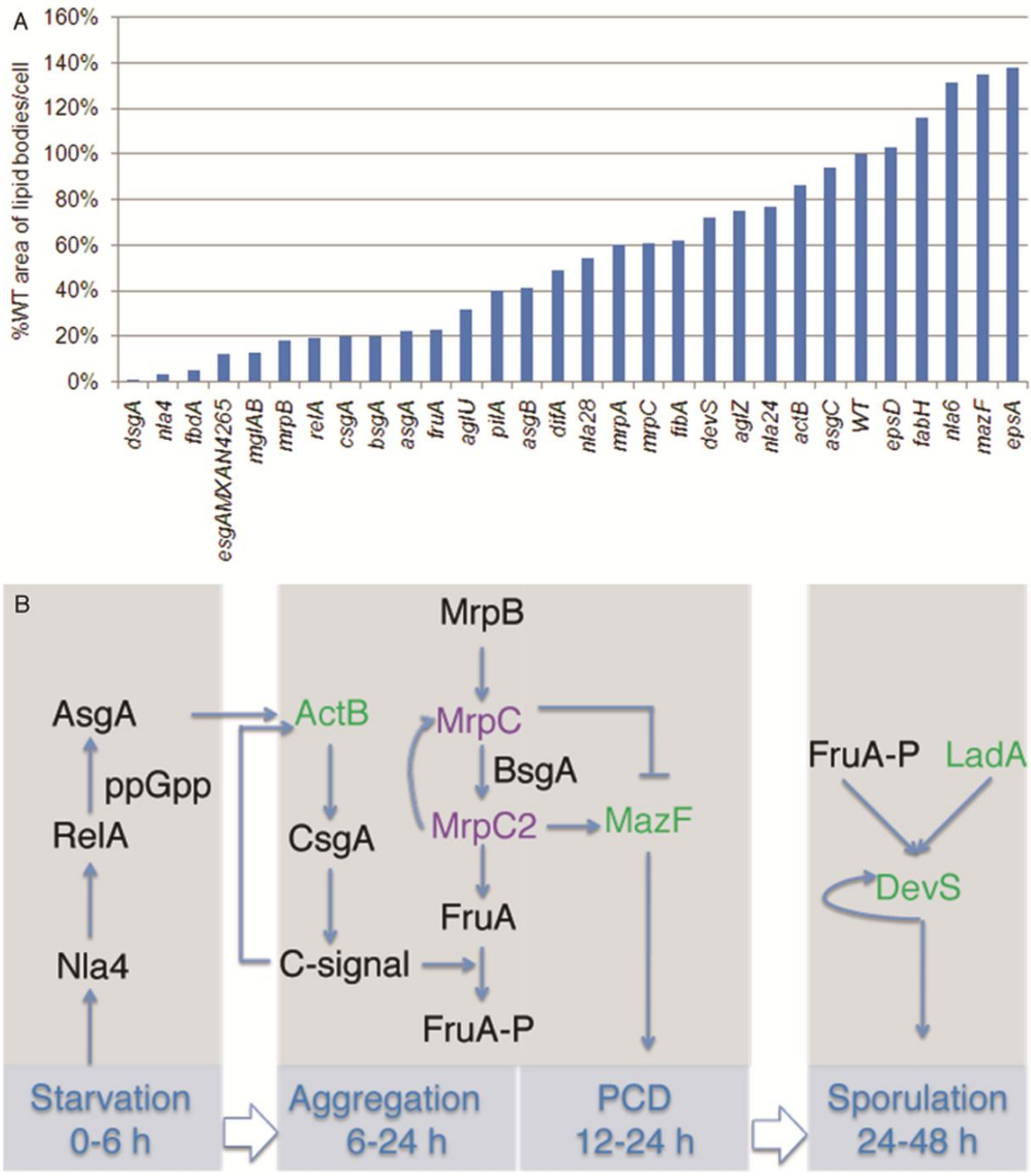

Figure 4-5: Regulation of lipid body production during *M. xanthus* fruiting body development. (A) Lipid body production in developmental mutants. Average lipid body area was calculated for 30 cells and compared with WT in terms of percentages. (B) Lipid body regulon. Mutants blocked in synthesis of proteins highlighted in black are deficient in lipid body synthesis (>20%), those in green produce WT levels (70-100%). Those in purple produce intermediate levels of lipid bodies (20-70%).

Development begins with amino acid deprivation. *relA* and *nla4*, which are essential for production of (p)ppGpp and the stringent response, are also blocked in lipid body production (Figure 4-5B) (Caberoy *et al.*, 2003, Singer & Kaiser, 1995). One gene is required for synthesis of the D-signal (*dsgA*, 1%). *dsgA* compromises lipid body production more seriously than any other mutation (figure 4-5A). *dsgA* is an essential gene that encodes translation initiation factor IF-3. This particular allele has a point mutation that impacts D-signaling while supporting translation initiation (Cheng et al., 1994). As lipid body synthesis is induced by inhibitors of translation, such as amino acid deprivation and kanamycin, it is possible that translation arrest, the stringent response, and D-signaling initiate lipid body production near the onset of development.

Starvation sensing leads to an unusual form of quorum sensing mediated by the A-signal that ascertains whether a sufficient cell density is available to form a fruiting body. Five genes are required for production of the A-signal, *asgA*, *asgB*, *asgC*, *asgD*, and *asgE*. While *asgA* (22%) and *asgB* (41%) deficient strains produce less lipid, the *asgC* (94%) mutant produces nearly normal levels. These results argue that lipid body production is not dependent on the A-signal but requires some secondary function provided by *asgA* and *asgB*. AsgA is a hybrid histidine kinase/response regulator (Plamann et al., 1995). AsgB is a putative DNA binding protein that seems to be essential for growth (Plamann et al., 1994). It is possible that AsgA and AsgB directly or indirectly activate genes required for lipid body production in addition to regulating A-signal production.

A-signaling initiates the expression of *actB*, which encodes a transcriptional activator of the *act* operon along with *actA* (Gronewold & Kaiser, 2007) (Figure 4-5B).

ActA and ActB are required for enhanced expression of the *csgA* gene (Gronewold & Kaiser, 2007). *csgA* produces the intercellular C-signal, which is essential for aggregation and sporulation (Shimkets et al., 1983). C-signaling activates response regulator FruA, a transcriptional activator of many morphogenesis genes (Søgaard-Andersen et al., 1996). Curiously, *csgA* mutants are blocked in aggregation, sporulation, and lipid body synthesis whereas *actB* mutants form aggregates, but are unable to sporulate, and produce nearly normal levels of lipid bodies. This anomaly may be explained by the difference in C-signal levels observed during different stages of development (Gronewold & Kaiser, 2001). As levels of C-signal rise, aggregates are formed. Only at the highest levels of C-signal is sporulation is induced (Kim & Kaiser, 1991). Gronwold et al showed that although ActB is essential for increasing C-signaling, *actB* mutants produce one-fourth of WT level of *csgA* protein which is sufficient to induce aggregation (Gronewold & Kaiser, 2002). This level of C-signaling is perhaps also sufficient to induce lipid body formation. *mglAB* is nonmotile and consequently defective in C-signaling, which requires cell alignment for efficient transmission of C-signal (Kim & Kaiser, 1990). *mglAB* makes fewer and smaller lipid bodies than *csgA* mutants.

Among the cell fate determination genes are *mrpC*, *mazF* and *fruA*. MrpC activates transcription of *fruA*, and together with FruA activates transcription of many genes responsible for sporulation (Figure 4-5B) (Ueki & Inouye, 2003, Sun & Shi, 2001a, Mittal & Kroos, 2009). In addition, MrpC is the antitoxin for the MazF toxin that mediates PCD (Nariya & Inouye, 2008). *mrpC* and *fruA* mutants under produce lipid bodies while the *mazF* mutant overproduces them (Figure 4-5A). One gene is required for

synthesis of the B-signal, a Lon protease referred to as BsgA (Gill & Bornemann, 1988, Gill *et al.*, 1988). Loss of BsgA (20%) leads to dramatic reductions in lipid bodies. BsgA activates MrpC by hydrolyzing 25 amino acids from the N-terminus (Nariya & Inouye, 2006). The developmental phenotype and lipid body phenotype of *bsgA* is far different from MrpC suggesting that BsgA may have more than one developmental function.

The sporulation of cells within the fruiting bodies is triggered by the *devTRS* genes, which are activated in part by FruA-P (Julien *et al.*, 2000, Thony-Meyer & Kaiser, 1993) (Viswanathan et al., 2007b). *devTRS* is also regulated by a second LysR-type activator, LadA, which also directly binds to the *dev* region. Both LadA and FruA binding are essential for full activation of *dev* (Figure 4-5B) (Viswanathan et al., 2007b). While *fruA* expression is required for lipid body synthesis, both *ladA* (data not shown) and *dev* mutants produce nearly WT level of lipid bodies. These results suggest that lipid body synthesis is probably not regulated by late developmental genes.

Many mutants produce reduced levels of ECM, which is at least partially responsible for the cap on the top of the fruiting bodies and stimulation of twitching (S) motility (Behmlander & Dworkin, 1994, Shi *et al.*, 2000). Several mutants were examined to determine whether lipid body production depends on synthesis of the protein and exopolysaccharide portions of the ECM. FibA is the major protein in the ECM (Kearns et al., 2002). A *fibA* mutant produces 62% of wild type levels while *pilA*, which is required for S-motility and ECM production, produces 40% of the wild type levels The exopolysaccharide portion of the ECM requires the *epsA* and *espD* genes (Lu et al., 2005b). The *epsA* mutant makes excessive amounts of lipid bodies (138%) and the *epsD* mutant normal levels (103%). Thus blocking the synthesis of the protein and

exopolysaccharide portion of the ECM does not dramatically diminish lipid body production. However, lipid body production may be necessary for ECM production. Mutants that are most dramatically impaired for lipid body production (<20%) have reduced ECM production. These include *fbdA, nla4, relA, mrpB,* and *mglAB* (Bonner & Shimkets, 2006, Ossa *et al.*, 2007, Singer & Kaiser, 1995, Sun & Shi, 2001a). The results suggest that lipid synthesis may be required for optimal production of other extracellular materials.

Discussion

During myxospore formation the rod-shaped cells shorten and eventually form spherical spores (Shimkets & Seale, 1975, Voelz & Dworkin, 1962). By 24 h cell length is less than 50% compared to vegetative cells. Such a drastic change requires reduction of a large portion of the cell membrane. It appears as if lipid bodies are synthesized from membrane turnover. While direct evidences supporting this hypothesis is lacking, the observation of small lipid bodies close to the membrane early in development suggests that lipid bodies are probably produced on the cell membrane (figure 4-1C). This is similar to what has been observed in other organisms. Lipid body studies in other bacteria have revealed the cytoplasmic membrane as the site of lipid body synthesis while in eukaryotes, lipid bodies are produced between the two leaflets of endoplasmic reticulum (Waltermann et al., 2005) (Robenek et al., 2006).

As the cell length diminishes the lipid body area increases until 18 h when it reaches its peak. Lipid bodies are absent in peripheral rods, which are unaltered in cell length over the course of development. In addition, the lengths of several lipid body deficient mutants such as *nla4*, *relA* and *asgA* remain unchanged. These results suggest

that lipid body synthesis is a consequence of cell length reduction. In this regard, the lipid bodies may protect cells by compartmentalizing free fatty acids and lipid species that are toxic to the cells (Rosenbluh & Rosenberg, 1990, Gelvan *et al.*, 1987)

The *M. xanthus* inner membranes are mainly composed of phosphotidylethanolamine (PE) with *iso* 15:0 being the most abundant fatty acid (Orndorff & Dworkin, 1980, Ware & Dworkin, 1973, Curtis *et al.*, 2006). To synthesize the most abundant lipid body lipids such as tri *iso* 15:0 requires hydrolysis of the phosphoethanolamine head group by phospholipase C producing diacylglycerol. A diacylglycerol acyltransferase (DGAT) could then catalyze synthesis of TAG. A gene encoding an *M. xanthus* homolog of DGAT was disrupted with no noticeable effect on triglyceride production (Hoiczyk et al., 2009). This suggests that TAG synthesis may utilize a novel mechanism in *M. xanthus*.

The lipid bodies, which are released by PCD, contain at least one developmental morphogen, the E-signal. MALDI analysis of the purified active lipid fraction identified two branched chain lipids, TG-1 and a second ether lipid that contains *iso* 17:0 at the *sn*-2 position. The concentration required to restore sporulation of E-signaling mutant LS1191 was as low as 100 ng. Further evaluation of TG-1 as the E-signal requires chemically synthesized TG-1.

Methods and Materials

Bacterial strains and growth condition. Table 4-1 lists the bacterial strains used in this study. *M. xanthus* strains were grown in CYE broth [1% Bacto casitone (Difco), 0.5% yeast extract (Difco), 10 mM 4-morpholinepropanesulfonic acid (MOPS) (pH 7.6), and

Table 4-1: Bacterial strains used in this study.

Bacterial strain	Genotype	Reference or source
DK1622	WT	(Kaiser, 1979)
DK3260	*dsgA*	(Cheng & Kaiser, 1989)
DK4398	*asgB*	(Kuspa et al., 1986)
DK5057	*asgA*	(Hagen et al., 1978)
DK5061	*asgC*	(Kuspa & Kaiser, 1989)
DK5614	*fabH*	(Bode et al., 2006a)
DK6204	*mglAB*	(Hartzell & Kaiser, 1991)
DK8606	Δ*pilA aglB1* P_{pilA}-*gfp*	(Wall & Kaiser, 1998)
DK10410	*ΔpilA*	(Wu & Kaiser, 1997)
DK10603	*actB*	(Gronewold & Kaiser, 2007)
DK11063	*fruA*	(Søgaard-Andersen et al., 1996)
DK11209	*devS*	(Viswanathan et al., 2007a)
LS1191	*esgA MXAN4265*	This study
LS2208	Δ*fibA*	Lawrence Shimkets
LS2225	*fbdA*	(Bonner & Shimkets, 2006)
LS2442	*ΔcsgA*	Lawrence Shimkets
LS2472	Δ*difA*, P_{pilA}-*gfp*	This study
MS10	*relA*	(Harris et al., 1998)
AG328	*nla28*	(Caberoy et al., 2003)

AG304	*nla4*	(Caberoy et al., 2003)
AG306	*nla6*	(Caberoy et al., 2003)
MTH8-1	*MXAN4265*	(Hao et al., 2002)
MXH1777	*aglU*	(White & Hartzell, 2000)
MXH2265	*aglZ*	(Yang et al., 2004)
AG324	*nla24*	(Caberoy et al., 2003)
M252	*bsgA*	(Gill et al., 1988)
SW810	Δ*epsA*	(Lu et al., 2005a)
SW813	Δ*epsD*	(Lu et al., 2005a)
SW2802	Δ*mrpB*	(Sun & Shi, 2001c)
SW2807	Δ*mrpA*	(Sun & Shi, 2001c)
SW2808	Δ*mrpC*	(Sun & Shi, 2001c)
SW600	*frzE*	(Shi et al., 2000)
YZ601	Δ*difA*	(Xu et al., 2005)
LS1193	*mazF*	Lawrence Shimkets

0.1% $MgSO_4$)] at 32°C with vigorous shaking. Kanamycin and agar (Difco) were added to CYE at final concentrations of 50 µg/ml and 1.5% respectively. Starvation was induced on TPM agar plates [10 mM Tris HCl, pH 7.6, 1 mM $KH(H_2)PO_4$, pH 7.6, 10 mM $MgSO_4$, 1.5% agar (Difco)].

Nile red staining. *M. xanthus* strains were grown to a density of 5×10^8 cells/ml then resuspended in 100 µl dH_2O to a final density of 5×10^9 cells/ml. 10 µl of cells were spotted on TPM agar and incubated for various times. Lipid body staining was carried out as described by Hoiczyk et al with modifications (Hoiczyk et al., 2009). A 0.5 mg/ml stock solution of Nile red (Sigma Aldrich) prepared in 100% ethanol, was diluted in dH_2O to a final concentration of 1.25 µg/ml and added directly on top of developing cells on TPM agar. The plates were incubated for 2 h at 32°C. Cells were resuspended in a drop of TPMF buffer [TPM buffer containing 10% ficoll], and examined with a fluorescence microscope (Leica Microsystems, DM5500B). Digital images were obtained using a QICAM FAST 1394 camera (Q Imaging systems, Compix Inc.).

The fluorescence images were digitally altered using the Simple PCI software (Hamamatsu Corporation), which removed background noise and improved contrast. Each lipid body was highlighted and the area calculated. Average lipid body area and cell length were calculated from 30 to 50 cells. Those cells that did not make lipid bodies were not discounted while averaging.

Submerged culture. Submerged culture development was carried out as described by Kuner and Kaiser (Kuner & Kaiser, 1982). *M. xanthus* cells were grown to a density of 5×10^8 cells and diluted to 1.25×10^8 cells/ml in CYE broth. 10 ml of the cell suspension and 4 to 5 (25×25 mm) coverslips were transferred to a 60 × 15 mm petri plate. The plate

was incubated at 32°C for 12 h while a thin biofilm formed on the surfaces of the coverslips. Starvation was induced by replacing the CYE broth with cohesion buffer [10 mM MOPS, pH 6.8, 1 mM $MgCl_2$, 1 mM $CaCl_2$] and incubated at 32°C. Coverslips with developing cells were stained with Nile red at a final concentration of 1.25 µg/ml in cohesion buffer containing 15% ficoll, for 2 h at 32°C. The coverslips were gently pressed against a glass slide to break fruiting bodies in order to view extracellular lipid bodies.

Construction of *M. xanthus* strains Mx4 generalized transduction was used for strain construction (Campos et al., 1978). The *esg258* allele from JD300 was transduced into MTH8-1 to create LS1191 by selecting for kanamycin resistance (Kroos *et al.*, 1986, Downard et al., 1993). To create LS2472 (*difA* P_{pilA}-*gfp*), Mx4 was grown on DK8606, which contains *gfp* under the control of *pilA* promoter (Wall & Kaiser, 1998). This gene was transferred into Δ*difA* strain YZ601 by Mx4 transduction with selection for kanamycin resistance (Xu et al., 2005).

Extracellular complementation. *M. xanthus* strains, DK1622 (WT) and LS2472, were grown to a density of 5×10^8 cells/ml, and resuspended in water to a final cell density of 5×10^9 cells/ml. Cells were mixed in a 1:1 ratio by vortexing. 10 µl of the mixture was spotted on TPM agar and incubated at 32°C. Cells spots were stained with Nile red as described above. Cells were fixed by resuspending in TPM buffer containing 2% paraformaldehyde and 10% ficoll. Simultaneously, cells were also examined using a fluorescence microscope for lipid body production. Cross-linked cells were sonicated and enumerated using a Petroff Hausser counting chamber.

Scanning electron microscopy *M. xanthus* development was examined by scanning electron microscopy (SEM) as described by Kuner and Kaiser with a few modifications (Kuner & Kaiser, 1982). *M. xanthus* cells were grown to a density of 5×10^8 cells and diluted to 1.25×10^8 cells/ml in CYE broth. 1 ml of the cell suspension and a sterile circular coverslip (12 mm diameter) was transferred to each well of a polystyrene, tissue culture plate (Becton Dickinson Labware). The plate was incubated at 32°C for 12 h during which a thin biofilm formed on the coverslip. Starvation was induced by replacing the CYE broth with cohesion buffer and incubated at 32°C. 2.5% glutaraldehyde was added to one well every 6 h until 48 h. Glutaraldehyde was removed and the coverslips were washed twice with dH_2O. 4% osmium tetroxide in 1x PBS [137 mM NaCl, 2.7 mM KCl, 10 mM Na_2HPO_4, 1.76 mM KH_2PO_4, pH 7.4] was added, and incubated for 1 h at room temperature. The coverslips were dehydrated in a series of ethanol solutions including 10%, 25%, 50%, 75%, and twice with 100% ethanol. The coverslips were subjected to critical point drying and sputter coated with gold. The fruiting bodies were viewed in a scanning electron microscope (Zeiss 1450EP variable pressure).

Lipid purification from developing cells *M. xanthus* strain DK5614 was grown to a density of 5×10^8 cells/ml and resuspended to a final density of 5×10^9 cells/ ml. The cells were plated on TPM agar and incubated at 32°C for 18 h. Cells were resuspended in 5 ml of dH_2O. Lipids were extracted with chloroform-methanol as described by Bligh and Dyer (Bligh & Dyer, 1959). *M. xanthus* cells were disrupted by sonication followed by addition of chloroform-methanol (2:1). The mixture was vigorously vortexed and incubated on ice for 10 min. One volume of chloroform and one volume of water were

added, and the mixture was centrifuged for 15 min at 5000×g. The chloroform layer was collected in a beaker and the solvent evaporated.

Lipids were fractionated by solid phase extraction using Sep-pak columns (Supelco) (Hamilton & Comai, 1984). The columns were washed with 4 ml of hexane/methyl-tertiarybutylether (MTBE) (96:4) followed by 12 ml hexane. Lipids, dissolved in hexane/MTBE (200:3), were loaded on to the column. 10 ml of hexane/MTBE (200:3) was added, and eluted (Fraction 1). Then 12 ml of hexane/MTBE (96:4) was added for the elution of triglycerides (Fraction 2). The column was acidified by the addition of hexane/acetic acid (100:0.2). This was followed by addition of 12 ml hexane/MTBE/acetic acid (100:2:02) to obtain free fatty acids (Fraction 3). Then 12 ml of MTBE/acetic acid (100:0.2) was added to elute diglycerides and monoglycerides (Fraction 4). Finally, phospholipids were eluted using MTBE:methanol:ammonium acetate (100:4:1) (Fraction 5). The five fractions were dried in pre-weighed vials, dissolved in chloroform/methanol (2:1), and stored at -20°C.

Thin layer chromatography (TLC). Fraction 1 was resolved with chloroform/cyclohexane (1:1) on a silica gel TLC plate (*Silica gel GF, Fisher scientific*) (Sherma, 2004). Iodine vapor was used to identify the lipid spots. Lipid was harvested from the silica gel in an Erlenmeyer flask equipped with a sintered funnel and vaccum aspirator using 5-10 ml chloroform/methanol (2:1) with stirring for 5 min. The silica gel was washed two more times with the same solvent. All three extracts were combined and the solvent evaporated. Lipids were weighed, dissolved in chloroform:methanol (2:1), and stored at -20°C.

Lipid bioassay. Lipid fractions were assayed for their ability to rescue sporulation of LS1191. Cells were grown to a density of 5×10^8 cells/ml, harvested, and resuspended in dH_20 to a final density of 5×10^8 cells/ml. 50 µl of cells were spotted on TPM plates, allowed to air dry and incubated at 32°C for 24 h. Lipid amounts ranging from 0 to 10 µg were applied to sterile, circular, Whatman #2 filter paper discs (7 mm), dried, and then placed on top of cell spots. The plates were incubated for 96 h at 32°C. The plates were incubated at 50°C for 2 h to kill vegetative cells. The plates were cooled and filter discs were then transferred to CYEK plates. The plates were incubated for 24-48 h until swarms of cells appeared around the filter disc. The swarm sizes at five equidistant points were recorded using a phase contrast microscope (Leitz Laborlux) with an ocular micrometer (Kaiser & Crosby, 1983). The average swarm size was plotted against lipid concentration.

Acknowledgements

We would like to thank Dr. John P. Shields and Ricky Patel for their assistance with TEM. This work was supported by research grant MCB 0742976 from the National Science Foundation.

References

Almahbobi, G. & P. F. Hall, (1990) The role of intermediate filaments in adrenal steroidogenesis. *J Cell Sci* **97 (Pt 4)**: 679-687.

Alvarez & Steinbüchel, (2002) Triacylglycerols in prokaryotic microorganisms. *Appl Microbiol and Biotechnol* **60**: 367-376.

Behmlander, R. M. & M. Dworkin, (1994) Biochemical and structural analyses of the extracellular matrix fibrils of *Myxococcus xanthus*. *J Bacteriol* **176**: 6295-6303.

Bell, M., H. Wang, H. Chen, J. C. McLenithan, D. W. Gong, R. Z. Yang, D. Yu, S. K. Fried, M. J. Quon, C. Londos & C. Sztalryd, (2008) Consequences of lipid droplet coat protein downregulation in liver cells: abnormal lipid droplet metabolism and induction of insulin resistance. *Diabetes* **57**: 2037-2045.

Bligh, E. G. & W. J. Dyer, (1959) A rapid method of total lipid extraction and purification. *Can J Biochem Physiol* **37**: 911-917.

Bode, H. B., M. W. Ring, D. Kaiser, A. C. David, R. M. Kroppenstedt & G. Schwar, (2006a) Straight-chain fatty acids are dispensable in the myxobacterium *Myxococcus xanthus* for vegetative growth and fruiting body formation. *J. Bacteriol.* **188**: 5632-5634.

Bode, H. B., M. W. Ring, G. Schwär, M. O. Altmeyer, C. Kegler, I. R. Jose, M. Singer & R. Müller, (2009) Identification of additional players in the alternative biosynthesis pathway to Isovaleryl-CoA in the myxobacterium *Myxococcus xanthus*. *ChemBioChem* **10**: 128-140.

Bode, H. B., M. W. Ring, G. Schwar, R. M. Kroppenstedt, D. Kaiser & R. Muller, (2006b) 3-Hydroxy-3-methylglutaryl-coenzyme A (CoA) synthase is involved in biosynthesis of isovaleryl-CoA in the myxobacterium *Myxococcus xanthus* during fruiting body formation. *J Bacteriol* **188**: 6524-6528.

Bonner, P. J. & L. J. Shimkets, (2006) Cohesion-defective mutants of *Myxococcus xanthus*. *J Bacteriol* **188**: 4585-4588.

Bozza, P. T., J. L. Payne, S. G. Morham, R. Langenbach, O. Smithies & P. F. Weller, (1996) Leukocyte lipid body formation and eicosanoid generation:

cyclooxygenase-independent inhibition by aspirin. *Proc Natl Acad Sci U S A* **93**: 11091-11096.

Caberoy, N. B., R. D. Welch, J. S. Jakobsen, S. C. Slater & A. G. Garza, (2003) Global mutational analysis of NtrC-like activators in *Myxococcus xanthus*: Identifying activator mutants defective for motility and fruiting body development. *J. Bacteriol.* **185**: 6083-6094.

Campos, J. M., J. Geisselsoder & D. R. Zusman, (1978) Isolation of bacteriophage MX4, a generalized transducing phage for *Myxococcus xanthus*. *J Mol Biol* **119**: 167-178.

Chang, B. Y. & M. Dworkin, (1994) Isolated fibrils rescue cohesion and development in the Dsp mutant of *Myxococcus xanthus*. *J Bacteriol* **176**: 7190-7196.

Cheng, Y. & D. Kaiser, (1989) *dsg*, a gene required for *Myxococcus* development, is necessary for cell viability. *J Bacteriol* **171**: 3727-3731.

Cheng, Y. L., L. V. Kalman & D. Kaiser, (1994) The *dsg* gene of *Myxococcus xanthus* encodes a protein similar to translation initiation factor IF3. *J Bacteriol* **176**: 1427-1433.

Curtis, P. D., R. Geyer, D. C. White & L. J. Shimkets, (2006) Novel lipids in *Myxococcus xanthus* and their role in chemotaxis. *Environ Microbiol* **8**: 1935-1949.

Downard, J., S. V. Ramaswamy & K. S. Kil, (1993) Identification of *esg*, a genetic locus involved in cell-cell signaling during *Myxococcus xanthus* development. *J. Bacteriol.* **175**: 7762-7770.

Downard, J. & D. Toal, (1995) Branched-chain fatty acids: the case for a novel form of cell-cell signalling during *Myxococcus xanthus* development. *Mol Microbiol* **16**: 171-175.

Gelvan, I., M. Varon & E. Rosenberg, (1987) Cell-density-dependent killing of *Myxococcus xanthus* by autocide AMV. *J Bacteriol* **169**: 844-848.

Gill, R. E. & M. C. Bornemann, (1988) Identification and characterization of the *Myxococcus xanthus bsgA* gene product. *J Bacteriol* **170**: 5289-5297.

Gill, R. E., M. G. Cull & S. Fly, (1988) Genetic identification and cloning of a gene required for developmental cell interactions in *Myxococcus xanthus*. *J Bacteriol* **170**: 5279-5288.

Gronewold, T. M. A. & D. Kaiser, (2001) The act operon controls the level and time of C-signal production for *Myxococcus xanthus* development. *Mol Microbiol* **40**: 744-756.

Gronewold, T. M. A. & D. Kaiser, (2002) *act* operon control of developmental gene expression in *Myxococcus xanthus*. *J. Bacteriol.* **184**: 1172-1179.

Gronewold, T. M. A. & D. Kaiser, (2007) Mutations of the Act promoter in *Myxococcus xanthus*. *J. Bacteriol.* **189**: 1836-1844.

Hagen, D. C., A. P. Bretscher & D. Kaiser, (1978) Synergism between morphogenetic mutants of *Myxococcus xanthus*. *Dev Biol* **64**: 284-296.

Hamilton, J. G. & K. Comai, (1984) Separation of neutral lipids and free fatty acids by high-performance liquid chromatography using low wavelength ultraviolet detection. *Journal of Lipid Research* **25**: 1142-1148.

Hao, T., D. Biran, G. J. Velicer & L. Kroos, (2002) Identification of the {Omega}4514 regulatory region, a developmental promoter of *Myxococcus xanthus* that is transcribed in vitro by the major vegetative RNA polymerase. *J. Bacteriol.* **184**: 3348-3359.

Harris, B. Z., D. Kaiser & M. Singer, (1998) The guanosine nucleotide (p)ppGpp initiates development and A-factor production in *Myxococcus xanthus*. *Genes & Development* **12**: 1022-1035.

Hartzell, P. & D. Kaiser, (1991) Function of MglA, a 22-kilodalton protein essential for gliding in *Myxococcus xanthus*. *J Bacteriol* **173**: 7615-7624.

Hoiczyk, E., M. W. Ring, C. A. McHugh, G. Schwär, E. Bode, D. Krug, M. O. Altmeyer, J. Z. Lu & H. B. Bode, (2009) Lipid body formation plays a central role in cell fate determination during developmental differentiation of *Myxococcus xanthus.* *Molecular Microbiology* **74**: 497-517.

Julien, B., A. D. Kaiser & A. Garza, (2000) Spatial control of cell differentiation in *Myxococcus xanthus*. *Proc Natl Acad Sci U S A* **97**: 9098-9103.

Kaiser, D., (1979) Social gliding is correlated with the presence of pili in *Myxococcus xanthus*. *Proc Natl Acad Sci U S A* **76**: 5952-5956.

Kaiser, D. & C. Crosby, (1983) Cell movement and its coordination in swarms of *Myxococcus xanthus*. *Cell Motility* **3**: 227-245.

Kearns, D. B., P. J. Bonner, D. R. Smith & L. J. Shimkets, (2002) An extracellular matrix-associated zinc metalloprotease is required for dilauroyl phosphatidylethanolamine chemotactic excitation in *Myxococcus xanthus*. *J Bacteriol* **184**: 1678-1684.

Kim, S. K. & D. Kaiser, (1990) C-factor: a cell-cell signaling protein required for fruiting body morphogenesis of *M. xanthus*. *Cell* **61**: 19-26.

Kim, S. K. & D. Kaiser, (1991) C-factor has distinct aggregation and sporulation thresholds during *Myxococcus* development. *J Bacteriol* **173**: 1722-1728.

Kroos, L., A. Kuspa & D. Kaiser, (1986) A global analysis of developmentally regulated genes in *Myxococcus xanthus*. *Dev Biol* **117**: 252-266.

Kuner, J. M. & D. Kaiser, (1982) Fruiting body morphogenesis in submerged cultures of *Myxococcus xanthus*. *J. Bacteriol.* **151**: 458-461.

Kuspa, A. & D. Kaiser, (1989) Genes required for developmental signalling in *Myxococcus xanthus*: three asg loci. *J Bacteriol* **171**: 2762-2772.

Kuspa, A., L. Kroos & D. Kaiser, (1986) Intercellular signaling is required for developmental gene expression in *Myxococcus xanthus*. *Dev Biol* **117**: 267-276.

Lang, P. D. & W. Insull, Jr., (1970) Lipid droplets in atherosclerotic fatty streaks of human aorta. *J Clin Invest* **49**: 1479-1488.

Law, J. H. & M. A. Wells, (1989) Insects as biochemical models. *J Biol Chem* **264**: 16335-16338.

Li, J. Z., J. Ye, B. Xue, J. Qi, J. Zhang, Z. Zhou, Q. Li, Z. Wen & P. Li, (2007) Cideb regulates diet-induced obesity, liver steatosis, and insulin sensitivity by controlling lipogenesis and fatty acid oxidation. *Diabetes* **56**: 2523-2532.

Lu, A., K. Cho, W. P. Black, X.-y. Duan, R. Lux, Z. Yang, H. B. Kaplan, D. R. Zusman & W. Shi, (2005a) Exopolysaccharide biosynthesis genes required for social motility in *Myxococcus xanthus*. *Mol Microbiol* **55**: 206-220.

Lu, A., K. Cho, W. P. Black, X. Y. Duan, R. Lux, Z. Yang, H. B. Kaplan, D. R. Zusman & W. Shi, (2005b) Exopolysaccharide biosynthesis genes required for social motility in *Myxococcus xanthus*. *Mol Microbiol* **55**: 206-220.

Mittal, S. & L. Kroos, (2009) Combinatorial regulation by a novel arrangement of FruA and MrpC2 transcription factors during *Myxococcus xanthus* development. *J Bacteriol* **191**: 2753-2763.

Moraleda-Munoz, A. & L. J. Shimkets, (2007) Lipolytic enzymes in *Myxococcus xanthus*. *J Bacteriol* **189**: 3072-3080.

Murphy, D. J., (1993) Structure, function and biogenesis of storage lipid bodies and oleosins in plants. *Prog Lipid Res* **32**: 247-280.

Murphy, D. J. & J. Vance, (1999) Mechanisms of lipid-body formation. *Trends in Biochem. Sci.* **24**: 109-115.

Nariya, H. & M. Inouye, (2008) MazF, an mRNA interferase, mediates programmed cell death during multicellular *Myxococcus* development. *Cell* **132**: 55-66.

Nariya, H. & S. Inouye, (2006) A protein Ser/Thr kinase cascade negatively regulates the DNA-binding activity of MrpC, a smaller form of which may be necessary for the *Myxococcus xanthus* development. *Mol Microbiol* **60**: 1205-1217.

O'Connor, K. A. & D. R. Zusman, (1991) Development in *Myxococcus xanthus* involves differentiation into two cell types, peripheral rods and spores. *J. Bacteriol.* **173**: 3318-3333.

Orndorff, P. E. & M. Dworkin, (1980) Separation and properties of the cytoplasmic and outer membranes of vegetative cells of *Myxococcus xanthus*. *J Bacteriol* **141**: 914-927.

Ossa, F., M. E. Diodati, N. B. Caberoy, K. M. Giglio, M. Edmonds, M. Singer & A. G. Garza, (2007) The *Myxococcus xanthus* Nla4 protein is important for expression of stringent response-associated genes, ppGpp accumulation, and fruiting body development. *J. Bacteriol.* **189**: 8474-8483.

Plamann, L., J. M. Davis, B. Cantwell & J. Mayor, (1994) Evidence that *asgB* encodes a DNA-binding protein essential for growth and development of *Myxococcus xanthus*. *J Bacteriol* **176**: 2013-2020.

Plamann, L., Y. Li, B. Cantwell & J. Mayor, (1995) The *Myxococcus xanthus asgA* gene encodes a novel signal transduction protein required for multicellular development. *J Bacteriol* **177**: 2014-2020.

Robenek, H., O. Hofnagel, I. Buers, M. J. Robenek, D. Troyer & N. J. Severs, (2006) Adipophilin-enriched domains in the ER membrane are sites of lipid droplet biogenesis. *J Cell Sci* **119**: 4215-4224.

Rodemer, C., T. P. Thai, B. Brugger, T. Kaercher, H. Werner, K. A. Nave, F. Wieland, K. Gorgas & W. W. Just, (2003) Inactivation of ether lipid biosynthesis causes male infertility, defects in eye development and optic nerve hypoplasia in mice. *Hum Mol Genet* **12**: 1881-1895.

Rosenbluh, A. & E. Rosenberg, (1990) Role of autocide AMI in development of *Myxococcus xanthus*. *J Bacteriol* **172**: 4307-4314.

Sell, H., D. Dietze-Schroeder & J. Eckel, (2006) The adipocyte-myocyte axis in insulin resistance. *Trends Endocrinol Metabol* **17**: 416-422.

Sherma, J., and Fried, B., (2004) Handbook of Thin-Layer Chromatography (3rd Edition), New York-Basel, 2003. **69**: 703-703.

Shi, W., Z. Yang, H. Sun, H. Lancero & L. Tong, (2000) Phenotypic analyses of *frz* and *dif* double mutants of *Myxococcus xanthus*. *FEMS Microbiology Letters* **192**: 211-215.

Shimkets, L. & T. W. Seale, (1975) Fruiting-body formation and myxospore differentiation and germination in Mxyococcus xanthus viewed by scanning electron microscopy. *J Bacteriol* **121**: 711-720.

Shimkets, L. J., (1986) Role of cell cohesion in *Myxococcus xanthus* fruiting body formation. *J. Bacteriol.* **166**: 842-848.

Shimkets, L. J., (1999) Intercellular signaling during fruiting body development of *Myxococcus xanthus*. *Ann Rev Microbiol* **53**: 525-549.

Shimkets, L. J., R. E. Gill & D. Kaiser, (1983) Developmental cell interactions in *Myxococcus xanthus* and the *spoC* locus. *Proc Natl Acad Sci U S A* **80**: 1406-1410.

Singer, M. & D. Kaiser, (1995) Ectopic production of guanosine penta- and tetraphosphate can initiate early developmental gene expression in *Myxococcus xanthus*. *Genes Dev* **9**: 1633-1644.

Søgaard-Andersen, L., F. J. Slack, H. Kimsey & D. Kaiser, (1996) Intercellular C-signaling in *Myxococcus xanthus* involves a branched signal transduction pathway. *Genes & Development* **10**: 740-754.

Søgaard-Andersen, L. & Z. Yang, (2008) Programmed cell death: Role for MazF and MrpC in *Myxococcus* multicellular development. *Curr Biol* **18**: R337-R339.

Sun, H. & W. Shi, (2001a) Analyses of mrp Genes during *Myxococcus xanthus* Development. *J. Bacteriol.* **183**: 6733-6739.

Sun, H. & W. Shi, (2001b) Genetic studies of *mrp*, a locus essential for cellular aggregation and sporulation of *Myxococcus xanthus*. *J Bacteriol* **183**: 4786-4795.

Sun, H. & W. Shi, (2001c) Genetic Studies of *mrp*, a locus essential for cellular aggregation and sporulation of *Myxococcus xanthus*. *J. Bacteriol.* **183**: 4786-4795.

Teigler, A., D. Komljenovic, A. Draguhn, K. Gorgas & W. W. Just, (2009) Defects in myelination, paranode organization and Purkinje cell innervation in the ether lipid-deficient mouse cerebellum. *Hum Mol Genet* **18**: 1897-1908.

Thony-Meyer, L. & D. Kaiser, (1993) *devRS*, an autoregulated and essential genetic locus for fruiting body development in *Myxococcus xanthus*. *J Bacteriol* **175**: 7450-7462.

Toal, D. R., S. W. Clifton, B. A. Roe & J. Downard, (1995) The *esg* locus of *Myxococcus xanthus* encodes the E1 alpha and E1 beta subunits of a branched-chain keto acid dehydrogenase. *Mol Microbiol* **16**: 177-189.

Ueki, T. & S. Inouye, (2003) Identification of an activator protein required for the induction of *fruA*, a gene essential for fruiting body development in *Myxococcus xanthus*. *Proc Natl Acad Sci U S A* **100**: 8782-8787.

Viswanathan, P., K. Murphy, B. Julien, A. G. Garza & L. Kroos, (2007a) Regulation of *dev*, an operon that includes genes essential for *Myxococcus xanthus* development and CRISPR-associated genes and repeats. *J. Bacteriol.* **189**: 3738-3750.

Viswanathan, P., T. Ueki, S. Inouye & L. Kroos, (2007b) Combinatorial regulation of genes essential for *Myxococcus xanthus* development involves a response regulator and a LysR-type regulator. *Proc Natl Acad Sci U S A* **104**: 7969-7974.

Voelz, H. & M. Dworkin, (1962) Fine structure of *Myxococcus xanthus* during morphogenesis. *J Bacteriol* **84**: 943-952.

Wall, D. & D. Kaiser, (1998) Alignment enhances the cell-to-cell transfer of pilus phenotype. *Proc Natl Acad Sci U S A Proc Natl Acad Sci U S A* **95**: 3054-3058.

Waltermann, M., A. Hinz, H. Robenek, D. Troyer, R. Reichelt, U. Malkus, H. J. Galla, R. Kalscheuer, T. Stoveken, P. von Landenberg & A. Steinbuchel, (2005) Mechanism of lipid-body formation in prokaryotes: how bacteria fatten up. *Mol Microbiol* **55**: 750-763.

Waltermann, M. & A. Steinbuchel, (2005) Neutral lipid bodies in prokaryotes: Recent insights into structure, formation, and relationship to eukaryotic lipid depots. *J. Bacteriol.* **187**: 3607-3619.

Ware, J. C. & M. Dworkin, (1973) Fatty acids of *Myxococcus xanthus*. *J Bacteriol* **115**: 253-261.

White, D. J. & P. L. Hartzell, (2000) AglU, a protein required for gliding motility and spore maturation of *Myxococcus xanthus*, is related to WD-repeat proteins. *Mol Microbiol* **36**: 662-678.

Wireman, J. W. & M. Dworkin, (1975) Morphogenesis and developmental interactions in myxobacteria. *Science* **189**: 516-523.

Wu, S. S. & D. Kaiser, (1997) Regulation of expression of the *pilA* gene in *Myxococcus xanthus*. *J Bacteriol* **179**: 7748-7758.

Xu, Q., W. P. Black, S. M. Ward & Z. Yang, (2005) Nitrate-dependent activation of the Dif signaling pathway of *Myxococcus xanthus* mediated by a NarX-DifA interspecies chimera. *J. Bacteriol.* **187**: 6410-6418.

Yang, R., S. Bartle, R. Otto, A. Stassinopoulos, M. Rogers, L. Plamann & P. Hartzell, (2004) AglZ is a filament-forming coiled-coil protein required for adventurous gliding motility of *Myxococcus xanthus*. *J. Bacteriol.* **186**: 6168-6178.

Yang, Z., X. Ma, L. Tong, H. B. Kaplan, L. J. Shimkets & W. Shi, (2000) *Myxococcus xanthus dif* genes are required for biogenesis of cell surface fibrils essential for social gliding motility. *J Bacteriol* **182**: 5793-5798.

CHAPTER 5

DISSERTATION SUMMARY AND CONCLUSION

M. xanthus β-barrel proteins.

β-barrel proteins are integral membrane proteins found exclusively in the OM that are important for passage of nutrients, waste products and signals (Wimley, 2003). The characteristic feature of β-barrel proteins, principally the antiparallel β-strands, has led to development of several bioinformatic programs for their identification from gene sequences (Punta *et al.*, 2007). However, these programs differ in accuracy, as demonstrated in chapter 3 when tested on known β-barrel and non β-barrel proteins. My major contribution was developing a strategy to eliminate cytoplasmic, lipoproteins and integral IM proteins using programs Signal P, LipoP and TMHMM, respectively (Bendtsen *et al.*, 2004, Juncker *et al.*, 2003, Krogh *et al.*, 2001). 228 putative β-barrel proteins out of 7331 protein coding genes were identified in the *M. xanthus* genome by using TMBETA-SVM and TMBETADISC-RBF (Ou *et al.*, 2008, Park *et al.*, 2005). The strategy described here for identification of β-barrel proteins can be applied in other organisms.

54 of the 228 β-barrel proteins were identified by LC-MS/MS of OM vesicles isolated from vegetative cells, which is equivalent to 0.7% of *M. xanthus* genome. Preparation of OM vesicles and subsequent solublization of membrane proteins is difficult, which led to failure in identification of polar protein complexes such as PilQ. While protein contamination from other cellular compartments is a common problem, it

was minimized by using bioinformatic tools to identify integral OM proteins. The OM β-barrel proteins identified in this study provide a dataset that can be used for identification of proteins essential for processes such as development, motility and predation. The availability of microarray data provides a tool to identify those OM β-barrel protein encoding genes that are differentially expressed during development. Such genes can be disrupted to see if they affect fruiting body development. One example, Oar, was examined in some detail.

Oar is required for C-signaling.

M. xanthus development is regulated by intercellular communication, which involves at least six extracellular signals (Shimkets, 1999). The OM pores through which these signals are imported or exported are unknown. One OM protein channel, Oar has been shown to be defective in aggregation and sporulation (Martinez-Canamero *et al.*, 1993). Bioinformatic analysis using BLASTP suggests that Oar is a TonB dependent receptor. Such receptors are required for energy dependent uptake of substrates that are present in low concentration in the environment. The most carefully studied examples are iron acquisition by FecA and vitamin B12 assimilation by BtuB (Ferguson & Deisenhofer, 2002).

The Oar protein is essential for C-signaling as demonstrated in chapter 3. The C-signal is produced by CsgA, a 25 kDa protein essential for aggregation and sporulation (Shimkets *et al.*, 1983). CsgA shares homology with members of the short chain alcohol dehydrogenase family proteins and is cell membrane bound (Baker, 1994, Shimkets & Asher, 1988, Simunovic *et al.*, 2003). Development in a Δ*csgA* mutant can be rescued by providing CsgA extracellulary or by mixing Δ*csgA* with strains that produce CsgA

(Shimkets & Rafiee, 1990, Shimkets & Asher, 1988). The C-signal is a short range signal whose intercellular passage is contact-dependent. This was demonstrated by using non-motile mutants such as *mglAB*, which are unable to transmit C-signal to Δ*csgA* cell in spite of being able to produce CsgA protein (Kim & Kaiser, 1990b, Kim & Kaiser, 1990a). However when cells were forced to arrange end-to-end, C-signaling was restored, suggesting CsgA is localized at the poles (Kim & Kaiser, 1990a). Direct proof of polar localization has never been accomplished.

Pair wise complementation of an *oar* mutant with each of the six intercellular signaling mutants revealed that *oar* cells can rescue development of all but the C-signal producing mutant *csgA.* Western blot analysis revealed that an *oar* mutant can produce WT levels of CsgA protein suggesting that Oar may be essential for export of the C-signal. The export of C-signal through Oar is intriguing because TonB dependent receptors that are involved in export have not been identified. If Oar is truly a TonB dependent receptor then the export of C-signal is energy dependent. Transport via TonB dependent receptors requires energy produced by proton motive force using ExbB and ExbD in the IM (Bradbeer, 1993). Future studies may focus on identification of IM components required for C-signal export.

While the export of C-signal via Oar is an interesting model it is possible that C-signaling may be inhibited due to abnormal cell shape of the *oar* cells. During development the *oar* cells are unable to maintain their cell shape and form spheroplasts, which are not observed in *oar* vegetative cells. By 24 h into development ~60% cells appear to bend then form spheroplasts (Figure 3-3). Most of the cells curve at the center as if there is cell wall degradation occurring at that point. As most cells perish the *oar*

mutant is unable to proceed beyond the aggregation phase. Spheroplast formation during development appears to be unique to *oar* cells. Although *M. xanthus* cells undergo programmed cell death during development bending has not been observed. The formation of spheroplasts may lead to loss of polarity, leading to C-signal inhibition. Interestingly the remaining 40% of *oar* cells that exhibit normal morphology are still unable to rescue Δ*csgA* development. It is possible that these cells may eventually form spheroplast, and block C-signaling and development.

It is not known why *oar* cells undergo spheroplasting. Assuming that the *oar* cells produce active CsgA protein, it is possible that CsgA accumulation in the membrane may cause toxicity. All attempts to overexpress CsgA without a bulky fusion tag such as MalE in *E. coli* have been unsuccessful, suggesting that CsgA is toxic to cells. Moreover, an *oar csgA* double mutant exhibits a normal morphology. The curving of cells at the center suggests that CsgA may be accumulating at that point in *oar* cells. The localization of CsgA in these cells can be examined further by generating a CsgA-mCherry fusion protein that can be visualized under a fluorescence microscope.

Lipoprotein sorting in *M. xanthus.*

Lipoproteins exist in the IM and OM of Gram-negative bacteria. *M. xanthus* is one of the few bacteria that secrete lipoproteins outside the cell where they become localized on the ECM (Curtis *et al.*, 2007a). In *E. coli*, the sorting of lipoproteins between IM and OM occurs via the Lol pathway (Masuda *et al.*, 2002). The sorting signal for the IM retention of lipoproteins is aspartate at the +2 position of the mature protein (Seydel *et al.*, 1999). Studies in several Gram-negative bacteria show that the '+2 rule' is applicable to only a few species of Enterobacteriaceae family (Tokuda &

Matsuyama, 2004). For example, in *Pseudomonas aeruginosa*, amino acid residues at positions +3 and +4 determine IM retention of lipoproteins (Tanaka *et al.*, 2007). Present work shows that *M. xanthus* possesses a novel system for lipoprotein sorting. Bioinformatic studies show that alanine at the +7 position is conserved in ECM lipoproteins and lysine at the +2 position is conserved in IM lipoproteins. The lysine at the +2 position as the IM sorting signal was recently confirmed by Wei et al (Wei *et al.*). In their study, the type II signal sequence of IM lipoprotein MXAN1176 that was identified by proteomics in Chapter 3 was fused with mCherry. This construct localized in the IM but not in the OM suggesting that *M. xanthus* IM sorting signal is different than *E. coli*.

Chapter 3 demonstrated that substituting +7 alanine with aspartate in the major ECM lipoprotein FibA leads to OM retention suggesting that +7 alanine is an essential ECM sorting signal. However, having lysine at the +2 position in FibA does not prevent ECM localization. These results suggest that the presence of alanine at the +7 position overrides the +2 lysine IM sorting signal and does not diminish ECM localization of lipoproteins.

While this work provides the first insight into sorting signals utilized for subcellular localization of lipoproteins in *M. xanthus*, the mechanism is not known. The *E. coli* Lol system consists of five proteins, LolA through LolE (Narita & Tokuda, 2006). The LolCDE forms an ATP-binding cassette in the IM. LolA is a periplasmic carrier protein, which binds to lipoproteins and transports them to the OM receptor LolB that incorporates the lipoprotein in to the OM. *M. xanthus* possesses LolA (MXAN1473), LolC (MXAN4730 and MXAN5419), LolD (MXAN4729) homologs that may be

involved in the transport of lipoproteins to the OM (Bhat, S unpublished). It remains unknown whether the Lol system is also involved in the export of lipoproteins to the ECM or whether a novel transport system exists for this purpose. Some bacteria use the type II secretion system for the transport of lipoproteins to the outer surface. *Klebsiella oxytoca* uses the Lol system for transport of lipoproteins to the OM while it uses type II secretion system for the export of the cell surface exposed lipoprotein PulA (Poquet *et al.*, 1993, Pugsley, 1993). The *M. xanthus* genome predicts the presence of two type II secretion systems that may be involved in the secretion of ECM lipoproteins (MXAN2504-MXAN2515) and (MXAN3105-3107) (Konovalova *et al.*). Although the latter appears to be an incomplete type II secretion system, MXAN3106 encodes the OM secretin (GspD), which was identified by proteomics in chapter 3. This suggests that MXAN3106 is a functional secretin.

The information obtained from this research is valuable in identifying other ECM lipoproteins in *M. xanthus* and possibly other myxobacterial species based on amino acid sequence data alone. Because the ECM proteome is essential for lipid chemotaxis and development it is important to identify its various components. Out of 425 lipoproteins encoded by *M. xanthus*, 34 have alanine at the +7 position and represent putative ECM lipoproteins (Table 5-1). Mutational analysis of these proteins may help identify developmentally essential lipoproteins.

Lipid body synthesis during fruiting body development.

Many bacteria store energy in the form of biopolymers for long term usage. The storage granules are generally produced during stationary phase in response to an excess

Table 5-1 Lipoproteins with +7 alanine.

MXAN No.	Function
MXAN0035	aliphatic sulfonate ABC transporter substrate-binding protein
MXAN0235	putative lipoprotein
MXAN0432	metallo-beta-lactamase family protein
MXAN0527	RND family efflux transporter MFP subunit
MXAN1485	putative cytochrome C
MXAN1623	M16 family peptidase
MXAN1706	kelch domain-containing protein
MXAN1721	putative lipoprotein
MXAN1724	putative lipoprotein
MXAN1921	TPR repeat-containing protein
MXAN1928	putative lipoprotein
MXAN2091	M16 family peptidase
MXAN2107	putative lipoprotein
MXAN2221	M27 family peptidase
MXAN2251	Glycine betaine/L-proline ABC transporter, periplasmic substrate-binding protein
MXAN2691	hypothetical protein
MXAN3045	putative lipoprotein
MXAN3440	M13 family peptidase
MXAN3504	putative lipoprotein
MXAN3574	von Willebrand factor type A domain-containing protein
MXAN3772	putative lipoprotein
MXAN3835	putative lipoprotein
MXAN4107	putative lipoprotein
MXAN4964	putative lipoprotein
MXAN5010	FG-GAP repeat-containing protein

MXAN5036	hypothetical protein
MXAN5213	alpha/beta fold family hydrolase
MXAN5251	phospholipase/carboxylesterase family protein
MXAN5293	putative lipoprotein
MXAN5337	putative lipoprotein
MXAN5580	hypothetical protein
MXAN5683	putative lipoprotein
MXAN5737	putative lipoprotein
MXAN6106	FibA

of carbon but shortage of other essential nutrients such as nitrogen, phosphorous, sulfur, or oxygen. Polyhydroxyalkanoates, glycogen and polyphosphates are some of the most common energy stores in bacteria that have been reviewed in some detail (Fuller, 1999, Shively, 1974). Unlike eukaryotes, very few bacterial species accumulate triacylglycerol (TAG) lipid bodies.

Starvation induces *M. xanthus* fruiting body formation, which initiates several morphological and physiological changes in a cell. One of the earliest changes observed is the synthesis of lipid bodies, which consist of TAGs, diacylglycerols and monoacylglycerols surrounded by a phospholipid monolayer (Hoiczyk *et al.*, 2009). The synthesis of lipid bodies during fruiting body development is fascinating because they are made when carbon substrates have depleted. This suggests lipid bodies are synthesized from recycled cellular components. During development structural changes convert a rod-shaped cell to a spherical spore with a smaller surface area (Voelz & Dworkin, 1962). To make a spherical spore, a cell has to degrade a major portion of its membrane. The average cell length measured at 18 h is approximately 40% shorter than that observed at 12 h. The area of lipid bodies synthesized at 18 h is approximately 8-fold higher than at 12 h. Nile red staining of early developing cells show small lipid bodies close to the membrane. Studies in other organisms suggest that lipid bodies are synthesized on the cell membrane. For example in *Rhodococcus opacus*, lipid accumulation begins at the cell membrane by depositing an oleogenous layer that form lipid pre-bodies which are released into the cytoplasm where they aggregate to form larger lipid bodies (Waltermann *et al.*, 2005). In eukaryotes lipid bodies are formed between the two endoplasmic reticulum leaflets which are released into the cytoplasm by budding (Murphy & Vance,

1999). A possible method to identify mechanism of lipid body synthesis is by utilizing tomography on developing cells.

The *M. xanthus* cell membrane consists primarily of phosphotidylethanolamine (PE) with iso 15:0 fatty acid being the most abundant. The synthesis of TAG such as the tri-iso 15:0 glycerol from phospholipids would require removal of the phosphate head group by a phospholipase C followed by addition of an iso 15:0 by DGAT (diacylglycerol acyl transferase). While the *M. xanthus* genome can potentially encode several phospholipases, only one DGAT homolog was identified and its deletion did not disrupt triglyceride synthesis (Hoiczyk et al., 2009). The synthesis of ether lipid TG-1 that contains alkyl-linked iso 15:0 at the *sn*-1 position and ester-linked iso 15:0 at the *sn*-2 and *sn*-3 position involves additional steps. In this case a fatty alcohol is derived from fatty acyl CoA catalyzed by fatty acyl reductase. The ether bond is then introduced by replacing the acyl group with the fatty alcohol at the *sn*-1 position by alkyl dihydroxyacetone phosphate synthase. However disruption of *M. xanthus* fatty acyl reductase homolog did not affect fruiting body development suggesting that lipid body synthesis in *M. xanthus* may a involve novel mechanism (Curtis *et al.*, 2007b).

Lipid body synthesis precedes PCD.

During fruiting body development cells differentiate into three distinct cell types. A few cells (5-10%) become peripheral rods that do not respond to developmental signals to enter fruiting bodies, or undergo sporulation, and remain rod shaped (O'Connor & Zusman, 1991). While only 15-20% of the cell population forms spores, the majority of the cells undergo programmed cell death (PCD) (Shimkets, 1986, Nariya & Inouye,

2008). PCD is induced by the MazF toxin, an RNA interferase (Nariya & Inouye, 2008). MazF is inactivated by the MrpC anti-toxin.

Currently the role of PCD during development is unknown. However, PCD appears to be essential for development since mutants blocked in PCD (e.g *mazF*, *difA*) fail to undergo development (Nariya & Inouye, 2008, Shimkets, 1986). Interestingly PCD can be stimulated in *difA* cells when mixed with WT cells (Figure 4-2) (Shimkets, 1986). This suggests extracellular factors may stimulate PCD during development. Nariya and Inouye proposed that PCD may be required to provide nutrients to the sporulating cells (Nariya & Inouye, 2008). I believe it has a temporally and spatially important regulation function. PCD is induced 12 h into development when lipid body synthesis is well underway. The number of cells containing lipid bodies declines in proportion with PCD as development progresses, suggesting that lipid bodies are produced by cells undergoing PCD. Thus lipid bodies are released during PCD. Extracellular lipid bodies appear to form a cap-like structure on top of fruiting bodies. It is unclear how or why lipid bodies are deposited on top of the fruiting body. As cells aggregate in tiers, those present on top layers may undergo cell lysis while those cells buried deep within the fruiting body may form spores (Curtis et al., 2007b). If this is true then using the Live/Dead Baclight Bacterial Viability kit (Invitrogen) and confocal microscopy should reveal the presence of dead cells on the top layers of fruiting bodies while live sporulating cells should appear in the middle or at the base of the fruiting bodies. In this technique SYTO 9 and propidium iodide stains are used. The SYTO 9 labels all cells while the propidium iodide can permeate only damaged cell membrane causing the dead cells to fluoresce red while live cells to fluoresce green.

The E-signal.

The E-signal is an extracellular factor essential for sporulation (Toal *et al.*, 1995). Mutants deficient in E-signaling can be restored for fruiting body formation by mixing with WT cells. While the role of the E-signal remains to be explored, micro-cinematography provides some clue. WT cells initiate development within 6-8 h of starvation by a sudden increase in motility (Curtis et al., 2007b). Within 12 h of starvation small cell aggregates are formed which constantly assemble, diffuse and merge with other aggregates ultimately forming larger stable fruiting bodies (Curtis et al., 2007b, Xie *et al.*). In contrast the E-signaling mutants form several small, stable aggregates that never diffuse, which suggests E-signal is essential for destabilizing smaller aggregates. E-signal is essential for destabilizing smaller aggregates (Xie et al.). Identification of E-signal is the first step in understanding its role during development.

The E-signal is synthesized by the *esg* gene product, which is a branched chain keto acid dehydrogenase (BCKAD) required for the synthesis of short branched chain fatty acids such as isovaleric acid (Toal et al., 1995). These primers can then be extended to synthesize long chain fatty acids such as iso 15:0 or iso 17:0. The iso-FAs can also be synthesized by a novel, alternative pathway using LiuC, MvaS, MXAN4264, MXAN4265 and MXAN4266 (Bode *et al.*, 2009, Bode *et al.*, 2006). This pathway is highly induced in *esg* mutants during development. The double mutants that are blocked in both pathways are deficient in synthesis of fatty acid primer derived triglycerides and fruiting body development. Development can be restored in these mutants by supplying isovaleric acid or iso 15:0 suggesting that the E-signal is a lipid (Ring *et al.*, 2006, Toal et al., 1995).

The lipid bodies are primarily composed of branched chain fatty acids that are esterified into various triacylglycerol species (Hoiczyk et al., 2009). Lipids isolated from lipid bodies have the ability to restore sporulation in E-signaling mutants suggesting that the lipid bodies contain the E-signal. The purified lipids were fractionated using the solid phase extraction and thin layer chromatography, which led to purification of E-signal by 50-fold. The active fraction was analyzed using *Matrix-assisted laser desorption/ionization* (MALDI). Because MALDI uses a soft ionization technique, it is ideal for identification of large organic molecules as it does not cause their fragmentation. TG-1 and the derivative of TG-1 with iso 17:0 at the *sn*-2 position were identified. Although MALDI analysis does not provide any information regarding the abundance of TG-1 in the fraction, indirect evidence suggests that TG-1 is the E-signal. TG-1 is one of the major lipid synthesized during development but absent in vegetative cells (Ring et al., 2006). Chemically synthesized TG-1 has been shown to partially complement sporulation defect in the E-signaling mutants, while other triglycerides such as tri iso 15:0 triglyceride failed (Ring et al., 2006). These results suggest that TG-1 The bioassay described in chapter 4 is a sensitive method to identify the active lipid and the concentration required to rescue sporulation of E-signaling mutants. If TG-1 is the E-signal then the chemically synthesized TG-1 will rescue development of E-signal mutant at even lower concentration than the purified lipid fractions obtained from *M. xanthus*. Our lab is currently testing this hypothesis.

Relevance of lipid body study.

The physiology and function of lipid bodies in *M. xanthus* is strikingly similar to those of eukaryotes. Firstly, lipid bodies in both systems are long term energy storages. Secondly, they are a source of cell signaling molecules such as E signal in case *M. xanthus* and cholesterol in eukaryotes that dictate cellular functions such as differentiation. Lastly, lipid bodies are highly regulated. Several developmental mutants analyzed in chapter 4 have aberrant lipid body synthesis. Similarly, a recent analysis in *Drosophila* has discovered 227 genes are required for lipid body synthesis and utilization (Guo *et al.*, 2008). These findings suggest that *M. xanthus* is a simple system to understand various roles of lipid body lipids and their regulation in the physiology of a cell.

References.

Baker, M. E., (1994) *Myxococcus xanthus* C-factor, a morphogenetic paracrine signal, is similar to *Escherichia coli* 3-oxoacyl-[acyl-carrier-protein] reductase and human 17 beta-hydroxysteroid dehydrogenase. *Biochem J* **301 (Pt 1)**: 311-312.

Bendtsen, J. D., H. Nielsen, G. von Heijne & S. Brunak, (2004) Improved prediction of signal peptides: SignalP 3.0. *J Mol Biol* **340**: 783-795.

Bode, H. B., M. W. Ring, G. Schwär, M. O. Altmeyer, C. Kegler, I. R. Jose, M. Singer & R. Müller, (2009) Identification of additional players in the alternative biosynthesis pathway to Isovaleryl-CoA in the myxobacterium *Myxococcus xanthus*. *ChemBioChem* **10**: 128-140.

Bode, H. B., M. W. Ring, G. Schwar, R. M. Kroppenstedt, D. Kaiser & R. Muller, (2006) 3-Hydroxy-3-methylglutaryl-coenzyme A (CoA) synthase is involved in

biosynthesis of isovaleryl-CoA in the myxobacterium *Myxococcus xanthus* during fruiting body formation. *J Bacteriol* **188**: 6524-6528.

Bradbeer, C., (1993) The proton motive force drives the outer membrane transport of cobalamin in *Escherichia coli*. *J Bacteriol* **175**: 3146-3150.

Curtis, P. D., J. Atwood, 3rd, R. Orlando & L. J. Shimkets, (2007a) Proteins associated with the *Myxococcus xanthus* extracellular matrix. *J Bacteriol* **189**: 7634-7642.

Curtis, P. D., R. G. Taylor, R. D. Welch & L. J. Shimkets, (2007b) Spatial organization of *Myxococcus xanthus* during fruiting body formation. *J Bacteriol* **189**: 9126-9130.

Ferguson, A. D. & J. Deisenhofer, (2002) TonB-dependent receptors--structural perspectives. *Biochim Biophys Acta- Biomembranes* **1565**: 318-332.

Fuller, R. C., (1999) Microbial inclusions with special reference to PHA inclusions and intracellular boundary envelopes. *Int J Biol Macromol* **25**: 21-29.

Guo, Y., T. C. Walther, M. Rao, N. Stuurman, G. Goshima, K. Terayama, J. S. Wong, R. D. Vale, P. Walter & R. V. Farese, (2008) Functional genomic screen reveals genes involved in lipid-droplet formation and utilization. *Nature* **453**: 657-661.

Hoiczyk, E., M. W. Ring, C. A. McHugh, G. Schwär, E. Bode, D. Krug, M. O. Altmeyer, J. Z. Lu & H. B. Bode, (2009) Lipid body formation plays a central role in cell fate determination during developmental differentiation of *Myxococcus xanthus*. *Molecular Microbiology* **74**: 497-517.

Juncker, A. S., H. Willenbrock, G. Von Heijne, S. Brunak, H. Nielsen & A. Krogh, (2003) Prediction of lipoprotein signal peptides in Gram-negative bacteria. *Protein Sci* **12**: 1652-1662.

Kim, S. K. & D. Kaiser, (1990a) Cell alignment required in differentiation of *Myxococcus xanthus*. *Science* **249**: 926-928.

Kim, S. K. & D. Kaiser, (1990b) Cell motility is required for the transmission of C-factor, an intercellular signal that coordinates fruiting body morphogenesis of *Myxococcus xanthus*. *Genes Dev* **4**: 896-904.

Konovalova, A., T. Petters & L. Sogaard-Andersen, Extracellular biology of *Myxococcus xanthus*. *FEMS Microbiol Rev* **34**: 89-106.

Krogh, A., B. Larsson, G. von Heijne & E. L. Sonnhammer, (2001) Predicting transmembrane protein topology with a hidden Markov model: application to complete genomes. *J Mol Biol* **305**: 567-580.

Martinez-Canamero, M., J. Munoz-Dorado, E. Farez-Vidal, M. Inouye & S. Inouye, (1993) Oar, a 115-kilodalton membrane protein required for development of *Myxococcus xanthus*. *J Bacteriol* **175**: 4756-4763.

Masuda, K., S. Matsuyama & H. Tokuda, (2002) Elucidation of the function of lipoprotein-sorting signals that determine membrane localization. *Proc Natl Acad Sci U S A* **99**: 7390-7395.

Murphy, D. J. & J. Vance, (1999) Mechanisms of lipid-body formation. *Trends in Biochem. Sci.* **24**: 109-115.

Narita, S.-i. & H. Tokuda, (2006) An ABC transporter mediating the membrane detachment of bacterial lipoproteins depending on their sorting signals. *FEBS Lett.* **580**: 1164-1170.

Nariya, H. & M. Inouye, (2008) MazF, an mRNA interferase, mediates programmed cell death during multicellular *Myxococcus* development. *Cell* **132**: 55-66.

O'Connor, K. A. & D. R. Zusman, (1991) Development in *Myxococcus xanthus* involves differentiation into two cell types, peripheral rods and spores. *J. Bacteriol.* **173**: 3318-3333.

Ou, Y. Y., M. M. Gromiha, S. A. Chen & M. Suwa, (2008) TMBETADISC-RBF: Discrimination of beta-barrel membrane proteins using RBF networks and PSSM profiles. *Comput Biol Chem* **32**: 227-231.

Park, K. J., M. M. Gromiha, P. Horton & M. Suwa, (2005) Discrimination of outer membrane proteins using support vector machines. *Bioinformatics* **21**: 4223-4229.

Poquet, I., M. G. Kornacker & A. P. Pugsley, (1993) The role of the lipoprotein sorting signal (aspartate +2) in pullulanase secretion. *Mol Microbiol* **9**: 1061-1069.

Pugsley, A. P., (1993) The complete general secretory pathway in gram-negative bacteria. *Microbiol Rev* **57**: 50-108.

Punta, M., L. R. Forrest, H. Bigelow, A. Kernytsky, J. Liu & B. Rost, (2007) Membrane protein prediction methods. *Methods* **41**: 460-474.

Ring, M. W., G. Schwär, V. Thiel, J. S. Dickschat, R. M. Kroppenstedt, S. Schulz & H. B. Bode, (2006) Novel Iso-branched ether lipids as specific markers of developmental sporulation in the myxobacterium *Myxococcus xanthus*. *Journal of Biological Chemistry* **281**: 36691-36700.

Seydel, A., P. Gounon & A. P. Pugsley, (1999) Testing the '+2 rule' for lipoprotein sorting in the *Escherichia coli* cell envelope with a new genetic selection. *Mol Microbiol* **34**: 810-821.

Shimkets, L. J., (1986) Role of cell cohesion in *Myxococcus xanthus* fruiting body formation. *J. Bacteriol.* **166**: 842-848.

Shimkets, L. J., (1999) Intercellular signaling during fruiting body development of *Myxococcus xanthus. Annu Rev Microbiol* **53**: 525-549.

Shimkets, L. J. & S. J. Asher, (1988) Use of recombination techniques to examine the structure of the *csg* locus of *Myxococcus xanthus*. *Mol Gen Genet* **211**: 63-71.

Shimkets, L. J., R. E. Gill & D. Kaiser, (1983) Developmental cell interactions in *Myxococcus xanthus* and the spoC locus. *Proc Natl Acad Sci U S A* **80**: 1406-1410.

Shimkets, L. J. & H. Rafiee, (1990) CsgA, an extracellular protein essential for *Myxococcus xanthus* development. *J Bacteriol* **172**: 5299-5306.

Shively, J. M., (1974) Inclusion bodies of prokaryotes. *Annu Rev Microbiol* **28**: 167-187.

Simunovic, V., F. C. Gherardini & L. J. Shimkets, (2003) Membrane localization of motility, signaling, and polyketide synthetase proteins in *Myxococcus xanthus*. *J Bacteriol* **185**: 5066-5075.

Tanaka, S. Y., S. Narita & H. Tokuda, (2007) Characterization of the *Pseudomonas aeruginosa* Lol system as a lipoprotein sorting mechanism. *J Biol Chem* **282**: 13379-13384.

Toal, D. R., S. W. Clifton, B. A. Roe & J. Downard, (1995) The *esg* locus of *Myxococcus xanthus* encodes the E1 alpha and E1 beta subunits of a branched-chain keto acid dehydrogenase. *Mol Microbiol* **16**: 177-189.

Tokuda, H. & S. Matsuyama, (2004) Sorting of lipoproteins to the outer membrane in *E. coli*. *Biochim Biophys Acta* **1693**: 5-13.

Voelz, H. & M. Dworkin, (1962) Fine structure of *Myxococcus xanthus* during morphogenesis. *J Bacteriol* **84**: 943-952.

Waltermann, M., A. Hinz, H. Robenek, D. Troyer, R. Reichelt, U. Malkus, H. J. Galla, R. Kalscheuer, T. Stoveken, P. von Landenberg & A. Steinbuchel, (2005) Mechanism of lipid-body formation in prokaryotes: how bacteria fatten up. *Mol Microbiol* **55**: 750-763.

Wei, X., D. T. Pathak & D. Wall, Heterologous protein transfer within structured myxobacteria biofilms. *Mol Microbiol*.

Wimley, W. C., (2003) The versatile beta-barrel membrane protein. *Curr Opin Struct Biol* **13**: 404-411.

Xie, C., H. Zhang, L. J. Shimkets & O. A. Igoshin, Statistical image analysis reveals features affecting fates of *Myxococcus xanthus* developmental aggregates. *Proc Natl Acad Sci U S A* **108**: 5915-5935.

APPENDIX A

CHAPTER 3 SUPPLEMENTARY TABLES

Table A-1. 228 OM proteins identified by bothTMBETA-SVM and TMBETADISC-RBF.

MXAN	Gene name	Protein function
MXAN0021		Hypothetical protein
MXAN0033		Hypothetical protein
MXAN0063		Hypothetical protein
MXAN0129		Hypothetical protein
MXAN0162		Hypothetical protein
MXAN0182		PQQ enzyme repeat domain protein
MXAN0219		Hypothetical protein
MXAN0224		Hypothetical protein
MXAN0251		Mce family protein
MXAN0271		Hypothetical protein
MXAN0272		TonB-dependent receptor
MXAN0355		Putative pilus biogenesis operon protein
MXAN0391		Oxidoreductase, aldo/keto reductase family
MXAN0413		Hypothetical protein
MXAN0500		Hypothetical protein
MXAN0518		TonB-dependent receptor
MXAN0538		Hypothetical protein

MXAN0551		Hypothetical protein
MXAN0562		Phosphate-selective porin O and P
MXAN0585		Hypothetical protein
MXAN0589		Hypothetical protein
MXAN0653		Peptidase, S8A (subtilisin) subfamily
MXAN0662		Hypothetical protein
MXAN0679		Hypothetical protein
MXAN0751		Amino acid/amide ABC transporter substrate-binding protein
MXAN0774		Oxidoreductase, short chain dehydrogenase/reductase family
MXAN0794		Hypothetical protein
MXAN0821		TonB dependent receptor
MXAN0855		Putative chemotaxis motb protein
MXAN0856		TonB dependent receptor
MXAN0924		Hypothetical protein
MXAN0940		Hypothetical protein
MXAN0945		Tetratricopeptide repeat protein
MXAN0959	*sbcC*	Nuclease sbccd, C subunit
MXAN0990		Cation efflux system protein cusc
MXAN1003		Hypothetical protein

MXAN1020		Hypothetical protein
MXAN1021		Hypothetical protein
MXAN1051		Hypothetical protein
MXAN1070	*dacB*	D-alanyl-D-alanine carboxypeptidase/D-alanyl-D-alanine-endopeptidase
MXAN1147		Hypothetical protein
MXAN1183		Spermine/spermidine synthase family protein
MXAN1226		Fibronectin type III domain protein
MXAN1242		Hypothetical protein
MXAN1263		Hypothetical protein
MXAN1316		TonB dependent receptor
MXAN1329		Hypothetical protein
MXAN1368		Hypothetical protein
MXAN1369		Prepilin-type N-terminal cleavage/methylation domain protein
MXAN1426		Hypothetical protein
MXAN1559		Hypothetical protein
MXAN1608		Hypothetical protein
MXAN1688		TonB dependent receptor
MXAN1700		Tetratricopeptide repeat protein
MXAN1897		Hypothetical protein

MXAN1904		Hypothetical protein
MXAN1916		Hypothetical protein
MXAN1923		Hypothetical protein
MXAN1948		Tetratricopeptide repeat protein
MXAN1967		Putative peptidase, S8 (subtilisin) family
MXAN1999		Hypothetical protein
MXAN2203		Hypothetical protein
MXAN2277		Hypothetical protein
MXAN2374		Hypothetical protein
MXAN2380		Hypothetical protein
MXAN2412		Hypothetical protein
MXAN2417		Hypothetical protein
MXAN2422		Hypothetical protein
MXAN2426		Hypothetical protein
MXAN2466		Hypothetical protein
MXAN2481		Hypothetical protein
MXAN2508		Putative prepilin-type N-terminal cleavage/methylation domain protein
MXAN2514	*gspD*	General secretion pathway protein D
MXAN2515	*gspC*	General secretion pathway protein C

MXAN2520	MORN variant repeat protein
MXAN2537	TldD/PmbA family protein
MXAN2539	Hypothetical protein
MXAN2552	Tetratricopeptide repeat protein
MXAN2561	Prepilin-type N-terminal cleavage/methylation domain protein
MXAN2562	Hypothetical protein
MXAN2584	Hypothetical protein
MXAN2619	Tetratricopeptide repeat protein
MXAN2659	Hypothetical protein
MXAN2690	AsmA family protein
MXAN2782	Hypothetical protein
MXAN2850	Hypothetical protein
MXAN2864	Hypothetical protein
MXAN2915	Putative adventurous gliding motility protein
MXAN2952	Hypothetical protein
MXAN2995	Peptidase, S1C (protease Do) subfamily
MXAN3106	Protein transporter, outer bacterial membrane secretin (secretin) family
MXAN3129	Prolyl oligopeptidase, serine peptidase
MXAN3165	Hypothetical protein

MXAN3242		Hypothetical protein
MXAN3373		Hypothetical protein
MXAN3424		Outer membrane efflux protein
MXAN3482		Hypothetical protein
MXAN3483		Hypothetical protein
MXAN3553		Hypothetical protein
MXAN3564		Peptidase, M36 (fungalysin) family
MXAN3676		Hypothetical protein
MXAN3719		Fibronectin type III domain protein
MXAN3723		Hypothetical protein
MXAN3729		PQQ enzyme repeat domain protein
MXAN3745		Hypothetical protein
MXAN3768		Mce family protein
MXAN3774		Hypothetical protein
MXAN3774		Dipeptidyl-peptidase 7, serine peptidase
MXAN3780		Patatin-like phospholipase family protein
MXAN3814		Hypothetical protein
MXAN3824	*gspG*	General secretion pathway protein G
MXAN3883		Protein transporter, outer membrane fimbrial usher porin (FUP) family

MXAN3905	Outer membrane efflux protein
MXAN3953	Hypothetical protein
MXAN4014	Von Willebrand factor type A domain protein
MXAN4092	Hypothetical protein
MXAN4109	Hypothetical protein
MXAN4115	Transposase orf3, IS66 family
MXAN4153	Hypothetical protein
MXAN4175	Efflux transporter, RND family, MFP subunit
MXAN4176	Outer membrane efflux protein
MXAN4181	Hypothetical protein
MXAN4198	Putative outer membrane macrolide efflux protein
MXAN4200	Putative macrolide-specific efflux protein
MXAN4293	Hypothetical protein
MXAN4308	Hypothetical protein
MXAN4365	Transporter, outer membrane receptor (OMR) family
MXAN4381	Hypothetical protein
MXAN4382	Hypothetical protein
MXAN4390	BNR/Asp-box repeat domain protein
MXAN4407	Hypothetical protein

MXAN4559		TonB dependent receptor
MXAN4561		Tetratricopeptide repeat protein
MXAN4652		Putative Flp pilus assembly protein CpaB
MXAN4658		Pilus biogenesis protein, TadE family
MXAN4695		Spo IID/lytB domain protein
MXAN4728	*omp85*	Outer membrane protein, OMP85 family
MXAN4746		TonB dependent receptor
MXAN4821		Sulfate ABC transporter, periplasmic sulfate-binding protein
MXAN4837	*celA*	Endoglucanase
MXAN4859		Ankyrin repeat protein
MXAN4876		Hypothetical protein
MXAN4897		Hypothetical protein
MXAN4911		Hypothetical protein
MXAN5013		Hypothetical protein
MXAN5023		TonB dependent receptor
MXAN5030		Efflux transporter, HAE1 family, outer membrane efflux protein
MXAN5117		Hypothetical protein
MXAN5191		Hypothetical protein
MXAN5200		Hypothetical protein

MXAN5291	*mtgA*	Monofunctional biosynthetic peptidoglycan transglycosylase
MXAN5292		Hypothetical protein
MXAN5299		Peptidase, S9C (acylaminoacyl-peptidase) subfamily
MXAN5304		Hypothetical protein
MXAN5326		Putative phytase
MXAN5375		Hypothetical protein
MXAN5391		Hypothetical protein
MXAN5442		Thermolysin, metallo peptidase
MXAN5453		Hypothetical protein
MXAN5454		Peptidase, M36 (fungalysin) family
MXAN5491		Hypothetical protein
MXAN5522		Lactonizing lipase
MXAN5685		Hypothetical protein
MXAN5693		DNA/RNA non-specific endonuclease
MXAN5720		Metallo-beta-lactamase family protein
MXAN5743		Hypothetical protein
MXAN5756	*tolB*	TolB protein
MXAN5772	*pilQ*	Type IV pilus secretin PilQ
MXAN5809		Hypothetical protein

MXAN5819	Hypothetical protein
MXAN5822	Hypothetical protein
MXAN5835	Hypothetical protein
MXAN5869	Hypothetical protein
MXAN5875	Hypothetical protein
MXAN5931	Hypothetical protein
MXAN5970	Peptidase, S8 (subtilisin) family
MXAN5998	Putative lipase
MXAN6040	Hypothetical protein
MXAN6044	TonB-dependent receptor
MXAN6090	Hypothetical protein
MXAN6196	Hypothetical protein
MXAN6236	Putative polysaccharide-degrading enzyme
MXAN6246	OmpA domain protein
MXAN6272	Hypothetical protein
MXAN6333	Hypothetical protein
MXAN6404	Hypothetical protein
MXAN6405	Hypothetical protein
MXAN6409	Putative beta-lactamase

MXAN6429		Hypothetical protein
MXAN6465		Hypothetical protein
MXAN6487		Outer membrane efflux protein domain protein
MXAN6547		TonB-dependent receptor
MXAN6579		TonB-dependent receptor
MXAN6674		Hypothetical protein
MXAN6679		Hypothetical protein
MXAN6703		Gliding motility protein
MXAN6716		TonB dependent receptor
MXAN6737		TonB-dependent receptor
MXAN6767		Hypothetical protein
MXAN6774		Hypothetical protein
MXAN6845		TonB-dependent receptor
MXAN6911		TonB-dependent receptor
MXAN7034		Hypothetical protein
MXAN7037		MotB chemotaxis proteins
MXAN7039		Hypothetical protein
MXAN7040	*oar*	TonB dependent receptor
MXAN7112		Hypothetical protein

MXAN7210	Hypothetical protein
MXAN7331	TonB-dependent receptor
MXAN7407	Hypothetical protein
MXAN7436	Outer membrane efflux protein
MXAN7464	Hypothetical protein
MXAN7497	Peptidase, M16B (mitochondrial processing peptidase beta-subunit) family
MXAN7513	Hypothetical protein

Table A-2. List of non-outer membrane integral proteins identified by LC-MS/MS

MXAN	Function	No. of peptides
MXAN0403	ATP synthase F0, C subunit	1
MXAN0791	Peptidase, M16 (pitrilysin) family	1
MXAN0870	conserved hypothetical protein	8
MXAN0875	Hypothetical protein	1
MXAN0976	Putative lipoprotein	3
MXAN1080	NADH dehydrogenase I, N subunit	1
MXAN1111	Propionyl-CoA carboxylase, alpha subunit	3
MXAN1389	Putative alkaline phosphatase	13
MXAN1448	Transporter, MotA/TolQ/Exbb proton channel family	4
MXAN1449	Putative TonB protein	1
MXAN1564	Alkyl hydroperoxide reductase C	5
MXAN1671	V-type H(+)-translocating pyrophosphatase	1
MXAN1994	Ribosomal protein S9	1
MXAN2016	Prolyl endopeptidase precursor Pep	12
MXAN2666	Pyruvate dehydrogenase complex	10
MXAN2667	Pyruvate dehydrogenase complex, E1 component, pyruvate dehydrogenase, beta subunit	11
MXAN2668	Pyruvate dehydrogenase complex , E2 component, dihydrolipoamide	7

	acetyltransferase	
MXAN2719	Hypothetical protein	1
MXAN2720	Hypothetical protein	1
MXAN2728	Putative NADH dehydrogenase I, G subunit	1
MXAN2787	Homogentisate 1,2-dioxygenase	2
MXAN2814	Putative N-acetylmuramoyl-L-alanine amidase	1
MXAN2967	RND transporter, hydrophobe/amphiphile efflux-1 (HAE1) family	3
MXAN3206	DSBA-like thioredoxin domain protein	15
MXAN3296	Ribosomal protein S7	4
MXAN3305	Ribosomal protein S3	1
MXAN3309	Ribosomal protein L14	1
MXAN3311	Ribosomal protein L5	1
MXAN3316	Ribosomal protein S5	5
MXAN3323	Ribosomal protein S13	4
MXAN3326	DNA-directed RNA polymerase, alpha subunit	1
MXAN3327	Ribosomal protein L17	4
MXAN3370	Ribosomal protein L3	3
MXAN3539	Succinate dehydrogenase, flavoprotein subunit	4
MXAN3549	Ribosomal protein L19	6
MXAN3549	Ribosomal protein L19	6

MXAN3556	Hypothetical protein	3
MXAN3743	Hypothetical protein	1
MXAN3779	Non-ribosomal peptide synthetase/polyketide synthase	5
MXAN4217	Alpha keto acid dehydrogenase complex, E2 component	13
MXAN4219	Alpha keto acid dehydrogenase complex, E3 component	18
MXAN4289	Hypothetical protein	4
MXAN4293	Hypothetical protein	4
MXAN4299	Non-ribosomal peptide synthase/polyketide synthase	1
MXAN4327	Glu/Leu/Phe/Val dehydrogenase family protein	3
MXAN4467	Chaperonin GroEL	36
MXAN4564	2-oxoisovalerate dehydrogenase complex, E1 component, alpha subunit	15
MXAN4565	2-oxoisovalerate dehydrogenase complex, E1 component, beta subunit	15
MXAN4650	Type II secretion system protein F domain protein	1
MXAN4690	Protein-export membrane protein SecF	4
MXAN4691	Protein-export membrane protein SecD	1
MXAN4692	Preprotein translocase, YajC subunit	1
MXAN4808	Conserved hypothetical protein	5
MXAN4860	hypothetical protein MXAN_4860	10

MXAN4895	Chaperonin GroEL	33
MXAN5143	Tol-pal system protein YbgF	3
MXAN5152	OmpA family protein	3
MXAN5344	Ribosomal protein S2	3
MXAN5743	Hypothetical protein	11
MXAN6000	Iron compound ABC transporter, periplasmic iron compound-binding protein	1
MXAN6035	2-oxoglutarate dehydrogenase, E1 component	18
MXAN6036	2-oxoglutarate dehydrogenase, E2 component, dihydrolipoamide succinyltransferase	13
MXAN6247	Terpene synthase, metal binding domain protein	5
MXAN6248	Cyclic nucleotide-binding domain protein	20
MXAN6249	Cyclic nucleotide-binding domain protein	14
MXAN6483	MotA/TolQ/Exbb proton channel family protein	3
MXAN6574	Putative lipoprotein	6
MXAN6601	Peptidase, S9C (acylaminoacyl-peptidase) subfamily	3
MXAN6601	Peptidase, S9C (acylaminoacyl-peptidase) subfamily	3
MXAN6665	Putative branched chain amino acid ABC transporter, periplasmic amino acid-binding protein	2
MXAN6805	Ribosomal protein S4	2

MXAN6829	Putative late embryogenesis abundant-like protein	4
MXAN6862	MotA/TolQ/Exbb proton channel family protein	1
MXAN6884	Hypothetical protein	3
MXAN6913	Cytochrome d ubiquinol oxidase, subunit I	1
MXAN6976	Hypothetical protein	9
MXAN7028	ATP synthase F1, alpha subunit	4
MXAN7104	Peptidase, M3 (thimet oligopeptidase) family	10
MXAN7340	Hypothetical protein	3
MXAN7437	Heavy metal efflux pump, CzcA family	1